Høgskulen på Vestlandet

Master's Thesis in Climate Change Management

GE4-304-O-2022-VÅR-FLOWassign

Predefinert informasjon

Startdato:	24-05-2022 00:00	**Termin:**	2022 VÅR
Sluttdato:	07-06-2022 14:00	**Vurderingsform:**	Norsk 6-trinns skala (A-F)
Eksamensform:	Masteroppgave		
Flowkode:	203 GE4-304 1 O 2022 VÅR		
Intern sensor:	(Anonymisert)		

Deltaker

Kandidatnr.:	420

Informasjon fra deltaker

Antall ord *:	21556

Egenerklæring *: Ja

Jeg bekrefter at jeg har registrert oppgavetittelen på norsk og engelsk i StudentWeb og vet at denne vil stå på vitnemålet mitt *: Ja

Jeg godkjenner avtalen om publisering av masteroppgaven min *

Ja

Er masteroppgaven skrevet som del av et større forskningsprosjekt ved HVL? *

Ja, JOSTICE

Er masteroppgaven skrevet ved bedrift/virksomhet i næringsliv eller offentlig sektor? *

Nei

Høgskulen på Vestlandet

MASTER'S THESIS

Monitoring glacial lakes and outburst floods around Jostedalsbreen ice cap, Norway

Manoj Pariyar

Master in Climate Change Management

Department of Environmental Sciences/Western Norway

University of Applied Sciences/ Høgskulen på Vestlandet (HVL)

Supervisors: Thorben Dunse (HVL), Jacob Clement Yde (HVL), Halvor Dannevig (HVL), Liss Marie Andreassen (NVE)

Submitted on: June 7, 2022

I confirm that the work is self-prepared and that references/source references to all sources used in the work are provided, cf. Regulation relating to academic studies and examinations at the Western Norway University of Applied Sciences (HVL), § 12-1.

Monitoring glacial lakes and outburst floods around Jostedalsbreen ice cap, Norway

Master's thesis by

Manoj Pariyar

Master in Climate Change Management

Western Norway University of Applied Sciences/

Høgskulen på Vestlandet (HVL)

June 7, 2022

Sogndal, Norway

Høgskulen på Vestlandet

NVE

DECLARATION

I, Manoj Pariyar, hereby declare that this thesis titled **"Monitoring glacial lakes and outburst floods around Jostedalsbreen ice cap, Norway"** is my original work and all the sources of information used are duly acknowledged. I have not submitted it or any part of it to any other academic institutions for any degree or for any evaluation and publications.

……

Manoj Pariyar

Western Norway University of Applied Sciences/ Høgskulen på Vestlandet (HVL),

Sogndal, Norway

Email: 590114@stud.hvl.no, pariyarm982@gmail.com

Western Norway University of Applied Sciences/ Høgskulen på Vestlandet (HVL),

Sogndal, Norway

Mailing Address: HVL, Røyrgata 6, 6856 Sogndal, Norway

Email: post@hvl.no

Website: www.hvl.no

CITATION

Pariyar, M. (2022). "Monitoring glacial lakes and outburst floods around Jostedalsbreen ice cap, Norway"

A thesis submitted to Western Norway University of Applied Sciences/ Høgskulen på Vestlandet (HVL), Sogndal, Norway as a partial fulfilment of the requirement for the Degree of Master of Science in Climate Change Management.

ACKNOWLEDGEMENTS

I would like to express my sincere gratitude to all my supervisors, Thorben Dunse (HVL), Jacob Clement Yde (HVL), Halvor Dannevig (HVL), Liss Marie Andreassen (NVE) for providing me intellectual ideas, concepts, guidance, suggestions and encouragement in research development and further proceedings till the completion of my thesis. This is a great opportunity for me to write my thesis on such an interesting topic. I knew a lot about how glacial lakes are varying over time in recent years in Jostedalsbreen, Norway with ongoing climate change. The knowledge and experience I gained from this thesis will certainly help me boost further in my career.

I sincerely appreciate the coordination of the JOSTICE project in Western Norway University of Applied Sciences and NVE which helped a lot to compile relevant resources for my thesis. I would also like to thank the data providers Copernicus Satellite Service, Planet Labs, NVE, Meteorological Institute Norway, Norge in bilder, Geonorge, and others to help me acquire the data needed to accomplish my thesis.

The outlines (polygons) of glacial lakes produced in this study will be available in NVE's Copernicus Glacier Service Website https://www.nve.no/hydrology/glaciers/copernicus-glacier-service/glacier-lakes/

Lastly, I am very much grateful to my family members who encouraged and inspired me a lot to work on my research.

Manoj Pariyar

Sogndal, Norway, 7 June 2022

ABSTRACT

As a result of global climate change, glacial lakes are undergoing rapid changes and are becoming more dynamic, posing a risk of outburst floods for communities and infrastructures nearby (Shugar et al., 2020). With no doubt, mainland Europe's largest glacier, Jostedalsbreen has already experienced 20 GLOF events, out of 147 in Norway, with 4-5 events in the last 2 decades (Andreassen, Nagy, Kjøllmoen, & Leigh, 2022; Nagy & Andreassen, 2019). NVE has been closely monitoring glacial lakes in Norway including Jostedalsbreen through satellite-based application www.xgeo.no and inventories of glacial lakes in certain years. This study, however, analyzes the time series of higher frequency data to study rapid drainage events, month-to-month (seasonal)/year-to-year (annual) variations, and trend in growth of glacial lakes around Jostedalsbreen both with and without history of GLOF events in recent years.

The approach of the study is to calculate the Normalized Difference Water Index (NDWI) of Sentinel 2 and PlanetScope imageries acquired from Copernicus Satellite Services and Planet Labs websites, use a threshold NDWI value to separate the water pixels from non-water pixels and manually digitize where necessary to obtain the lake area. A threshold NDWI value which best represents the area of lakes and reduces the need for digitization is obtained with reference to manually digitized high resolution ortho-imagery of same lakes in Jostedalsbreen.

The study found no significant evidence of rapid drainage events indicative of GLOF. However, lake L2 (*Associated Glacier: Marabreen/Glacier ID: 2364/type: glacier-dammed*) and L19 (*Associated Glacier: Supphellebreen/Glacier ID – 2352/type: moraine-dammed*) both with history of GLOF events were found to be significantly reduced in size within an interval of 1 to 2 months, but the intermediate imageries showed no evidence of rapid drainage. Further, percentage variation (SD) in normalized maximum annual surface area of lakes *connected-to-glacier* was significantly higher (p-value = 0.01) than for lakes *not-connected-to-glacier*. Among all lakes, lake L23 (*Glacial ID: 2293/type: supraglacial*) showed the highest variation in overall 6 years. Though not significant, lakes *connected-to-glacier* including *moraine-dammed* lakes showed an increasing trend in maximum annual surface area in 6 years.

In recent years in Western Norway, the temperature has risen even higher (Meteorological Institute Norway, 2021), causing the ablation process to accelerate, resulting in an increased surface area of lakes (meaning more water or a rise in water level). Simultaneously, the glacier is also calving which might be a trigger factor for outburst in lakes *connected-to-glacier*. In such a scenario, the risk of damage due to potential outburst might be higher than before. Therefore, the need for a regular monitoring of glacial lakes, especially for lakes with high potential of outburst, is a most in Jostedalsbreen region.

Key words: *Climate change, glacial lakes, glacial lake types, GLOFs, variations, trend, satellite imageries, NDWI, threshold, manual digitization, surface area, trigger factor, risk.*

Table of Contents

List of Tables

List of Figures

ACRONYMS

BGR	Blue, Green, and Red
BOA	Bottom-Of-Atmosphere
CSS	Copernicus Satellite Service
DN	Digital Numbers
DOS	Dark Object Subtraction
ESA	European Space Agency
GLOF	Glacial Lake Outburst Flood
LIA	Little Ice Age
m.s.l.	Mean Sea Level
NDWI	Normalized Difference Water Index
NIR	Near-Infrared
NVE	Norwegian Water Resources and Energy Directorate
PS	PlanetScope
S2	Sentinel 2
SD	Standard Deviation
TOA	Top-Of-Atmosphere
AG	Associated Glacier
GID	Glacier ID

1 INTRODUCTION

1.1 Background

Glacial lakes are evolving rapidly and are becoming more dynamic globally in response to climate change in recent years, posing risk of outburst floods to communities and infrastructures in their proximity (Aggarwal, Rai, Thakur, & Emmer, 2017; Bajracharya, Mool, & Shrestha, 2008; Jackson & Ragulina, 2014; Komori, 2008; Mohanty & Maiti, 2021; Wang, Xiang, Gao, Lu, & Yao, 2015). It is therefore crucial to understand their dynamics regarding their evolution, distribution, and driving forces for rapid expansion and drainage to prepare the communities and planners to reduce the potential impacts of glacial lake outburst floods (GLOF) (M. Zhang, Chen, Tian, Liang, & Yang, 2020). However, the inaccessibility due to their remoteness and the lack of advanced technology to assess them remotely and more frequently had always been a challenge until the arrival of Copernicus Satellite Service (CSS) in 2015 which provides free available high spatial resolution (10 meter) and high temporal resolution (revisit time of 5 days) imageries of earth surfaces including glacial lakes, good enough to monitor them frequently and more precisely (The European Space Agency, n.d.). In addition, Planet lab, despite having some limitation in data acquisition, provides even higher spatial (3-4 m) resolution and higher temporal (revisit time of 1 day) resolution satellite data to researchers and students to observe the daily changes on earth surface (Planet Labs, n.d.-a). Therefore, combining both the satellite services data a continuous and higher frequency time series can be obtained (Sadeh et al., 2021) which helps us regularly monitor and better understand the changes in glacial lake surfaces (Andreassen et al., 2022; Qayyum, Ghuffar, Ahmad, Yousaf, & Shahid, 2020; M. Zhang et al., 2020).

In the global context, the average surface temperature has increased by 0.14 ºC per decade since 1880 but the rate has doubled in past 4 decades with the top 10 warmest years recorded since 2005 and the global surface temperature averaged across ocean and land is recorded at 0.98 ºC hotter than the average of 20th century. Meanwhile, the polar regions are warming at even faster rates (Lindsey & Dahlman, 2022). The updated climate record since 1900 from Meteorological Institute of Norway has depicted that the regional annual temperature of Western Norway has increased by 1.5 ºC by 2020 as compared to normal (1961 - 1990) temperature, with sharp increase since 1985. The summer temperature is 1.3 ºC and the winter temperature is 2.5 ºC above normal temperature. Likewise, the annual precipitation is 16 % above normal

(Meteorological Institute Norway, 2021).

Several studies have already concluded since last few decades that the glaciers in mid-latitude regions, and especially those in maritime region in Norway are highly sensitive to rising temperature and reduced mass balance (Braithwaite & Zhang, 1999; Jóhannesson, Sigurdsson, Laumann, & Kennett, 1995; Laumann & Reeh, 1993). Moreover, in about 100 to 200 years, many glaciers and ice caps are expected to disappear, alongside increasing the runoff from glaciated areas by 25 to 50 % in about 30 to 100 years in Nordic countries (Jóhannesson et al., 2006). Quite evidently, things are happening as expected as there is huge reduction in glacier area and ice volume since the Little Ice Age (LIA). In Jostedalsbreen region, during LIA, maximum ice-covered area was 586 km^2 which is reduced by 19 % and the ice volume was ranged between 61 km3 to 91 km3 which is now reduced by 18 % (Carrivick, Andreassen, Nesje, & Yde, 2022). As this reduction continues, new glacial lakes are formed and glacier-related hazards are increased in the region (Andreassen et al., 2022; Jackson & Ragulina, 2014). Particularly, the moraine-dammed GLOF events are predicted to increase in frequency in coming decades and in 22nd century (Harrison et al., 2018).

Until 2014, several GLOFs events have been recorded in 20 different glaciers in Norway (4 around Jostedalsbreen ice cap alone), of which 12 are expected to repeat the events and additional 8 glaciers are likely to have potential GLOF events in future. Marabreen (*Glacier ID: 2364*) and Supphellebreen (*Glacier ID: 2352*) are active and potentially dangerous sites for GLOF in Jostedalsbreen with history of 1 event and 4 events respectively, the last events being recorded in 2004 in both the sites. Tunsbergdalsbreen (*Glacier ID: 2320*), being the largest glacier unit in Jostedalsbreen ice cap, has a history of 10 GLOF events from 1896 and 1999. Likewise, Brenndalsbreen (*Glacier ID: 2305*) has 2 events from 1720 to 1743 (Jackson & Ragulina, 2014).

In such a scenario, it is crucial to understand the geomorphology and variations in glacial lakes and identify potential candidate lakes for GLOF events so that necessary actions are taken in time to save lives and properties of people living in proximity. Particularly, it is important to assess the seasonal and annual variation in their surface aera and the annual trend in their maximum size in recent years that helps us compare between different lakes and their types regarding the degree of risk they possess in near future.

1.2 Research problem and rationale of the study

Jostedalsbreen ice cap, being the largest continental glacier in Europe has a history of high occurrence of GLOFs. According to the updated data source from Norwegian Water Resources and Energy Directorate (NVE), 147 GLOF events have been recorded in whole Norway until 2021, majority of which happening in the past 2 decades in Jostedalsbreen region (Norwegian Water Resources and Energy Directorate, 2022a). A recent inventory of glacial lakes in Norway has also revealed a general increase in lake area as well as the formation of new glacial lakes around Jostedalsbreen (Andreassen et al., 2022). This trend is expected to continue, as glacier retreat in response to climate change. Time and again, such inventories are conducted and there are certain web applications (www.xgeo.no) designed to monitor glaciers and glacial lakes. However, a continuous series of high temporal data is not produced yet to assess the variations and trend in glacial lakes around Jostedalsbreen in recent years. Therefore, this study aims to develop a time series of data in melting seasons starting from 2016 until 2021 on a monthly-basis to monitor and look for evidence of outburst, month-to-month (seasonal) variation, year-to-year (inter-annual variation), overall (6 years variation) and trend in maximum annual seasonal extent (surface area) of different lakes and their types. The compiled data is thus expected to disclose potentially dangerous lakes regarding outburst, and rank the lakes based on their variation. In addition, it will reveal how glacier fronts in contact with glacial lakes are retreating or advancing in recent years and how lakes are changing their forms (types) over time.

Glacial lakes are of different types, based on how they are dammed with and how they interface with the glacier (Yao, Liu, Han, Sun, & Zhao, 2018). Therefore, the variation they show and the risk they pose in case of outburst are also different from each other. Specially, the lakes in direct contact with glacier and dammed with moraine are of more the interest as they are more dynamic (Nagy & Andreassen, 2019; Wang et al., 2015; G. Zhang, Yao, Xie, Wang, & Yang, 2015). Therefore, to assess the variations in glacial lakes, it is primarily important to categorize the lakes into their lake type.

The approach of the study is to calculate the Normalized Difference Water Index (NDWI) of imageries acquired from Copernicus Satellite Service website https://scihub.copernicus.eu/ (Copernicus Open Access Hub, n.d.) and from Planet Labs website https://www.planet.com/ (Planet Labs, n.d.-b), use suitable threshold NDWI values to separate the water pixels from non-water pixels and manually digitize where necessary to obtain the lake area. A threshold

NDWI value which best represents the area of lakes and reduces the need for digitization is obtained with reference to manually digitized high resolution ortho-imagery of same lakes in Jostedalsbreen. Meanwhile, an over- or under-estimation of lake areas using the selected threshold value will be quantified in percentage and represented in the result.

In the meantime, the study had some limitations in acquisition of high-resolution images of glacial lakes due to the presence of clouds, shadows, and floating ices on lakes which limited the number of usable images. However, the images are selected with very keen observation to optimize the quality of the research.

1.1.1 Research questions

The study is designed and expected to answer following questions:

- Is there any rapid events indicative of outburst flood around Jostedalsbreen in recent years (2016-2021)?
- How does surface area of glacial lakes and their types vary around Jostedalsbreen region in recent years (2016-2021)?
- How are glacial lakes expanding around Jostedalsbreen region in recent years (2016-2021)?

1.3 Objective of the study

The major objectives of the study are as follows:

- Map and monitor the extent of glacial lakes during melting seasons from 2016 to 2021 using optical satellite (airborne) imagery of high spatial and temporal resolution.
- Identify rapid drainage events, indicative of glacier-lake outburst floods.
- Follow up potential sites for new glacier-lakes, previously identified by (Nagy & Andreassen, 2019).

1.4 Glacial lakes and their classification

There are a lot of definitions on “Glacial Lake”, but the commonly accepted concept is that the glacial lakes are formed by glaciation. The only inconsistency is in the distance between the glacier feeding the lake which differentiate the glacial lake from the natural lake. Because of

this inconsistency, the results of different studies on glacial lakes are not feasible for comparison. However, in simple words, glacial lakes are those lakes which are originated from meltwater of glaciers. The process involves erosion of land by glacier as it slides down, followed by its melting, leaving a depression on the land which is then filled up by the melt water as the glacier continues melting (Norwegian Water Resources and Energy Directorate, 2022b; Yao et al., 2018). Like "Glacial Lake", its classification system is also different between scholars. For instant, the classification system used by (Yao et al., 2018) includes 6 major classes, glacial erosion lake, moraine-dammed lake, ice-blocked lake, supraglacial lake, subglacial lake and other glacial lake. According to the paper, glacial erosion lakes are those formed in the depression created by erosion and abrasion of glacier while the glacier slides over the slope. Moraine-dammed lakes are those that are formed in between the glacier margin and the ridge created by the moraine whereas ice-blocked lakes are formed by glacier ice which when separated from the main glacier acts as a wall for water accumulation. Supraglacial lakes are formed on the surface of glacier because of difference in ablation while subglacial lakes are formed within the glacier and they develop channel underneath the glacier to drain out water (Yao et al., 2018). However, for the basic purpose of this study, lakes are broadly classified into two categories, (1) *connected-to-glacier* and (2) *not-connected-to-glacier* with slight modification in classification followed by (Nagy & Andreassen, 2019). Simply, the lakes which are connected to the glacier are assigned to lake class *connected-to-glacier* and those which are not in direct contact with the glacier and reside at certain distance but close to the glacier are assigned to lake class *not-connected-to-glacier*. Images acquired for each lake were subjectively explored while processing and assigned to different classes. Those lakes which happened to change its class (for instant, from lake class *connected-to-glacier* to *not-connected-to-glacier*) during 6 years' time-period were keenly observed and assigned to certain class where they appeared to in most of the images.

Technically, *Glacier-dammed* and *Moraine-dammed* lakes are also *connected-to-glacier*, but in this study, there were only 2 *Glacier-dammed* and 1 (clearly identifiable) *Moraine-dammed* lakes so these lakes were analyzed separately. In addition, there were 2 largest lakes with *artificial-water-level-regulation* system; Styggevatnet and Kupvatnet, so these lakes were also analyzed separately. There was a *supraglacial-lake* which eventually found a drainage pathway at the end year (2021). However, it was kept in the lake class *connected-to-glacier*. In fact, the number of glacial lakes *connected-to-glacier* was the highest and there was just one *supraglacial-lake* included in this study.

Table 1: Glacial lakes classification

Types	Number of Lakes	Description
1	14	*Not-connected-to-glacier*
2	31	*Connected-to-glacier*
3	2	*Glacier-dammed*
4	1	*Moraine-dammed*
5	2	*Artificial-water-level-regulation*
6	1	*Supraglacial*
Total	**51**	

1.5 Glacial lakes and their seasonal and annual variation

As glaciers, the glacial lakes are very sensitive to climate change and the variation in surface area of glacial lakes are strongly associated with temperature and precipitation (Dai et al., 2022). Unlike normal lakes, glacial lakes pass through two different phases in a year (1) melting phase and (2) freezing phase. Generally, melting season starts from May and ends in September in Norway (Imhof, Nesje, & Nussbaumer, 2012). During this time, the glacier lakes show variation in their size depending on the type they belong to. In a normal scenario, the glacial lakes start melting from early summer collecting more and more water and normally drain out through natural drainage pathway. As it approaches the winter phase, the lake water starts to freeze (Dai et al., 2022; Green, 2011; Sugiyama et al., 2021). However, this is not always the case. There might be different scenarios, (1) the water level may rise alongside increasing the surface area of lake, (2) the lake may drain out abruptly emptying the lake, (3) the lake may drain out slowly causing reduced water level and surface area, (4) the lake may remain frozen underneath the ice for the whole season, and lastly (5) there might be negligible change in the surface area. Moreover, these variations may be the same or alter year after year giving an overall variation in a couple of year. Besides, a trend might also be obtained in annual growth (annual maximum surface area) of lake. All these variations are important to understand how a particular lake, or a lake type (class) is responding to or might respond to changing climate and hence they are assessed in this study.

Glacial lake expansion and reduction is a natural phenomenon, but a rapid expansion and rapid drainage is dangerous because a rapid expansion puts more mechanical pressure on dam and a rapid drainage signifies outburst leading to loss of lives and properties downstream. The major factors contributing to lake expansion are precipitation, ablation, calving, glacier retreat, and positive feedback loop enhancing the melting process as the glaciers retreat exposing earth surface underneath. Likewise, the factors contributing to lake area reduction are geomorphological characteristics of dams (Begam, Sen, & Dey, 2018; Emmer & Cochachin,

2013).

1.6 Glacial lake outburst floods (GLOFs) and trigger mechanisms

Glacial lake outburst flood (GLOF) occurs due to release of meltwater collected in glacial lakes dammed by either moraine or ice. The GLOF often occurs suddenly (or sometimes in a cyclic order) and the release of water from the lake lasts for few hours to days. The dam failure fundamentally depends on the coalition of the dam materials and the type of the trigger mechanism (Bendle, 2020). As mentioned earlier, glacial lakes are dammed by either moraine or ice but basically the moraine-dams which hold the glacial lake water are weak dams as they are composed of unconsolidated materials, and have usually unstable slopes and freeboard (Bendle, 2020; Emmer & Cochachin, 2013; Neupane, Chen, & Cao, 2019). Dam failure mechanism is generally triggered by a number of factors such as landslide, rock or ice avalanches, degradation of ice core in the dam, glacier calving, earthquake, or atmospheric events which stimulates the breaching of dams through waves that overtops the dam or leakage of water through the dam (Begam et al., 2018; Bendle, 2020; Emmer & Cochachin, 2013; Neupane et al., 2019).

According to (Bendle, 2020), the process of dam failure in moraine-dammed lakes can be summarized in 3 steps – displacement wave, breach incision and moraine degradation. At first, the displacement wave is produced in the lake when an external material suddenly drops or slides into the lake. These materials can be the chunk of ice calved from the terminus or glacier margin, rocks fallen from higher altitude and other earth materials swept by avalanches into the lake. In addition, meltwater from upstream glacier, and precipitation as rainfall or snow which rapidly raises the water level and earthquake shaking the moraine dam materials could also be the triggering elements. The displacement wave hence produced overtops the moraine dam causing an incision in the dam. The incision or small channel initially allows rapid flow of lake water through the dam. As this continues, the flow of water is accompanied by the unconsolidated materials present in the lake which intensifies the magnitude of flow into debris flow. Another factor to degrade or weaken the moraine is the seepage of water through it or the melting of ice core in the dam that dismantles the dam materials (Bendle, 2020).

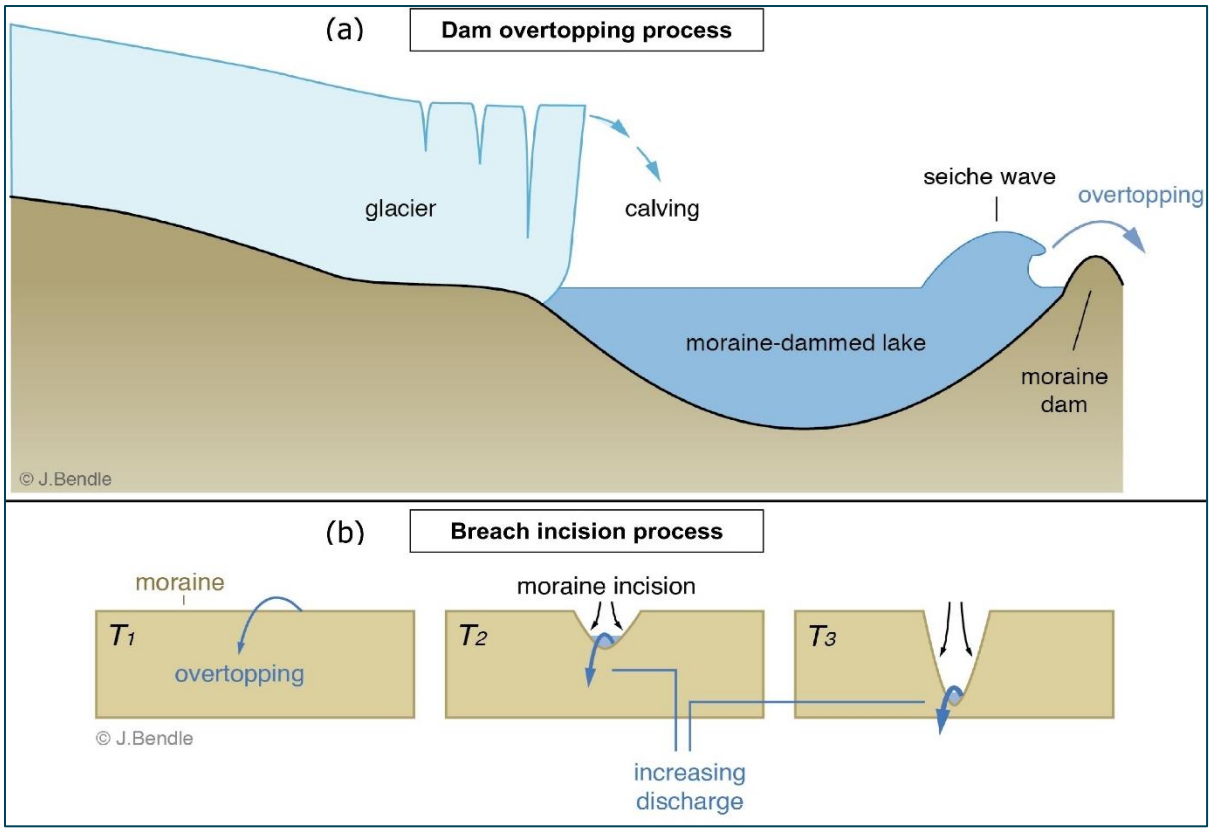

Figure 1: Overtopping displacement wave in moraine-dammed lake due to glacier calving and breach incision process, derived from (Bendle, 2020). (a) Dam overtopping process and (b) Breach incision process

According to (Bendle, 2020), outburst flood in ice- or glacier-dammed lakes is different as it does not need a dam to destroy rather it works in a dam-lifting or dam-floating mechanism. As the water level in the lake rises to more than 90 % of the height of the ice dam, it is lifted from the bed making some space (subglacial conduit) for the water to drain from underneath. This happens because of difference between density of ice (~0.9 g/cm^3) and water (~1.0 g/cm^3). Besides the ice-lifting phenomenon, ice-dammed lake also drains out through spillover when the lake water level rises due to heavy rainfall or melting of snow. This phenomenon is common in cold-based glaciers where the bed of the glacier is impermeable (Bendle, 2020).

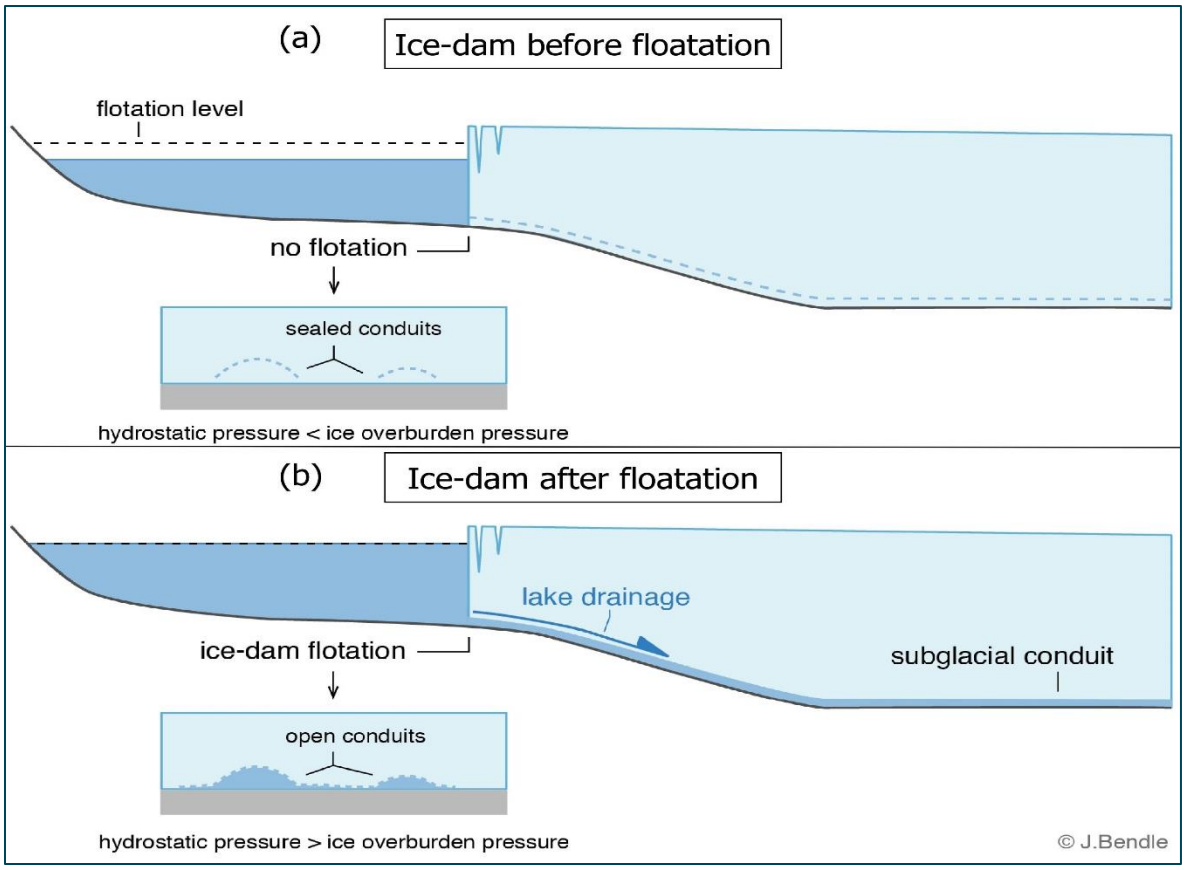

Figure 2: Ice-dam floatation process in ice-dammed lake. (a) Ice-dam before floatation and (b) Ice-dam after floatation Derived from (Bendle, 2020)

Since the GLOF events emptying the whole lake might happen in few hours to few days, the (1 month) temporal resolution of images taken in this study may not be able to detect this exact event but, on the other hand, it takes some time to refill the lake as well or may remain empty rest of the year, so the variation is detectable. Even though the intermediate images are not included in the study for all lakes, they are visually inspected in daily earth monitoring platforms like www.xgeo.no, Copernicus website https://scihub.copernicus.eu/ , and Planet Labs interface https://www.planet.com/ to observe any significant changes indicative of GLOF.

1.7 Summary of previous inventories of glacial lakes around Jostedalsbreen

Inventory of outlines of glacial lakes in mainland Norway has been conducted a couple of times by NVE using different techniques. In 2014, the lake outlines were mapped with manual digitization of Landsat imageries where the lakes in direct contact or within 50 m distance from the glacier margin mapped during inventory of conducted in (1999-2006) were only included. In 2018, the lakes were mapped using semi-automatic classification, thresholding, and manual digitization in Sentinel 2 (S2) satellite imageries. Categorization of lakes was done based on

the interface of lakes with the glacier (Nagy & Andreassen, 2019). The inventory was updated with additional data in 2019 with manually corrected outlines (Andreassen et al., 2022). Therefore, the lake outlines mapped in this study are compared with the previous inventories.

1.8 Remote sensing and use of satellite images

Remote sensing is "the art or science of telling something about an object without touching it." (Fischer, Hemphill, & Kover, 1976). Earth observation has been revolutionized since the beginning of remote sensing in past few decades. Especially, its application in glacier or glacial lake observation has been very useful, which otherwise would have been extremely difficult. For instance, NVE makes use of Sentinel imageries for continuous monitoring of glaciers and glacial lakes (Andreassen, Engeset, et al., 2021; Andreassen, Moholdt, et al., 2021; Andreassen et al., 2022; Kjøllmoen, Andreassen, Elvehøy, & Melvold, 2021; Nagy & Andreassen, 2019). With growing technology, the spatial and temporal resolution of images provided by the latest and updated remote sensing satellite services are high enough to capture the finer details (3-10 m) with frequent revisits (1-5 days). The different bands available in the electromagnetic spectrum of satellite sensors can be used to characterize and analyze the changes in natural processes. For instant, the visible (Blue, Green, and Red) and infrared bands in both Sentinel 2 (S2) and Planetscope (PS) images are highly useful in detecting and mapping the glacial lakes in this study (Davies, 2020). There are some limitations in image acquisition and issues of interferences due to atmospheric conditions in optical remote sensing. However, we can make the best out of available images in the study of glacier and glacial lakes.

2 MATERIALS AND METHODS

2.1 Study area

The mainland Europe's largest glacier, Jostedalsbreen, situated in Western Norway extending more than 60 km along its largest extent from southwest to northeast and a width of 10 to 15 km covers an area of 458 km^2 (Andreassen et al., 2022). It is surrounded by other smaller glaciers which are also included in this study. Meanwhile, in these last few decades, there has been some significant changes in the area due to climate change (Askheim, 2022).

Basically, Jostedalsbreen is sub-divided into more than 80 glacier units, among which Tunsbergdalsbreen is the largest, stretching more than 15 km long on the southern side (Andreassen et al., 2022; Andreassen, Winsvold, Paul, & Hausberg, 2012; Carrivick et al., 2022). There lie some major glacier arms namely Marabreen, Vetlebreen, Lundabreen, and Bøyabreen in the south-east, Sikilbreen, Sygneskarsbreen, and Tverrbyttnbreen in the north-east, Austerdalsbreen, Tunsbergdalsbreen, and Nigardsbreen in the south and Melkevollsbreen, Briksdalsbreen, and Brenndalsbreen in the north (Askheim, 2022). Jostedasbreen has the highest elevation of 1957 meters from the m.s.l., yet the highest glacial lake included in the study is at an elevation of 1713 m from m.s.l. and the lowest glacial lake is at 387 m from m.s.l. Many glacial lakes for the study are associated with the main glacier ice cap. However, the lakes from nearby glaciers such as Jostefonni, Grovabreen, Myklebustbreen, Ramnefjellbreen, Tystigbreen, and Spørteggbreen are also included in this study.

Jostedalsbreen has maritime climatic effect and so the snow is supplied heavily from mild and humid North Atlantic winds from the southwest. In Norway, in general, the melting season (ablation) ranges from May 1 and September 30 and the freezing season (snow accumulation) ranges from October 1 to April 30. Thus, changes in these local climatic conditions make the glacier sensitive over time (Imhof et al., 2012). A substantial increase in the number of glacial lakes has been observed along with glacier retreat, some of which are being drained and emptied, while others are being created. 87 new lakes were documented in the inventory conducted in 2018 by (Nagy & Andreassen, 2019), whereas some lakes were already disconnected with glacier compared to inventory conducted in 1999 and 2006 (Andreassen et al., 2022).

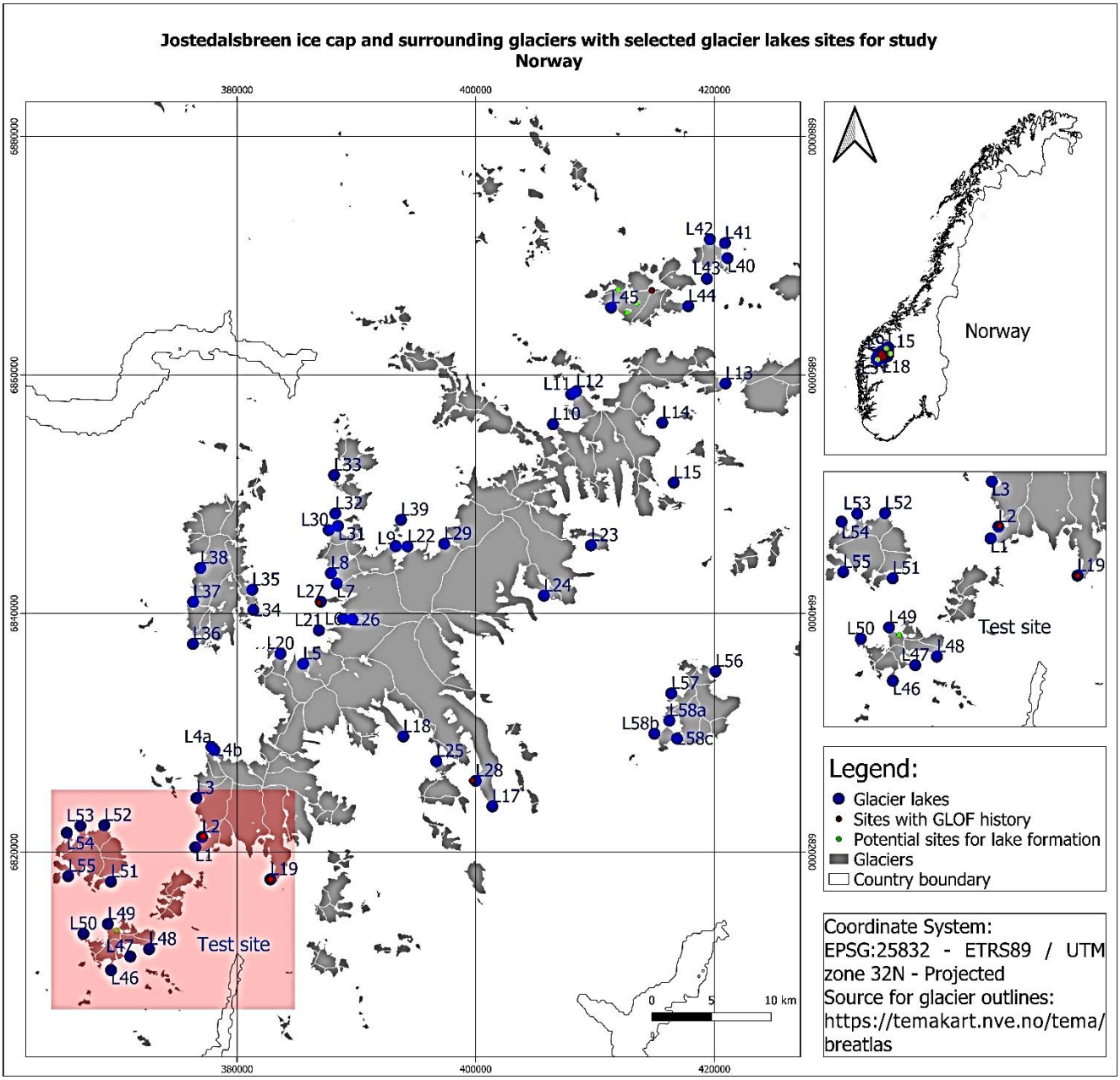

Figure 3: Study Area (Jostedalsbreen ice cap and surrounding glaciers, Norway)

Here is an overview on the types of glacial lakes and their associated glaciers.

Table 2: Some information about the selected lakes and associated glaciers. Source: (Nagy & Andreassen, 2019)

Lakes	Lake Type	Lake name	Associated Glacier (AG)	Glacier ID (GID)	Glacier Area (km2)	Glacier Slope	Glacier Aspect
L1	2		Marabreen	2364	2.524	8.6	245
L2	3		Marabreen (Potentially Dangerous)	2364	2.524	8.6	245
L3	2		Lundabreen	3906	8.86	7.2	253
L4a	2	Strupevatnet		2340	1.839	8.6	336
L4b	2			2340	1.839	8.6	336
L5	2	Oldevatn	Melkevollbreen	2324	6.553	10.5	330
L6	1						
L7	1						
L9	2		Ruteflotbreen	2294	6.038	11.4	350
L10	2		Erdalsbreen	2481	10.28	10.5	321
L11	1						
L12	2		Vesledalsbreen	2474	3.415	10.6	330
L13	2		Tverrbyttnbreen	2459	3.571	14	41
L14	5	Kupvatnet	Sygneskarsbreen	2471	3.054	9.1	78
L15	5	Styggevatnet	Austdalsbreeen	2478	10.35	5.2	133
L17	2		Tunsbergdalsbreen	2320	47.47	5.9	133
L18	2		Austerdalsbreen	2327	19.78	9.5	134
L19	4		Supphellebreen (Potentially Dangerous)	2352	12.82	8.6	161
L22	2		Ruteflotbreen	2294	6.038	11.4	350
L23	2			2293	0.349	4.7	232
L24	1						
L25	2			2346	1.34	11.3	318
L29	1						
L30	1						
L31	1						
L34	2		Myklebustbreen	2303	0.082	11.6	122
L35	2		Myklebustbreen	2295	1.368	18.9	88
L36	1		Myklebustbreen				
L37	2		Myklebustbreen	2302	2.949	9.4	243
L38	2		Myklebustbreen	2290	11.75	8.5	265
L40	2			2417	0.589	14.1	97
L41	2			3628	3.379	11.1	15
L42	1						
L43	1						
L44	2		(Tystigbreen) Maradalsbreen	2438	2.353	9.2	110
L45	2		Tystigbreen	2435	5.95	8.7	169
L46	1						
L47	1						
L48	2			2145	1.677	10	94
L49	2			2142	1.115	5.7	316
L50	2			3848	1.526	17	5
L51	1						
L52	2			2119	3.371	13.8	357
L53	2			3916	3.371	13.8	357
L54	2			2118	0.354	19.2	321
L55	2			2124	1.006	8.3	139
L56	2		(Spørtegg glacier) Leirbotnbreen	2520	2.514	10.8	55
L57	1		Spørtegg glacier				
L58a	2		Spørtegg glacier	2524	0.805	5.6	228
L58b	3			2531	0.32	10.5	328
L58c	2			2532	1.848	6.1	74

Note: Type 1 (*Not-connected-to-glacier*), Type 2 (*Connected-to-glacier*), Type 3 (*Glacier-dammed*), Type 4 (*Moraine-dammed*), Type 5 (*Artificial-water-level-regulation*), and Type 6 (*Supraglacial*)

2.2 Research design

The method for glacial lake outlines mapping is primarily based on semi-automatic classification of ground images which involves assessment and classification of spectral

reflectance values of each pixel and calculating the NDWI for water pixels. The semi-automatic classification method is followed by thresholding NDWI for water pixels and manual digitization (correction) where the method fails to classify the water pixel correctly.

2.2.1 Data Collection

The study is based on optical remote sensing, so the satellite imageries used for analysis were obtained from two satellite data services to obtain optimum number of imageries for a continuous timeseries. Sentinel 2 (S2) imageries were obtained from European Union's Earth Observation program, Copernicus website https://scihub.copernicus.eu/ (Copernicus Open Access Hub, n.d.) and PlanetScope (PS) imageries were obtained from Planet Labs website https://www.planet.com/ (Planet Labs, n.d.-b).

Table 3: Information on satellite services, their products, and scenes used for the study

Description	**Sentinel 2**	**PlanetScope**
Sensors used	Opto-electronic multispectral sensor	Dove Classic, Dove-R, and Super Dove
Resolution	10 m for BGR+NIR	3 m for BGR+NIR
Revisit time	5 days in equator and 2 to 3 days at middle latitudes	Daily
Data range used for scene analysis	1 scene per month for each lake starting from July to November (2016- 2021)	51 scenes (1 for each lake) on (2018-08-14) + 73 scenes to fill up gaps in Sentinel 2 series wherever needed
Number of scenes analysed	702 scenes for 51 lakes	124 scenes for 51 lakes
Total scenes used for analysis	826	
Expected scenes per lake	5 months (scenes) per year * 6 years = 30	
Available maximum scenes per lake	24	
Available minimum scenes per lake	8	

2.2.1.1 Satellite imageries

2.2.1.1.1 Sentinel 2 (S2) Imageries

S2 mission of Copernicus started with the launch of S2A satellite on 23 June 2015 followed by the launch of S2B satellite on 7 March 2017 on the same orbit placed at 180° from the previous one in sun-synchronous orbit (The European Space Agency, n.d.). The mission aims to contribute to several fields such as climate change and land monitoring including agriculture, forest, water, and disaster, and support the continuation of multispectral imageries from series of SPOT and USGS LANDSAT Thematic Mapper Instrument (ESA, n.d.-c). However, the temporal resolution until 2017 was low due to presence of single satellite and initial setting-up

operation phase. But after, the two satellites together had a revisit time of 5 days and the spatial resolution of 10 meter (ESA, n.d.-d). Therefore, as compared to LANDSAT, it is more useful for change detection with higher spatial and temporal resolution. The Multi-Spectral Instrument (MSI) mounted in the satellites captures 13 reflective bands of different wavelengths including four 10-meter bands of visible and near-infrared (BGR+NIR), six 20-meter bands of near-infrared (NIR) and short-wave infrared (SWIR), and three 60-meter bands of visible, near-infrared (NIR) and short-wave infrared (SWIR) (ESA, 2015). 10-meter bands of BGR+NIR are used for calculating NDWI and for image visualization in natural and false colors. The 60-meter bands are also known as atmospheric correction bands as they are useful to correct atmospheric interference in satellite images from aerosol, water vapor and cirrus to obtain atmospherically corrected images (Satellite Imaging Corporation, n.d.).

S2 satellites provide products of different levels, of which, Level-2A products are highly useful in this study as they are orthorectified and provide Bottom-Of-Atmosphere (BOA) reflectance or surface reflectance with necessary bands to calculate water indices (ESA, n.d.-b). But these products are not available for 2016 and 2017, so Level-1C products which provide the Top-Of-Atmosphere (TOA) reflectance were hence used for the study after the application of Dark Object Subtraction (DOS1) method – a simple method for atmospheric (haze) correction. The layers downloaded from the Copernicus websites contain Digital Numbers (DNs) for each pixel which need to be converted to reflectance values through image processing. This is done with the help of Semi-Automatic Classification Plugin in QGIS. S2 imageries are obtained in a square tile of 100 * 100 km^2 so, two such tiles of same day were downloaded for each month to cover the study area (Fig. 4).

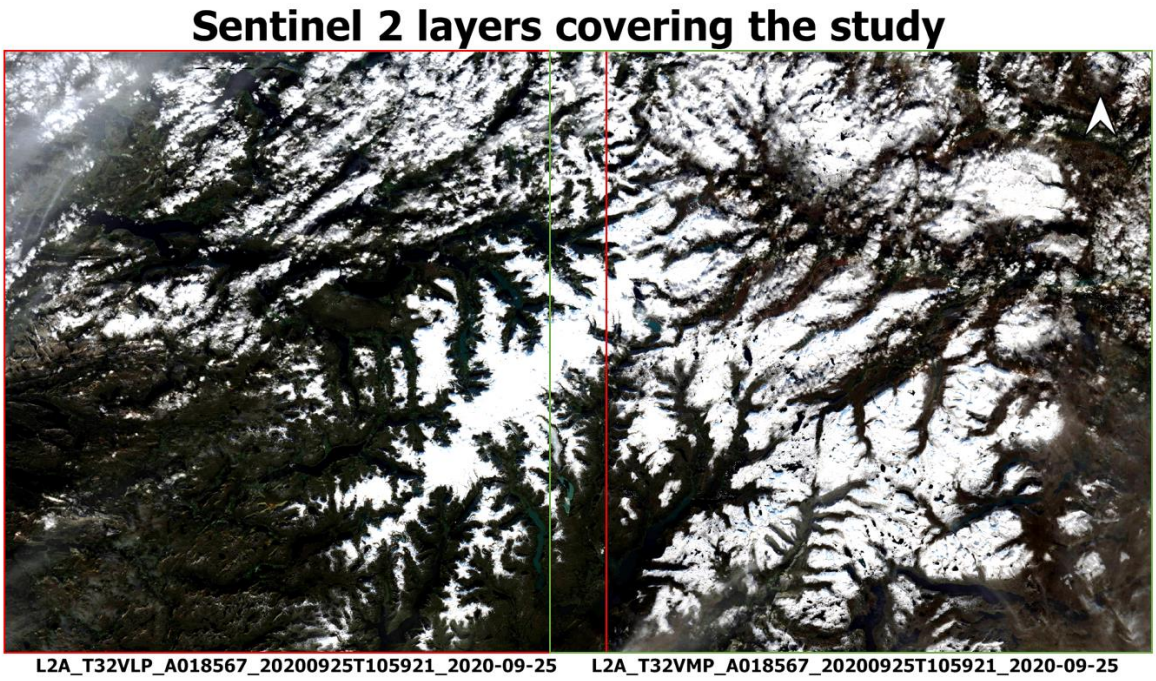

Figure 4: A mosaic of S2 natural colour composite band layers including bands 4, 3, and 2 covering the study area on 25-09-2020. Source: Copernicus Open Access Hub (https://scihub.copernicus.eu/)

2.2.1.1.2 PlanetScope (PS) Imageries

Together with approximately 130 satellites, PS is capable of imaging the whole land surface in just one day, so it can provide imageries every day. The spatial resolution is 3 meter which makes it highly useful for change detection in finer spatiotemporal scale as compared to Sentinel and LANDSAT. However, the service is not freely available for all, except to those scientific researchers whose project proposals are accepted upon submission by the Planet team. There was limitation to download only 5000 km^2 images per month so PS images were used to supplement the S2 images to fill up the gaps where S2 images are not available. Unlike S2 images, PS images can be obtained in desired dimension as per the need of the study. However, there might be some missing data in PS layers as shown in the Fig. 5

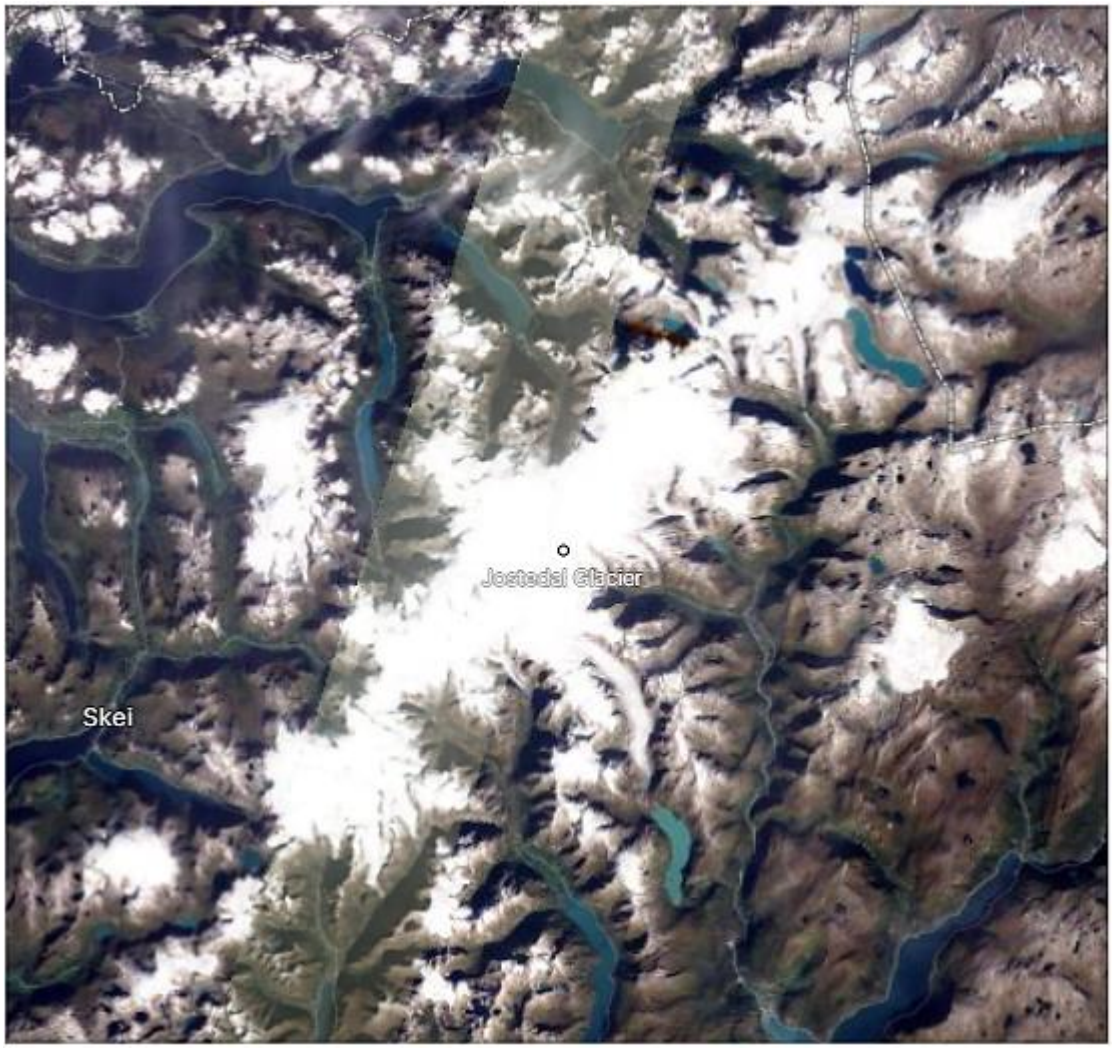

Figure 5: Mosaic of PS scenes covering the study area on September 13, 2021. Source: Planet Labs website (https://www.planet.com/)

PS satellites have three types of sensors which capture 3 to 8 different bands of different wavelengths including Visible (BGR) and near IR in Dove Classic sensor, Visible (BGR) and near IR with updated Bayer pattern and pass-band filter in Dove-R sensor, and Visible (BGR), near IR, red edge, green I, coastal blue, and yellow in SuperDove sensor (Planet Labs, n.d.-c). The scenes produced from Dove Classic sensor has the lowest coverage (25.0 * 11.5 km^2) whereas SuperDove sensor has the highest coverage (32.5 * 19.6 sq km.). Furthermore, these scenes obtained from these sensors are categorized into 4 asset types based on the number of bands they capture viz, PSScene Supported Assets, PSScene3Band Supported Assets, PSScene4Band Supported Assets, and PSOrthoTile Supported Assets. Among them, the most useful type is the PSScene4Band Supported Assets which contain 4 bands, BGR and Near-IR necessary for water index calculations (Tab. 2). This asset consists of orthorectified products providing both TOA (Analytic Radiance) and BOA (Surface Reflectance) reflectance (Planet

Labs, n.d.-d). However, due to technical issues in computation of NDWI, Analytic Radiance (TOA reflectance) products were used instead of Surface Reflectance (BOA reflectance) products.

Table 4: Comparison of Bands, Central Wavelengths, and Resolutions between Sentinel 2 (Satellite Imaging Corporation, n.d.) and Planetscope products (Sentinelhub, n.d.)

Sentinel-2 12 Bands (L2A and L1C products)			**Planetscope Scene 4 Bands (Analytic Radiance and Surface reflectance Products)**		
Bands available	**Central Wavelength (µm)**	**Resolution (m)**	**Bands available**	**Central Wavelength (µm)**	**Resolution (m)**
Band 1 – Coastal aerosol	0.443	60			
Band 2 – Blue	0.490	10	Band 1 – Blue	0.490	3m
Band 3 – Green	0.560	10	Band 2 – Green	0.566	3m
Band 4 – Red	0.665	10	Band 3 – Red	0.665	3m
Band 5 – Vegetation Red Edge	0.705	20			
Band 6 – Vegetation Red Edge	0.740	20			
Band 7 – Vegetation Red Edge	0.783	20			
Band 8 – NIR	0.842	10	Band 4 – Near Infrared	0.865	3m
Band 8A – Vegetation Red Edge	0.865	20			
Band 9 – Water vapour	0.945	60			
Band 10 – SWIR – Cirrus	1.375	60			
Band 11 - SWIR	1.610	20			
Band 12 - SWIR	2.190	20			

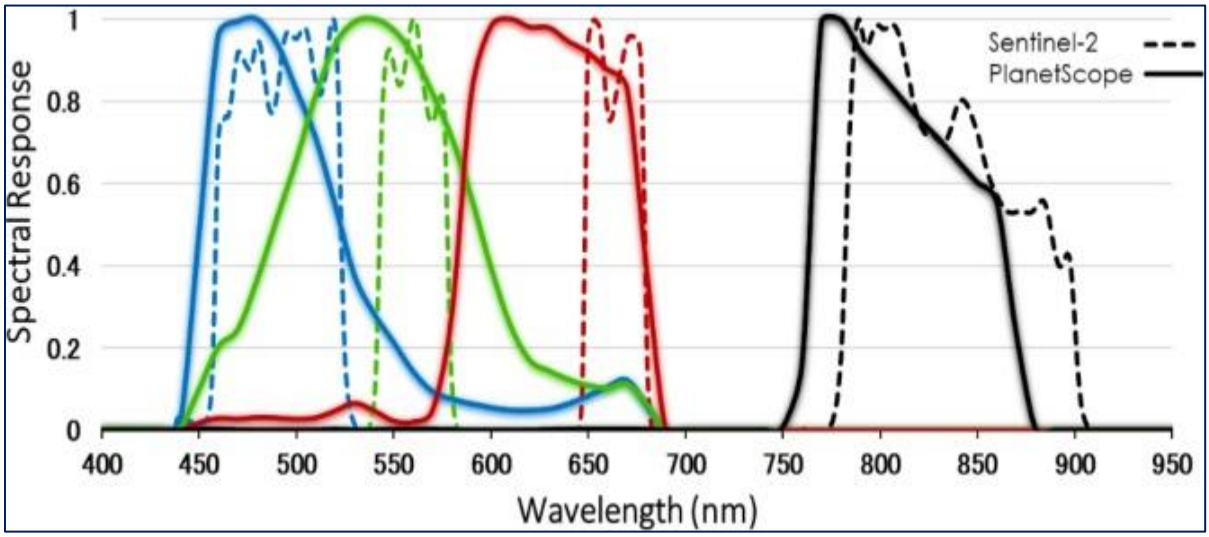

Figure 6: Spectral signatures of Planetscope and Sentinel 2 in blue, green, red, and infrared bands (Sadeh et al., 2021)

2.2.1.2 Image preprocessing and sub-setting

Multi-spectral multi-temporal image analysis may require image with true surface reflectance or BOA reflectance to compare the actual changes in different time frames. However, the images acquired from the satellite services are not necessarily preprocessed as required to meet the objective of the project. These images may have some radiometric and geometric distortions

which need to be corrected before proceeding to image analysis. Radiometric distortions involve effects on image due to sensor's sensitivity, sun angle, topography, and atmospheric scattering whereas geometric distortions involve inconsistency in coordinates of the image to actual point on the ground (Bashiri et al., 2021; ESA, n.d.-a).

The S2 Level-2A product readily provides BOA reflectance and are geometrically corrected, but, initially, they are acquired with DN values which needs to be converted to reflectance values through preprocessing tool under Semi-Automatic Classification Plugin in QGIS (ESA, 2013). It also involves haze correction through DOS method.

The surface reflectance product from Planet Lab is atmospherically corrected, orthorectified and is calibrated to BOA reflectance (Planet Labs, n.d.-d) but, due to technical issues, Analytic Radiance products are used which are also orthorectified but are not atmospherically corrected. To avoid the effect of atmospheric interference, the PS images were acquired for those days with very little or no cloud coverage.

S2 imageries are downloaded in layers of size 100 * 100 km^2 so, they are clipped to the extent of each glacial lakes for further processing while the PS imageries are possible to be downloaded directly to the extent of each glacial lakes.

2.2.1.2.1 Dark Object Subtraction (DOS) method

Dark Object Subtraction (DOS) method is a simple and commonly used technique in remote sensing for atmospheric correction. It is specifically effective in haze correction. The electromagnetic signals coming from the ground to the remote sensing satellite sensors are either scattered or absorbed by different gases and aerosols present in the atmosphere. Because of such phenomena, the sensors cannot detect the true reflectance value of the Earth's surface. DOS method assumes the presence of "dark objects" having significantly less to zero reflectance values in a satellite imagery and the reflectance from these objects is due to a considerable part of atmospheric scattering. Therefore, these "dark objects", at first, are identified in the imagery and their reflectance values are subtracted from every pixel in each band removing the scattering effect. The DOS method is therefore important in multispectral multi-temporal image analysis (Gilmore, Saleem, & Dewan, 2015; Song, Woodcock, Seto, Lenney, & Macomber, 2001).

2.2.2 Glacial lakes outline mapping method

The outline mapping method initiates with computation of NDWI for scenes including the glacial lakes. Outlines of test lakes using different threshold values of NDWI are compared with manually digitized outlines of the same lakes on orthophoto taken on 16.09.2017. A suitable threshold value is then selected which increases the chance of including maximum possible water pixel as well as reduce the need for manual correction at places where the water pixels are not distinguished with neighboring landcovers (ice, barren soil, vegetation, etc.) pixels. Lakes selected for testing the suitable threshold are the same selected by (Nagy & Andreassen, 2019) for Sentinel imageries (Fig.s 1; 8; 9). The same lakes were selected for testing thresholds in PS imageries.

2.2.2.1 Normalized Difference Water Index (NDWI)

Water has the highest reflectance in green band and the highest absorption in NIR band making it a distinct spectral signature and very easy to detect. Therefore, this signature can be used in the form of index to specify and delineate water bodies (Karabulut & Ceylan, 2005).

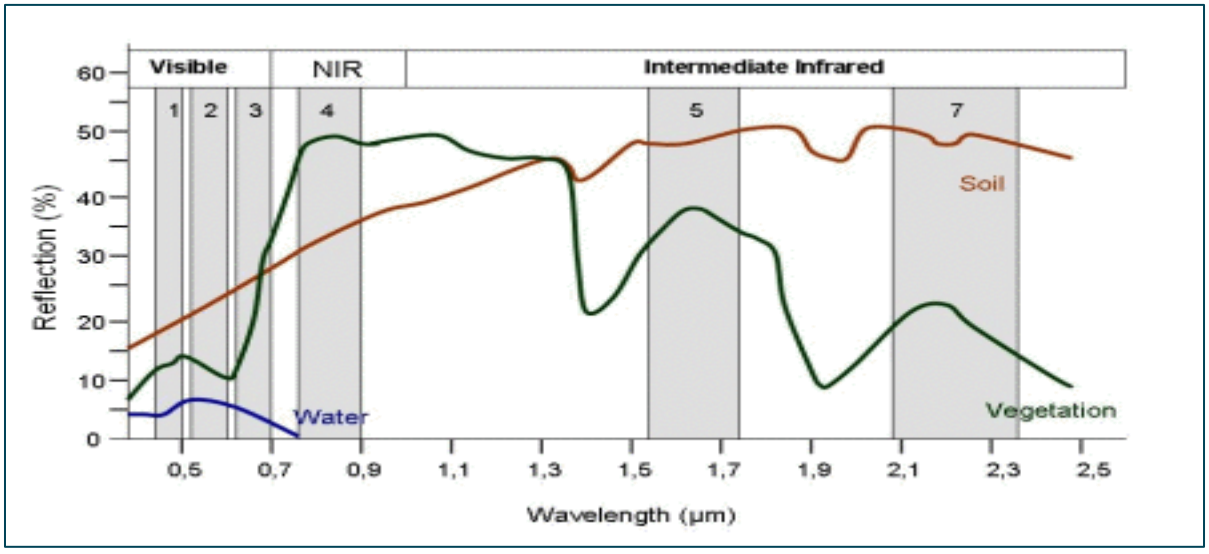

Figure 7: Spectral Reflectance Curve (Seos Project, n.d.)

A commonly used Normalized Difference Water Index (NDWI) proposed by (McFeeters, 2007) is thus used in this study.

NDWI = (Green – NIR)/(Green + NIR) ……. Eq (1)

For S2 imageries, green band corresponds to band 3 and NIR band corresponds to band 8 so

the equation (2) was used, whereas for PS imageries, green band corresponds to band 2 and NIR band corresponds to band 4, so the equation (3) was used for NDWI calculations.

NDWI = (Band 3 – Band 8)/(Band 3 + Band 8) ……. Equation (1) for S2 imageries

NDWI = (Band 2 – Band 4)/(Band 2 + Band 4) ……. Equation (2) for PS imageries

The NDWI value range from -1 to 1. The higher values represent water bodies, but it may vary based on various factors such as turbidity, sediments flowing in the water, depth of water, and underwater surface features. Reflectance is high for turbid water bodies (Nagy & Andreassen, 2019). However, in this study, it ranges from 0.23 and above in S2, and from 0.38 and above in PS.

2.2.2.2 Thresholding

A threshold NDWI of 0.23 for S2 imageries used by (Nagy & Andreassen, 2019) was tested again and was assured to be the most suitable threshold for glacial lakes outline mapping around Jostedalsbreen. The same procedure was applied to PS imageries at the same test lakes for new threshold and, hence a suitable threshold of 0.38 was obtained for PS imageries.

Table 5: Thresholding NDWI value for test lakes in Jostedalsbreen in PS scenes

Lake	Lake Type	Area (km^2) Orthophoto	T0.38(km^2)	%	T0.39(km^2)	%	T0.40(km^2)	%
L46	2	0.2761	0.2767	100.2	0.2740	99.2	0.2713	98.2
L47	1	0.1328	0.1304	98.2	0.1288	97.1	0.1275	96.0
L48	2	0.0218	0.0217	99.7	0.0212	97.0	0.0205	93.9
L49	2	0.0165	0.0139	84.6	0.0137	83.2	0.0131	79.8
L50	2	0.0187	0.0172	91.7	0.0168	89.8	0.0166	88.6
L52	2	0.0609	0.0586	96.2	0.0568	93.2	0.0560	92.0
L2	3	0.0333	0.0318	95.6	0.0315	94.5	0.0310	93.2
L1	2	0.0077	0.0069	90.4	0.0065	85.2	0.0061	79.7
L19	4	0.0080	0.0075	94.0	0.0071	89.2	0.0067	84.2
Total		**0.5758**	**0.5649**	**98.1**	**0.5565**	**96.6**	**0.5489**	**95.3**

According to the calculated thresholds for both types of images, 0.23T for S2 imageries represents 96.25% accuracy whereas 0.38T for PS imageries represents 98.1% accuracy to represent the water bodies. Therefore, an addition of 3.75% and 1.70% is recommended for outlines calculated from both S2 and PS images respectively.

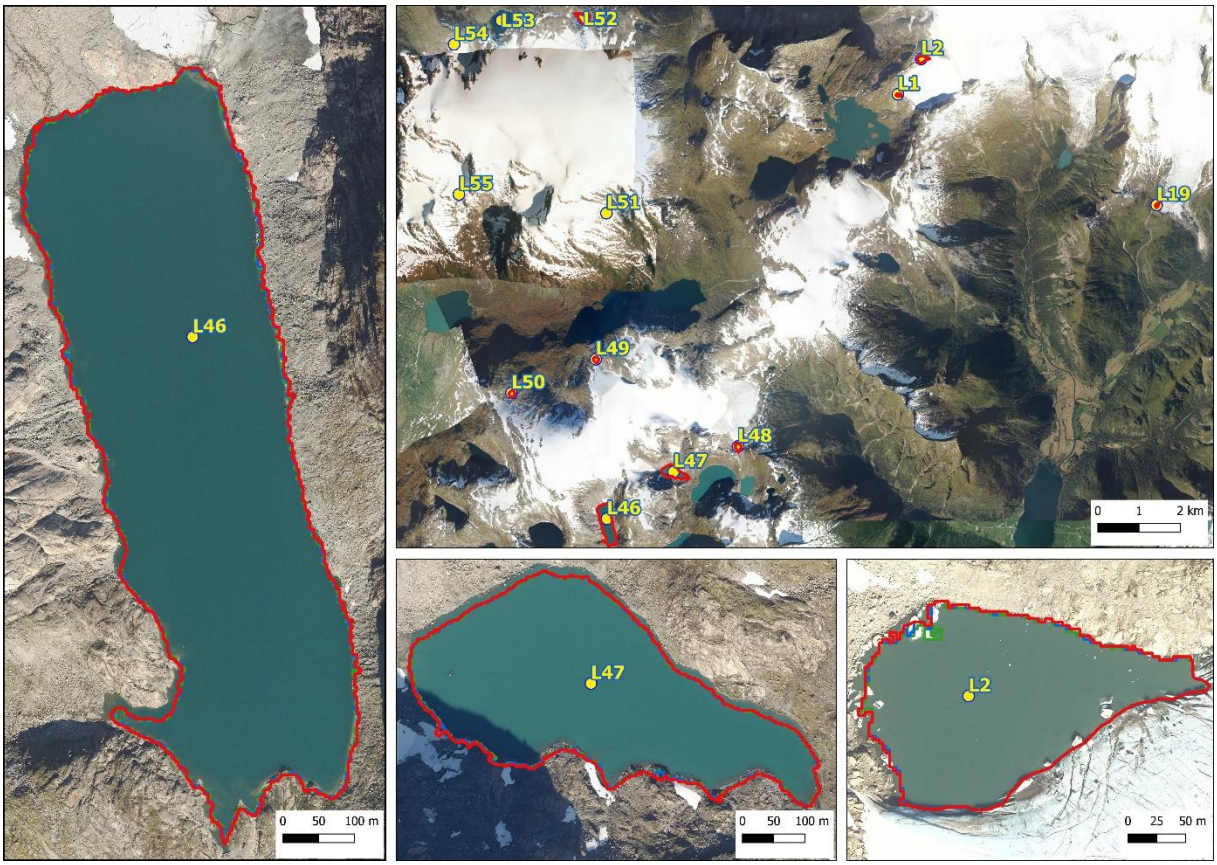

Figure 8: Thresholding on lakes (L46, L47 and L2 (GID: 2364) in test site while using PS imageries (Red: T0.38, Blue: T0.39 and Green: T0.40)

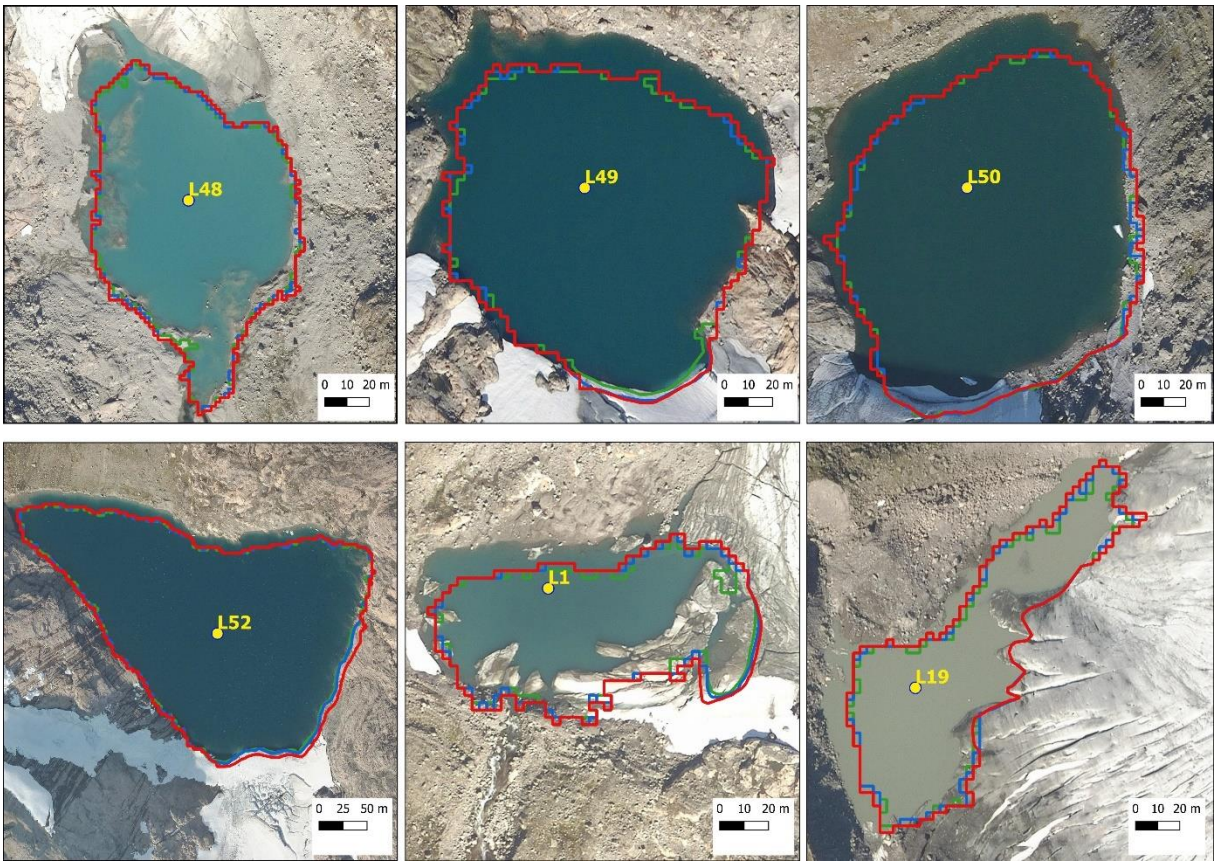

Figure 9: Thresholding on lakes (L1 (GID: 2364), L19 (GID: 2352), L48 (GID: 2145), L49 (GID: 2142), L50 (GID: 3848), and L52 (GID: 2119) in test site while using PS imageries (Red: T0.38, Blue: T0.39 and Green: T0.40)

Yet having high resolution, the positional accuracy of PS imageries with orthoimagery was poor. However, this discrepancy does not affect the study as our study deals with percentage representation of lake area using S2 and PS imageries, in which the PS imagery proves to be slightly better than S2. As expected, test lakes connected with glacier faced the problem of misclassification which was corrected manually and carefully to minimize biasness in representing the true water pixels.

2.2.2.3 Manual Digitization

Semi-automatic classification and thresholding is often challenging, especially in places where the adjacent classes are closely related in terms of spectral reflectance values. These spectrally adjacent classes while being close to each other may show similar spectral property, hence hampering the classification. For instance, in the study site, reflectance values of terrain ranges below -0.60, snow ranges from 0.03 to 0.07, ice ranges from 0.09 to 0.23, and water ranges above 0.23 (Nagy & Andreassen, 2019). Terrain and water classes are easily distinguishable as they fall far away from their spectral ranges, but water and ice have adjacent spectral ranges,

so they are misclassified even with our best suitable threshold value (Fig. 10). Therefore, in most water-ice interface areas, manual digitization was needed to achieve the lake outline. Natural and false color images of the lakes were used for digitization in those areas. In addition to partial digitization, few lakes were digitized for complete outlines where the thresholding was not functional but the natural color image with full visibility was available.

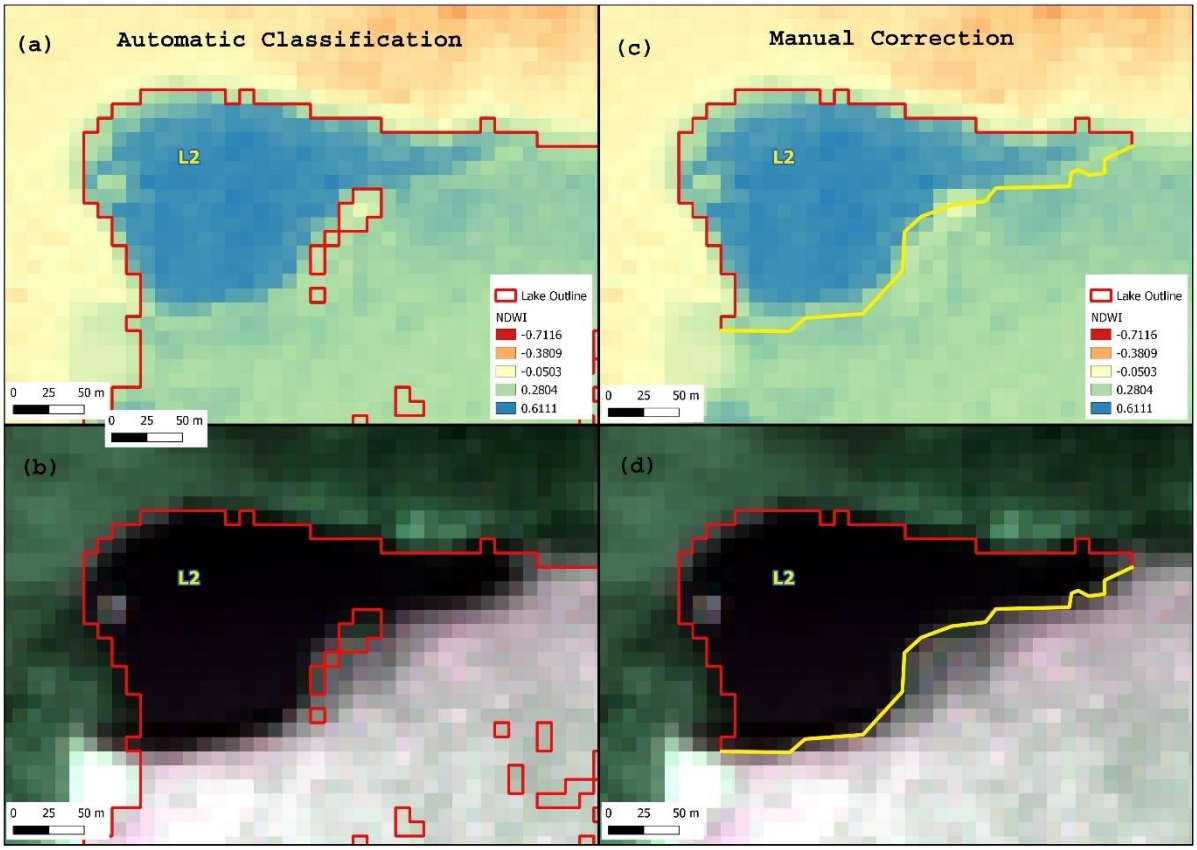

Figure 10: Misclassification of water pixel and manual correction using natural colour imagery as a background. Fig. (a) shows automatic classification of pixels and threshold of 0.23 used to delineate glacial lake but it also includes ice pixels as seen in Fig. (b). Fig. (c) shows manually corrected lake outline (yellow-highlighted line) to exclude ice pixels with the help of natural colour imagery in Fig. (d)

2.2.3 Temporal analysis of glacial lakes outlines

In line with the objective of the study, a time series of outlines of 51 glacial lakes starting from 2016 until 2021 were calculated. Each image per month were selected for 5 months for each year, starting from July to November, which corresponds to melting season in a year. However, due to unfavorable cloud conditions and unavailability of imageries in S2, the series discontinues in certain months. The gaps in the series, to some extent, were fulfilled from corresponding PS imageries.

2.2.3.1 Assessment of change in month-to-month surface area of glacial lakes to detect GLOF events

As mentioned earlier, GLOF events are sudden events (sometimes cyclic) which may take a few hours to days. However, it takes some time to refill the lake, so the variation seen in month-to-month scenes are further investigated with more scenes in between to verify the GLOF events.

2.2.3.2 Absolute monthly surface area of lake/lake types and annual and overall (6 years) variation expressed in terms of absolute SD

Annual variation in absolute surface area of lakes obtained in month-to-month basis in each melting season each year was computed in terms of Standard Deviation (SD). In addition, overall variation in terms of SD in 6 years was also computed. Besides bad cloud condition, casting shadows, and unavailability of images, some lakes were completely frozen at some point of time, so images with lake outlines only fully visible were included to compute the SD.

2.2.3.3 Normalized monthly surface area of lake/lake types and annual and overall (6 years) variation expressed in terms of percentage SD

Since the selected lakes for this study are different in size and are categorized into 6 types based on their nature of connection with the glacier and the way they are dammed, the variation in their surface area could be largely different so to compare between lakes, the data (month-to-month surface area) were normalized based on the median surface area of initial year (2016) making it 100%, and the lakes are ranked based on the SD of percentage change in lake area. Some lakes did not have data for the year 2016 so, the subsequent year with available data was taken as a base for normalization.

Since the lake types 3 (*Glacier-dammed*), 4 (*Moraine-dammed*) and 5 (*Artificial-water-level-regulation*) have very few lakes, they do not provide significant SD to make comparisons with others. So, lake types 1 (*Not-connected-to-glacier*), and 2 (*Connected-to-glacier*) were taken for Mann Whitney U test (Wilcoxon Rank Sum Test) to test if their SDs are significantly different from each other.

Mann Whitney U test (Wilcoxon Rank Sum Test) is a non-parametric test used to compare between two independently sampled groups and test if they are statistically significantly

different from each other (MacFarland & Yates, 2016; McKnight & Najab, 2010). Since the lakes in types 1 (*Not-connected-to-glacier*), and 2 (*Connected-to-glacier*) are independent from each other, and their calculated surface area do not follow a normal distribution, Mann Whitney U test was suitable to check if they show similar or different types of variation in their surface area.

2.2.3.4 Absolute annual maximum surface area of lake/lake types and overall (6 years) variation expressed in terms of absolute SD

Maximum surface area of glacial lakes is critical to potential outburst, so overall (6 years) variation (SD) of annual maximum surface area of 51 lakes was also computed and ranked accordingly.

2.2.3.5 Normalized annual maximum surface area of lake/lake types and overall (6 years) variation expressed in terms of percentage SD

To make comparison between lakes, the data was normalized again based on the maximum surface area of initial year (2016) making it 100%. The lakes were again ranked based on the SD of percentage change in maximum lake area.

As mentioned in section 2.2.3.3, Mann Whitney U test (Wilcoxon Rank Sum Test) was performed again between lake types 1 (*Not-connected-to-glacier*), and 2 (*Connected-to-glacier*) to test if their % SDs are significantly different from each other.

2.2.3.6 Time series of mean of annual maximum surface area of each lake types for each year

The lakes were grouped in separately based on their types and mean of annual maximum surface area of each lake types was computed for each year to form a time series. The same process was repeated for normalized annual maximum surface area for each lake types and represented graphically.

2.2.4 Usefulness of satellite imageries

Amid geographical remoteness and difficulty in accessibility of glacial lakes, remote sensing has no doubt become the most useful technique to continuously study such sites. Subsequent improvements in spatial and temporal resolutions of remote sensing systems have made it possible for the researchers to investigate finer scale details in earth observation. In this context,

the images freely provided by S2 mission have played vital role to achieve the objective of this study. Despite unfavorable cloud cover in the sites of interest, acquisition of useable images in an interval of around one month was possible for most of the lakes. PS images, however having limited access to the students (5000 km^2 per month download permission), was useful to fill up the gaps in the series. Altogether 826 useable images were obtained out of 1479, with the highest number of images in 2019 (168) and the lowest number of images in 2017 (118). Meanwhile, most of the images were obtained in August (272), September (228) and July (207) whereas in October (101) and November (18), there were considerably lesser number of images, so the SD calculated for each lake is influenced mostly by outline measurements in consecutive core melting months - July, August, and September. A median of 16 useable images were obtained per lake in 6 years with almost 3 images per year, most of which belonging to July, August, and September. Therefore, the available images were not sufficient to make a seasonal time series analysis in each year. However, it was enough to see the lake area fluctuations in core melting months through SD and perhaps, make a complete annual time series of maximum recorded surface area to observe the trend annually.

3 RESULTS

3.1 Glacial lakes area change

Generally, in Norway, the glacier melting season starts from May until September. However, most glacial lakes in the study area were clearly opened in July and remained open until November throughout the time frame (2016-2021) chosen, so the inventory was started from the month of July until November. During the melting season, the lakes generally expand in size, but it might also drain out slowly or rapidly depending on the type and geomorphology of its damming structure. Therefore, to observe these changes satellite images of 51 lakes were analyzed on a month-to-month basis in melting season from 2016 to 2021.

3.1.1 Reduction in surface area of glacial lakes indicative of GLOF events

The month-to-month changes in surface area of lakes were recorded from the inventory which showed both positive and negative changes. Some lakes also remained unchanged during certain timeframes. However, the negative changes observed in surface area alone was not enough to declare the GLOF events because the reduction in surface area might be because of ice cover developed at the margin of the lakes. This generally happens at the end of melting season and was also observed in the study area. Therefore, to verify the actual GLOF events, each image was carefully observed in natural color images in both Sentinel and PS imageries. PS imageries were more useful in such case as they have finer spatial (3 m) resolution. Nevertheless, no rapid drainage events indicative of GLOF events were found after scrutinizing month-to-month imageries of each lake. There were obviously some considerable numbers of lakes which were reduced in size, but they were not completely drained out. Those lakes which showed considerably higher reduction in surface area in our month-to-month inventory were re-examined with higher frequency of imageries in between the two consecutive months to check if any significant drainage incidents were missed. After examination of all possible lake candidates, it was found that no lakes out of 51 lakes in the study area were drained out completely or significantly highly enough to declare as GLOF events.

The summary of normalized surface area with respect to median surface area (i.e., 100 %) of each lake in the initial year (2016) is presented in the Tab.s 6 and 7. The Tab.s 6 and 7 show both positive and negative changes in surface area of 51 lakes compared to the last available month and it is presented under normalized surface area of each month. The negative changes

in % are highlighted in yellow. The Tab. 6 contains details of lake type 1 (*not-connected-to-glacier*), 3 (*glacier-dammed*), 4 (*moraine-dammed*) and 5 (*artificial-water-level-regulation*) whereas the Tab. 7 contains details of lake type 2 (*connected-to-glacier*).

Table 6: Normalized surface area of glacial lakes (in %) with respect to median surface area of 2016 and their month-to-month changes in surface area for lake type 1 (not-connected-to-glacier), 3 (glacier-dammed), 4 (moraine-dammed), and 5 (artificial-water-level-regulation)

Lake Type	Lake	Description	2016-07-23	2016-08-22	2016-09-04	2016-10-11	2016-11-03	2017-07-20	2017-08-22	2017-09-16	2017-10-09	2017-11-02	2018-07-26	2018-08-14	2018-10-01	2018-10-26	2018-11-20	2019-07-28	2019-08-27	2019-09-24	2019-10-06	2019-11-05	2020-07-25	2020-08-26	2020-09-25	2020-10-15	2021-07-25	2021-08-26	2021-09-13	2021-10-17	2021-11-04
1	L6	Area (%)	35	100	106	NA	NA	NA	93	93	NA	NA	106	110	NA	NA	NA	121	128	NA	NA	NA	15	91	92	92	111	108	117	NA	NA
		Change (%)		65	6					0				4					6					76	0	0		-3	9		
1	L7	Area (%)	62	110	117	90	NA	NA	84	127	48	NA	122	132	NA	NA	NA	120	85	NA	NA	NA	NA	101	92	141	145	158	143	NA	NA
		Change (%)		48	7	-27				43	-80			11					-35						-8	49		13	-15		
1	L11	Area (%)	NA	100	87	114	NA	106	99	99	NA	NA	100	100	106	NA	NA	107	106	89	NA	NA	102	84	96	100	99	101	NA	NA	NA
		Change (%)			-13	27			-7	0				0	6				-1	-18				-18	12	4		1			
1	L24	Area (%)	NA	NA	NA	NA	NA	NA	NA	NA	NA	NA	15	185	NA	NA	NA	62	163	83	NA	NA	NA	NA	NA	25	9	183	221	NA	NA
		Change (%)												171					101	-80								174	38		
1	L29	Area (%)	72	112	100	NA	NA	NA	30	91	NA	NA	151	148	148	NA	NA	137	141	128	NA	NA	NA	79	81	NA	141	140	139	NA	NA
		Change (%)		40	-12					60				-3	0				4	-13					2			-1	-1		
1	L30	Area (%)	88	112	NA	NA	NA	NA	106	NA	NA	NA	105	123	75	NA	NA	115	NA	113	NA	NA	48	NA	NA	NA	105	118	NA	NA	NA
		Change (%)		25										18	-48													13			
1	L31	Area (%)	NA	NA	NA	NA	NA	NA	NA	NA	NA	NA	11	189	NA	NA	NA	74	185	119	NA	NA	NA	NA	NA	NA	6	160	174	NA	NA
		Change (%)												178					110	-66								155	14		
1	L36	Area (%)	NA	100	100	94	NA	NA	95	97	92	NA	102	104	NA	NA	NA	101	102	97	92	NA	NA	NA	93	95	102	101	102	101	NA
		Change (%)			0	-6				2	-5			2					1	-5	-5					2		-2	1	-1	
1	L42	Area (%)	NA	100	NA	NA	NA	NA	149	123	NA	NA	114	197	NA	NA	NA	120	121	159	NA	NA	20	NA	NA	NA	126	143	132	NA	NA
		Change (%)								-25				83					1	38								17	-12		
1	L43	Area (%)	8	103	NA	100	NA	NA	42	90	87	NA	104	101	127	NA	NA	89	134	75	75	NA	NA	21	107	81	102	97	95	NA	NA
		Change (%)		96						48	-3			-3	26				46	-59	0				85	-26		-5	-1		
1	L46	Area (%)	NA	100	102	98	NA	NA	100	100	NA	NA	104	107	NA	NA	NA	104	104	105	100	94	NA	NA	100	97	103	103	102	106	102
		Change (%)			2	-4				-1				3					0	1	-4	-6				-3		0	-1	4	-4
1	L47	Area (%)	NA	96	100	101	NA	NA	93	96	NA	NA	101	104	NA	NA	NA	100	101	101	103	NA	NA	NA	94	99	97	96	97	NA	NA
		Change (%)			4	1				4				3					1	0	2					6		-1	1		
1	L51	Area (%)	NA	101	100	NA	0	NA	92	93	NA	NA	109	111	NA	NA	NA	107	107	100	92	NA	NA	88	93	96	106	104	104	NA	NA
		Change (%)			-1					1				2					0	-8	-7				5	3		-1	0		
1	L57	Area (%)	102	101	99	99	NA	NA	99	97	86	NA	101	102	NA	NA	NA	103	95	86	75	NA	NA	99	97	NA	101	99	98	NA	NA
		Change (%)		-1	-2	0				-2	-12			1					-8	-9	-11				-2			-2	-1		
3	L2	Area (%)	NA	101	99	NA	NA	88	85	59	NA	NA	86	89	63	NA	NA	88	55	NA	NA	NA	72	55	45	47	66	57	58	NA	NA
		Change (%)			-1				-4	-25				3	-26				-33					-17	-10	2		-9	1		
3	L58b	Area (%)	NA	NA	70	130	NA	NA	77	121	143	NA	145	150	NA	NA	NA	149	154	151	150	NA	NA	NA	NA	NA	NA	165	161	150	NA
		Change (%)				60				44	22			4					6	-3	-1								-4	-10	
4	L19	Area (%)	51	100	105	NA	NA	NA	64	NA	NA	NA	128	141	177	NA	NA	179	197	140	NA	NA	NA	112	140	118	173	144	92	NA	NA
		Change (%)		49	5									14	36				18	-57					27	-22		-29	-52		
5	L14	Area (%)	NA	98	NA	102	NA	NA	88	89	NA	NA	103	103	NA	NA	NA	101	103	103	NA	NA	NA	NA	NA	103	97	101	104	NA	NA
		Change (%)								1				0					2	0								4	3		
5	L15	Area (%)	NA	NA	99	101	NA	88	99	99	NA	NA	86	92	97	102	104	95	NA	97	98	97	NA	103	NA	104	84	88	91	NA	NA
		Change (%)				2			11	0				6	5	5	2				1	-1						5	3		

Note: Lakes belonging to type 1 (Not-connected-to-glacier), type 3 (Glacier-dammed), type 4 (Moraine-dammed), and type 5 (Artificial-water-level-regulation) are included in this table. The yellow highlighted numbers represent the reduction in surface area as compared to that of last available month.

Table 7: Normalized surface area of glacial lakes (in %) with respect to median surface area of 2016 and their month-to-month changes in surface area for lake type 2 (connected-to-glacier)

Lake Type	Lake	Description	2016-07-23	2016-08-22	2016-09-04	2016-10-11	2016-11-03	2017-07-20	2017-08-22	2017-09-16	2017-10-09	2017-11-02	2018-07-26	2018-08-14	2018-10-01	2018-10-26	2018-11-20	2019-07-28	2019-08-27	2019-09-24	2019-10-06	2019-11-05	2020-07-25	2020-08-26	2020-09-25	2020-10-15	2021-07-25	2021-08-26	2021-09-13	2021-10-17	2021-11-04
2	L1	Area (%)	71	105	100	NA	NA	NA	125	178	240	NA	136	396	798	NA	NA	278	666	521	394	NA	NA	86	182	103	139	296	408	NA	NA
		Change (%)		34	-5					52	62			260	402				388	-146	-126				95	-78		157	112		
2	L3	Area (%)	52	105	103	97	NA	NA	108	106	NA	NA	108	112	119	NA	NA	115	114	111	107	NA	NA	103	109	107	109	113	109	NA	110
		Change (%)		53	-2	-6				-2				4	6				0	-3	-4				5	-1		5	-4		
2	L4a	Area (%)	100	102	NA	100	NA	NA	104	100	100	NA	109	111	98	NA	NA	110	109	110	105	NA	63	111	105	112	112	111	104	NA	105
		Change (%)		2						-3	0			2	-12				-2	2	-5			48	-6	7		-1	-7		
2	L4b	Area (%)	93	100	100	122	NA	NA	96	90	94	NA	106	108	114	NA	NA	106	105	98	84	NA	89	99	98	103	104	105	103	NA	95
		Change (%)		7	0	22				-7	4			2	6				-1	-7	-14			10	-1	5		2	-2		
2	L5	Area (%)	80	100	102	NA	NA	NA	74	83	NA	NA	90	98	NA	NA	NA	133	144	NA	NA	NA	82	117	99	113	129	135	NA	NA	NA
		Change (%)		20	2					10				9					11					35	-18	14		6			
2	L9	Area (%)	NA	96	104	NA	NA	NA	68	109	NA	NA	114	137	141	NA	NA	116	153	148	NA	NA	NA	122	127	NA	141	164	166	NA	NA
		Change (%)			8					41				23	4				37	-5					5			23	2		
2	L10	Area (%)	96	100	NA	101	NA	103	104	NA	NA	NA	105	106	107	NA	NA	107	106	105	102	NA	102	106	105	NA	105	105	101	NA	NA
		Change (%)		4					1					0	1				-1	-1	-3			4	0			0	-4		
2	L12	Area (%)	74	103	NA	100	NA	NA	109	117	NA	NA	117	146	155	NA	NA	175	161	175	NA	NA	34	197	252	215	216	216	266	NA	NA
		Change (%)		29						8				29	8				-14	14				163	55	-37		0	51		
2	L13	Area (%)	21	179	NA	NA	NA	NA	85	135	NA	NA	443	593	900	NA	NA	550	999	NA	NA	NA	NA	NA	NA	NA	626	1019	1520	NA	NA
		Change (%)		157						49				151	307				448									393	501		
2	L17	Area (%)	100	100	101	91	NA	110	106	104	98	NA	118	117	105	NA	NA	130	128	123	113	NA	123	123	124	122	131	131	114	NA	NA
		Change (%)		-1	1	-10			-4	-2	-6			-1	-12				-2	-5	-10			0	1	-1		0	-18		
2	L18	Area (%)	110	74	153	90	NA	341	204	196	76	NA	429	409	477	NA	NA	502	548	520	335	430	530	559	592	494	728	711	673	NA	718
		Change (%)		-37	79	-63			-138	-7	-120			-20	68				46	-29	-184	94		30	33	-98		-17	-37		
2	L22	Area (%)	NA	92	108	NA	NA	NA	126	NA	NA	NA	311	267	NA	NA	NA	378	345	NA	NA	NA	NA	NA	NA	NA	NA	139	295	NA	NA
		Change (%)			16									-44					-32										157		
2	L23	Area (%)	NA	NA	NA	NA	NA	18	193	83	NA	117	133	773	1228	NA	NA	NA	2056	NA	NA	NA	NA	NA	NA	NA	NA	1444	3453	NA	NA
		Change (%)							175	-110				640	455														2009		
2	L25	Area (%)	NA	87	113	NA	NA	NA	NA	103	NA	NA	131	134	NA	NA	NA	173	176	139	NA	NA	161	183	138	132	149	156	173	NA	NA
		Change (%)			25									4					3	-37				22	-45	-7		7	16		
2	L34	Area (%)	NA	51	149	NA	NA	NA	98	128	NA	NA	201	284	2112	NA	487	287	1163	NA	NA	NA	57	63	299	352	209	540	987	NA	NA
		Change (%)			98					29				83	1828				876					6	236	53		331	447		
2	L35	Area (%)	35	100	111	NA	NA	NA	49	70	NA	NA	259	338	NA	NA	NA	294	284	243	NA	NA	NA	224	178	219	278	284	304	NA	NA
		Change (%)		65	11					22				78					-10	-41					-46	41		5	20		
2	L37	Area (%)	20	106	100	NA	NA	NA	87	110	NA	NA	107	190	NA	NA	NA	137	203	103	NA	NA	NA	10	NA	NA	103	180	177	221	NA
		Change (%)		86	-6					23				83					67	-100								77	-3	44	
2	L38	Area (%)	50	100	108	NA	NA	NA	59	96	NA	NA	124	152	NA	NA	NA	54	56	40	NA	NA	NA	NA	42	NA	33	27	27	NA	NA
		Change (%)		50	8					37				28					2	-17								-6	0		
2	L40	Area (%)	100	NA	NA	NA	NA	43	157	NA	NA	NA	298	352	143	NA	NA	35	16	NA	NA	NA	NA	NA	NA	NA	5	NA	11	NA	NA
		Change (%)							113					55	-210				-19												
2	L41	Area (%)	100	NA	NA	NA	NA	81	425	471	NA	NA	703	695	749	NA	NA	761	829	NA	NA	NA	304	541	645	NA	955	873	949	NA	NA
		Change (%)							344	46				-7	54				69					238	103			-82	77		
2	L44	Area (%)	100	NA	NA	NA	NA	NA	105	NA	98	NA	111	106	113	NA	NA	110	110	104	92	NA	NA	106	NA	NA	112	109	111	NA	NA
		Change (%)												-5	7				0	-6	-12							-3	2		
2	L45	Area (%)	NA	100	NA	NA	NA	NA	28	25	NA	NA	130	160	205	NA	NA	24	186	164	NA	NA	NA	NA	62	NA	55	169	202	NA	NA
		Change (%)								-3				31	45				162	-22								114	32		
2	L48	Area (%)	6	100	113	NA	NA	NA	108	117	NA	NA	140	132	NA	NA	NA	134	137	127	106	NA	NA	20	114	119	137	134	132	NA	NA
		Change (%)		94	13					9				-8					3	-10	-21				94	5		-4	-1		
2	L49	Area (%)	57	100	134	NA	NA	NA	102	140	NA	NA	134	174	NA	NA	NA	185	180	191	144	NA	NA	83	130	166	166	181	179	NA	NA
		Change (%)		43	34					38				40					-5	11	-48				47	36		15	-3		
2	L50	Area (%)	NA	111	89	NA	NA	NA	113	89	NA	NA	101	122	NA	NA	NA	106	116	114	97	NA	NA	94	95	108	100	114	117	NA	NA
		Change (%)			-22					-24				21					10	-2	-17				1	13		14	3		
2	L52	Area (%)	99	100	104	125	NA	122	109	114	NA	NA	107	119	132	NA	NA	112	109	117	117	NA	NA	112	118	116	106	109	107	NA	NA
		Change (%)		1	4	21			-13	5				12	13				-3	8	1				6	-2		3	-1		
2	L53	Area (%)	99	101	NA	103	NA	100	100	NA	105	NA	104	105	106	NA	NA	101	102	105	106	101	102	100	105	105	101	101	103	NA	104
		Change (%)		1					0					1	1				0	3	1	-4		-1	5	0		0	2		
2	L54	Area (%)	52	148	150	NA	0	42	255	266	NA	NA	258	350	446	NA	NA	373	404	243	NA	NA	27	64	58	613	574	515	547	NA	NA
		Change (%)		95	2				213	11				93	96				31	-161				37	-6	555		-59	32		
2	L55	Area (%)	NA	100	135	NA	0	NA	50	439	NA	NA	490	643	NA	NA	NA	756	904	963	1078	NA	NA	1258	1248	1260	967	1400	1437	NA	NA
		Change (%)			35					388				153					148	59	116				-9	12		433	37		
2	L56	Area (%)	64	96	108	104	NA	50	109	112	NA	NA	126	127	NA	NA	NA	136	NA	143	129	NA	NA	137	138	1053	161	158	159	NA	NA
		Change (%)		32	11	-4			59	3				1							-13				0	915		-3	1		
2	L58a	Area (%)	NA	NA	100	100	NA	NA	102	100	108	NA	107	118	NA	NA	NA	109	109	105	109	NA	NA	NA	NA	NA	NA	108	117	93	NA
		Change (%)				-1				-2	8			11					0	-4	4								8	-24	
2	L58c	Area (%)	NA	NA	101	99	NA	NA	102	107	98	NA	111	112	NA	NA	NA	115	116	118	106	NA	NA	NA	NA	110	111	120	117	114	NA
		Change (%)				-1				5	-9			1					0	2	-12							10	-3	-3	

Note: Lakes belonging to type 2 (Connected-to-glacier) are included in this table. The yellow highlighted numbers represent reduction in surface area as compared to that of last availble month

The Fig 9 shows outlines of lake L2 (*GID: 2364*) (*glacier-dammed*) and lake L19 (*GID: 2352*) (*moraine-dammed*) in both NDWI and natural colour images indicating the reduction in surface area in considerable amount in consecutive months. In case of L19, reduction in surface area was more evident in 2019 (Fig. 11c), 2020 (Fig. 11d), and 2021 (Fig. 11e). The reduction was comparatively huge in 2021 in two months' time interval from 173 % to 92 % (Tab. 6; Fig. 11e). However, the careful examination of intermediate images showed a gradual reduction, so it was not a candidate for GLOF. The situation was similar for L2 (*GID: 2364*) (Fig.s 11a; 11b).

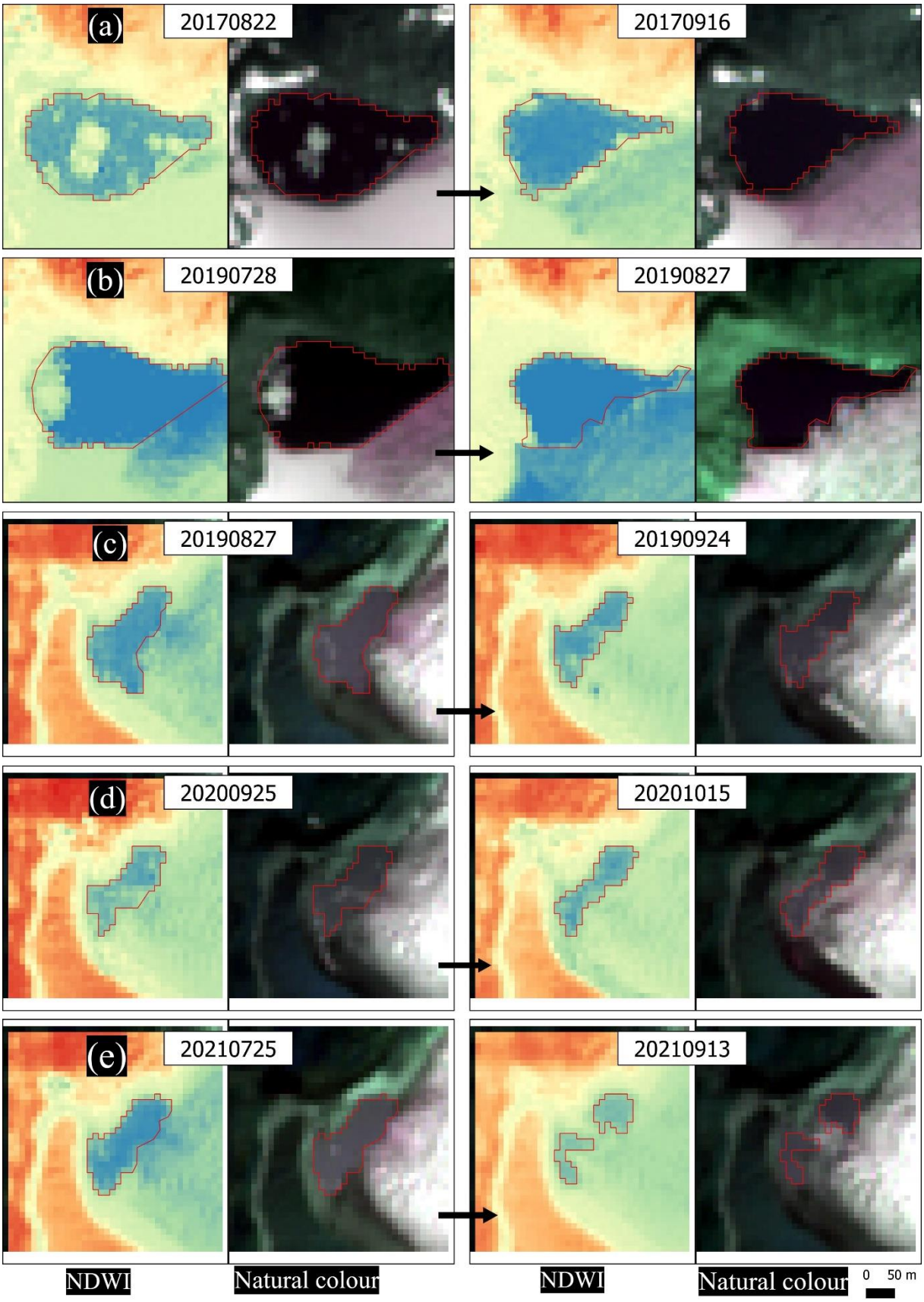

Figure 11: Indication of drainage events in L2 (GID: 2364) and L19 (GID: 2352). (a) and (b) represent the drainage events in 2017 and 2019 in L2 and (c), (d), and (e) represent the drainage events in 2019, 2010, and 2021 in L19

3.2 Variation in surface area of glacial lakes and their types

The degree of fluctuation or variation in surface area of a glacial lake in a melting season indicates or hints towards the expansion due to glacier melting as well as reduction due to drainage. This can be captured well through SD of its month-to-month recorded surface area assuming that a lake with higher accumulation and higher drainage will have a higher SD. Meanwhile, as mentioned earlier, it is not necessarily true that the expansion and reduction in surface area observed through outline mapping is due to accumulation or drainage as it might also be due to retreat and advance of glacier terminus (or margin) altering the room for water accumulation. However, the SD also helped to explore that dimension of glacial lakes. To correctly identify the cause, each image was carefully examined.

Since the surface area of glacial lakes may vary from month-to-month in a melting season in a year and also from year-to-year, both annual seasonal variation and overall (6 years) variation were calculated in terms of absolute SD. To make better comparison of surface area changes between different lakes and between their types, the absolute surface area of each lake was normalized in terms of percentage change with reference to the median surface area of initial year (2016) melting season, assuming it 100 %. Percentage changes in those lakes with no available data in 2016 are referenced with the next available year's median surface area.

3.2.1 Annual seasonal and overall (6 years) variation in surface area of each lake and their types (in both absolute and normalized terms)

The annual seasonal variation in each year starting from 2016 to 2021 and overall (6 years) variation in both absolute and normalized terms were calculated in SD and presented side by side (Tab. 8). The lakes in the table are arranged in a descending order based on overall (6 years) variation in normalized term (i.e., in %).

Table 8: Annual seasonal and overall (6 years) variation in surface area of each lake (in both absolute and normalized terms)

Lake type	Lake name	Absolute Median surface area	(a) SD of Absolute surface area (in km^2) of each lake in melting season each year and overall (6 years)							(b) SD of normalized surface area (in %) of each lake in melting season each year and overall (6 years)						
			2016	2017	2018	2019	2020	2021	Overall (6 years)	2016	2017	2018	2019	2020	2021	Overall (6 years)
2	L23	0.0011	NA	0.0007	0.0049	0.0000	NA	0.0109	0.0116	NA	63.05	449.09	NA	NA	1004.63	1067.44
2	L34	0.0009	0.0004	0.0001	0.0069	0.0039	0.0012	0.0028	0.0046	48.83	14.66	781.21	438.19	134.00	318.93	517.75
2	L55	0.0041	0.0023	0.0079	0.0031	0.0047	0.0002	0.0087	0.0195	57.23	194.05	76.47	116.18	5.06	213.31	479.29
2	L13	0.0009	0.0007	0.0002	0.0017	0.0020	NA	0.0033	0.0039	78.58	24.69	190.27	224.16	NA	366.09	437.01
2	L41	0.0045	0.0000	0.0079	0.0011	0.0016	0.0065	0.0017	0.0123	NA	173.91	23.91	34.26	142.76	37.52	271.04
2	L56	0.1591	0.0270	0.0455	0.0011	0.0086	0.6867	0.0021	0.3429	16.99	28.62	0.68	5.42	431.60	1.34	215.51
2	L18	0.0197	0.0058	0.0184	0.0056	0.0150	0.0071	0.0041	0.0413	29.60	93.76	28.48	76.55	36.23	20.74	210.07
2	L1	0.0017	0.0003	0.0008	0.0046	0.0024	0.0007	0.0019	0.0034	14.98	46.64	272.41	144.56	41.55	110.59	202.70
2	L54	0.0188	0.0120	0.0194	0.0144	0.0131	0.0458	0.0045	0.0366	64.00	103.28	76.96	69.79	244.26	24.14	195.23
2	L40	0.0087	0.0000	0.0049	0.0077	0.0008	NA	0.0002	0.0102	NA	56.62	88.73	9.46	NA	2.82	116.89
2	L22	0.0010	0.0001	0.0000	0.0002	0.0002	NA	0.0007	0.0010	7.83	NA	21.81	16.02	NA	78.41	105.61
2	L35	0.0037	0.0012	0.0004	0.0014	0.0008	0.0008	0.0004	0.0036	33.42	10.79	39.14	21.80	20.50	10.86	96.84
1	L24	0.0055	NA	NA	0.0047	0.0024	0.0000	0.0051	0.0043	NA	NA	85.39	43.36	NA	92.24	78.51
1	L31	0.0036	NA	NA	0.0032	0.0016	NA	0.0028	0.0026	NA	NA	88.96	45.35	NA	76.29	70.96
2	L45	0.0132	0.0000	0.0002	0.0041	0.0095	0.0000	0.0083	0.0089	NA	1.43	31.11	71.74	NA	62.87	67.35
2	L12	0.0043	0.0006	0.0002	0.0007	0.0003	0.0036	0.0010	0.0026	13.15	4.06	16.23	6.69	83.57	23.98	61.24
2	L37	0.0030	0.0012	0.0004	0.0012	0.0012	0.0000	0.0013	0.0018	39.32	11.67	41.65	41.57	NA	42.39	59.75
1	L42	0.0013	0.0000	0.0002	0.0006	0.0002	0.0000	0.0001	0.0005	NA	12.75	41.71	18.23	NA	7.18	39.90
4	L19	0.0073	0.0018	0.0000	0.0015	0.0017	0.0009	0.0024	0.0029	24.32	NA	20.81	23.85	11.84	33.45	39.75
2	L49	0.0080	0.0025	0.0015	0.0016	0.0015	0.0027	0.0005	0.0031	31.53	18.83	20.04	18.49	33.65	6.56	38.40
2	L38	0.0133	0.0034	0.0025	0.0018	0.0010	0.0000	NA	0.0051	25.35	18.42	13.86	7.35	NA	2.84	38.07
2	L48	0.0160	0.0076	0.0007	0.0006	0.0019	0.0073	0.0003	0.0060	47.50	4.39	3.83	12.07	45.60	2.13	37.47
1	L29	0.0043	0.0007	0.0013	0.0001	0.0002	0.0001	0.0000	0.0015	16.76	30.23	1.41	5.60	1.16	0.88	34.53
1	L43	0.0145	0.0064	0.0032	0.0017	0.0035	0.0052	0.0004	0.0045	44.28	22.11	11.71	24.17	35.72	2.97	31.20
1	L7	0.0086	0.0018	0.0028	0.0005	0.0015	0.0018	0.0006	0.0025	21.33	32.51	5.29	17.54	21.42	6.58	29.61
1	L6	0.0290	0.0093	0.0001	0.0006	0.0009	0.0096	0.0011	0.0083	32.20	0.18	2.04	3.19	33.04	3.75	28.71
3	L58b	0.1046	0.0312	0.0288	0.0023	0.0022	NA	0.0063	0.0292	29.81	27.50	2.19	2.10	NA	6.05	27.94
2	L25	0.0701	0.0088	0.0000	0.0013	0.0117	0.0141	0.0069	0.0190	12.58	NA	1.78	16.67	20.15	9.84	27.06
2	L9	0.1511	0.0059	0.0311	0.0182	0.0249	0.0038	0.0170	0.0394	3.93	20.56	12.02	16.51	2.51	11.23	26.08
2	L52	0.0482	0.0211	0.0026	0.0049	0.0017	0.0012	0.0006	0.0122	43.80	5.31	10.18	3.58	2.51	1.32	25.24
1	L51	0.0446	0.0211	0.0003	0.0006	0.0028	0.0015	0.0004	0.0109	47.35	0.56	1.24	6.29	3.35	0.81	24.50
2	L5	0.0320	0.0033	0.0016	0.0014	0.0018	0.0044	0.0009	0.0069	10.16	4.85	4.33	5.53	13.79	2.91	21.58
1	L30	0.0174	0.0022	0.0000	0.0034	0.0002	0.0000	0.0011	0.0037	12.39	NA	19.78	1.11	NA	6.34	21.18
2	L53	0.2456	0.1076	0.0054	0.0017	0.0045	0.0055	0.0028	0.0517	43.82	2.21	0.70	1.84	2.26	1.12	21.06
3	L2	0.0510	0.0004	0.0065	0.0060	0.0085	0.0054	0.0021	0.0091	0.70	12.85	11.75	16.65	10.68	4.20	17.83
2	L3	0.1689	0.0366	0.0017	0.0071	0.0054	0.0039	0.0031	0.0223	21.69	0.98	4.22	3.21	2.29	1.85	13.22
2	L17	0.2644	0.0112	0.0110	0.0156	0.0177	0.0013	0.0222	0.0314	4.24	4.15	5.89	6.69	0.51	8.39	11.88
2	L4a	0.0641	0.0006	0.0010	0.0035	0.0014	0.0130	0.0022	0.0065	0.89	1.60	5.45	2.12	20.29	3.39	10.18
2	L50	0.0144	0.0016	0.0017	0.0015	0.0011	0.0009	0.0011	0.0015	10.80	11.82	10.25	7.63	6.44	7.29	10.06
2	L4b	0.0380	0.0041	0.0011	0.0013	0.0033	0.0019	0.0015	0.0031	10.75	2.83	3.41	8.82	5.00	4.01	8.26
1	L11	0.0185	0.0020	0.0007	0.0005	0.0016	0.0013	0.0001	0.0013	11.07	3.52	2.90	8.54	6.85	0.54	7.19
1	L57	0.0599	0.0008	0.0036	0.0002	0.0063	0.0005	0.0008	0.0042	1.27	5.95	0.26	10.45	0.75	1.29	6.97
2	L58c	0.3949	0.0025	0.0141	0.0012	0.0176	0.0000	0.0145	0.0265	0.64	3.56	0.31	4.45	NA	3.68	6.72
2	L58a	0.1595	0.0004	0.0052	0.0085	0.0028	NA	0.0160	0.0104	0.27	3.26	5.30	1.76	NA	10.04	6.53
2	L44	0.3345	0.0000	0.0123	0.0104	0.0254	0.0000	0.0043	0.0199	NA	3.67	3.12	7.60	NA	1.28	5.96
5	L15	8.3145	0.1037	0.4297	0.5270	0.0926	0.0318	0.2480	0.4901	1.25	5.17	6.34	1.11	0.38	2.98	5.90
5	L14	4.0238	0.0610	0.0243	0.0006	0.0284	0.0000	0.1121	0.2013	1.52	0.60	0.01	0.71	NA	2.79	5.00
1	L36	0.1708	0.0047	0.0034	0.0016	0.0069	0.0015	0.0012	0.0065	2.75	2.01	0.94	4.03	0.89	0.68	3.79
1	L47	0.1268	0.0025	0.0023	0.0019	0.0015	0.0036	0.0007	0.0039	1.95	1.77	1.51	1.15	2.86	0.56	3.11
1	L46	0.2611	0.0041	0.0010	0.0041	0.0099	0.0038	0.0036	0.0079	1.56	0.38	1.58	3.79	1.44	1.36	3.04
2	L10	0.4568	0.0086	0.0013	0.0029	0.0084	0.0088	0.0086	0.0125	1.89	0.28	0.64	1.85	1.93	1.87	2.74

Note: Column (a) represents SD in absolute term (in km^2) and column (b) represents SD in normalized term (in % of median of lake area in 2016 or the next available year). They grey-highlighted and the blue-highlighted numbers represent the highest and the lowest SD (in absolute terms) in each year and in overall (6 years) whereas the red-highlighted and the green-highlighted numbers represent the highest and the lowest SD (in %) in each year and in overall (6 years).

Both annual seasonal and overall (6 years) variation in absolute and normalized surface area of lakes presented in Tab. 8 are also represented graphically in Fig. 12 and Fig. 13 for better visualization.

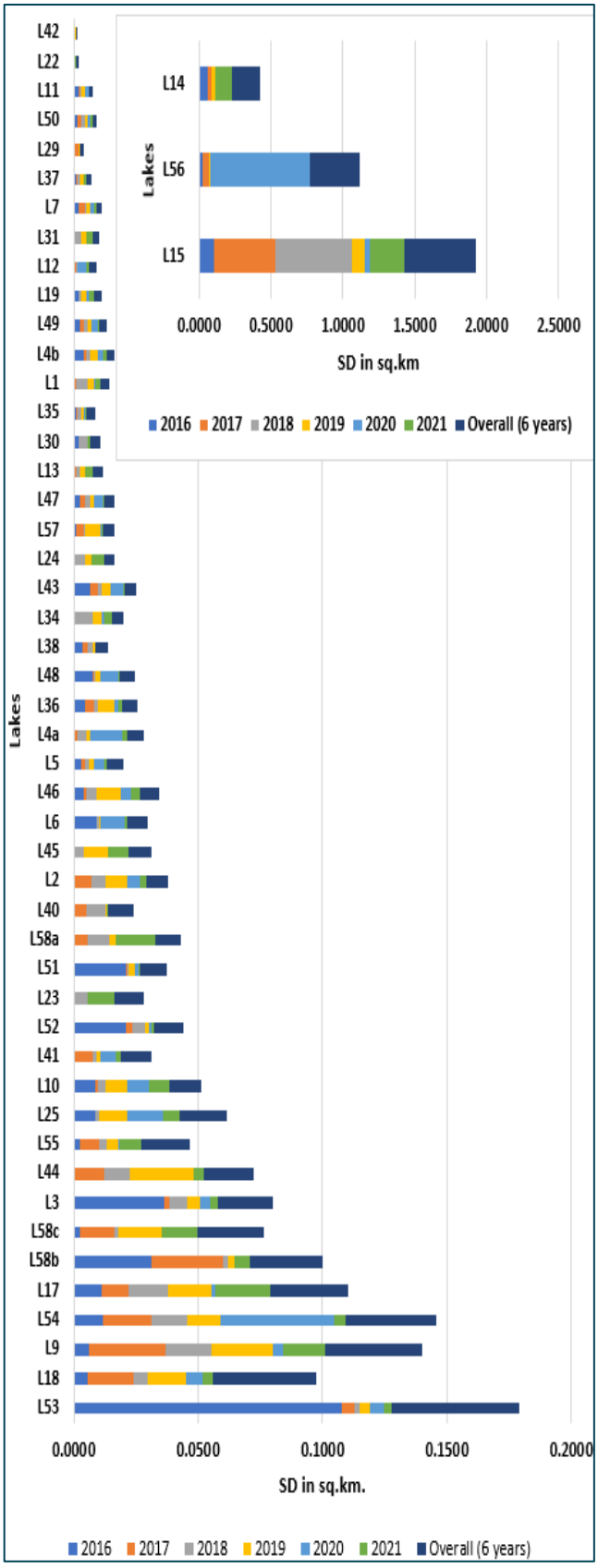

Figure 12: SD of absolute surface area in km^2. of each lake in melting season each year

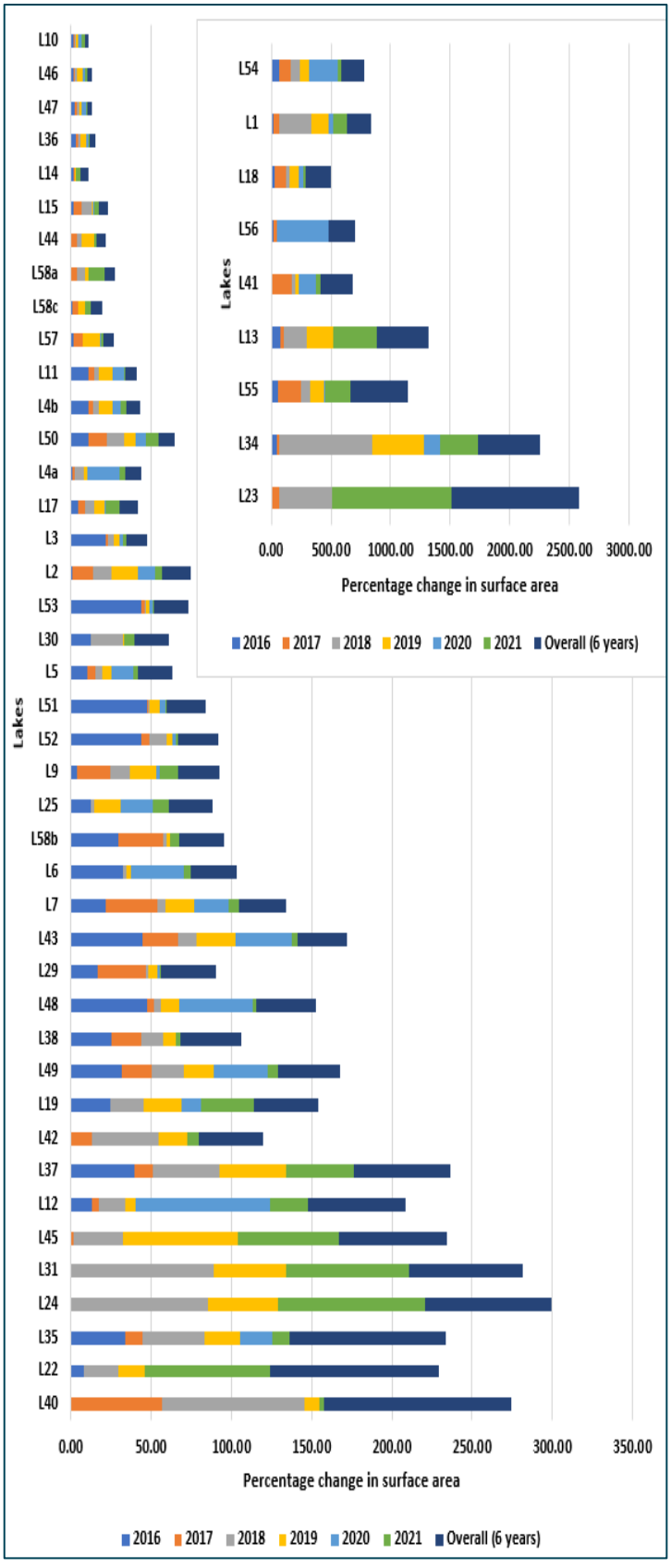

Figure 13: SD of normalized surface area (in %) of each lake in melting season each year

3.2.1.1 Annual seasonal and overall (6 years) variation in surface area of each lake and their types in absolute terms

The Tab. 8a and Fig. 12 show the highest overall (6 years) absolute SD (0.4901 km^2) in L15 (*GID: 2478*) (Fig. 15) and the lowest overall (6 years) absolute SD (0.0005 km^2) in L42. Likewise, L56 (Fig. 17) and L14 (*GID: 2471*) (Fig. 18) stand at second and third highest positions. Among top 20 lakes with the highest SDs, 16 lakes belong to type 2 (*connected-to-glacier*). Therefore, the initial part of Tab. 8 shows that glacial lakes type 2 (*connected-to-glacier*) are more variable compared to type 1 (*not-connected-to-glacier*), 3 (*glacier-dammed*), and 4 (*moraine-dammed*).

According to the Tab. 8a and Fig. 10, L53 had the highest SD (0.1076 km^2) in 2016. L15 had the highest variation in 2017, 2018, 2019, and 2021 with SDs 0.4297 km^2, 0.5270 km^2, 0.0926 km^2, and 0.2480 km^2 respectively. In 2020, L56 had the highest variation with SD 0.6867 km^2 which is also the highest absolute annual seasonal variation among all lakes in 6 years. On the other hand, in 2016, L44, L41, L40, L45, and L42 had almost no variation. In 2017, L25, L30, and L19 (*GID: 2352*) had almost no variation and in 2018, L29 has the least variation with SD 0.0001 km^2. In 2019, L23 (*GID: 2293*) shows no variation. In 2020, L14, L58c, L44, L45, L38, L30, L37, and L42 had no variation. Likewise, in 2021, L29 had no variation.

The Tab. 8a and Fig. 12 clearly shows that glacial lakes type 5 (*artificial-water-level-regulation*) shows extremely high absolute variation as compared to other lake types. This is because of their extremely large size. Even a small percentage change in such large lakes is significantly large to small lakes in absolute terms (Fig. 16).

The Fig. (14) shows the boxplot of each lake types with their SD. Lake type 4 (*moraine-dammed*) contains just one lake, whereas lake types 3 (*glacier-dammed*), and 5 (*artificial-water-level-regulation*) contain just 2 lakes each. As mentioned earlier, the lakes with *artificial-water-level-regulation* have extremely large surface area so the change in their size is largely influenced by their initial surface area. This can be clearly seen in the boxplot (Fig. 14) as they stand out among all. Lake type 1 (*not-connected-to-glacier*), and 2 (*connected-to-glacier*) contain considerably a greater number of lakes than others and their surface area are not significantly different from each other (p-value = 0.54) so the changes in their absolute surface area are meaningfully comparable to each other. The Fig. 14, therefore, shows that lake type 2 (*connected-to-glacier*) is more variable than lake type 1 (*not-connected-to-glacier*).

Meanwhile, there are two outliers in lake type (*connected-to-glacier*). They are L56 (0.3429 km^2) with almost similarly large variation as lake type 5 (*Artificial-water-level-regulation*) and L53 (0.0517 km^2.) which has the fourth highest absolute overall (6 years) variation among all. These two lakes clearly stand out because they (L56 and L53) had the highest SD in 2020 (0.6867 km^2.) and 2016 (0.1076 km^2.) respectively (Tab. 8a; Fig. 12).

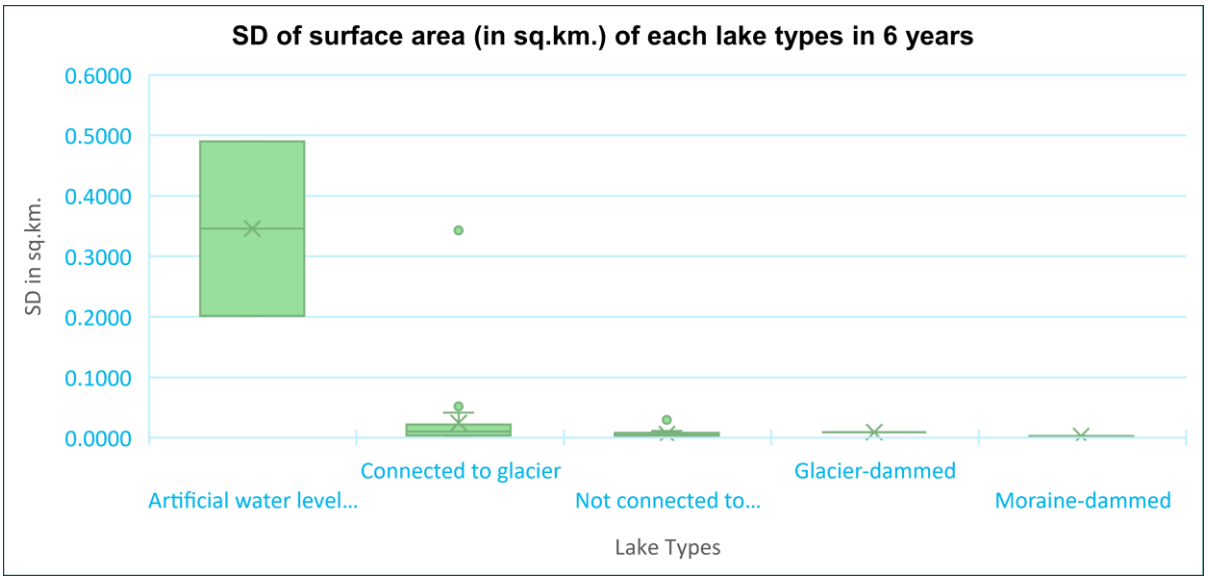

Figure 14: Boxplot of SD of surface area (in km^2) of each lake types in 6 years

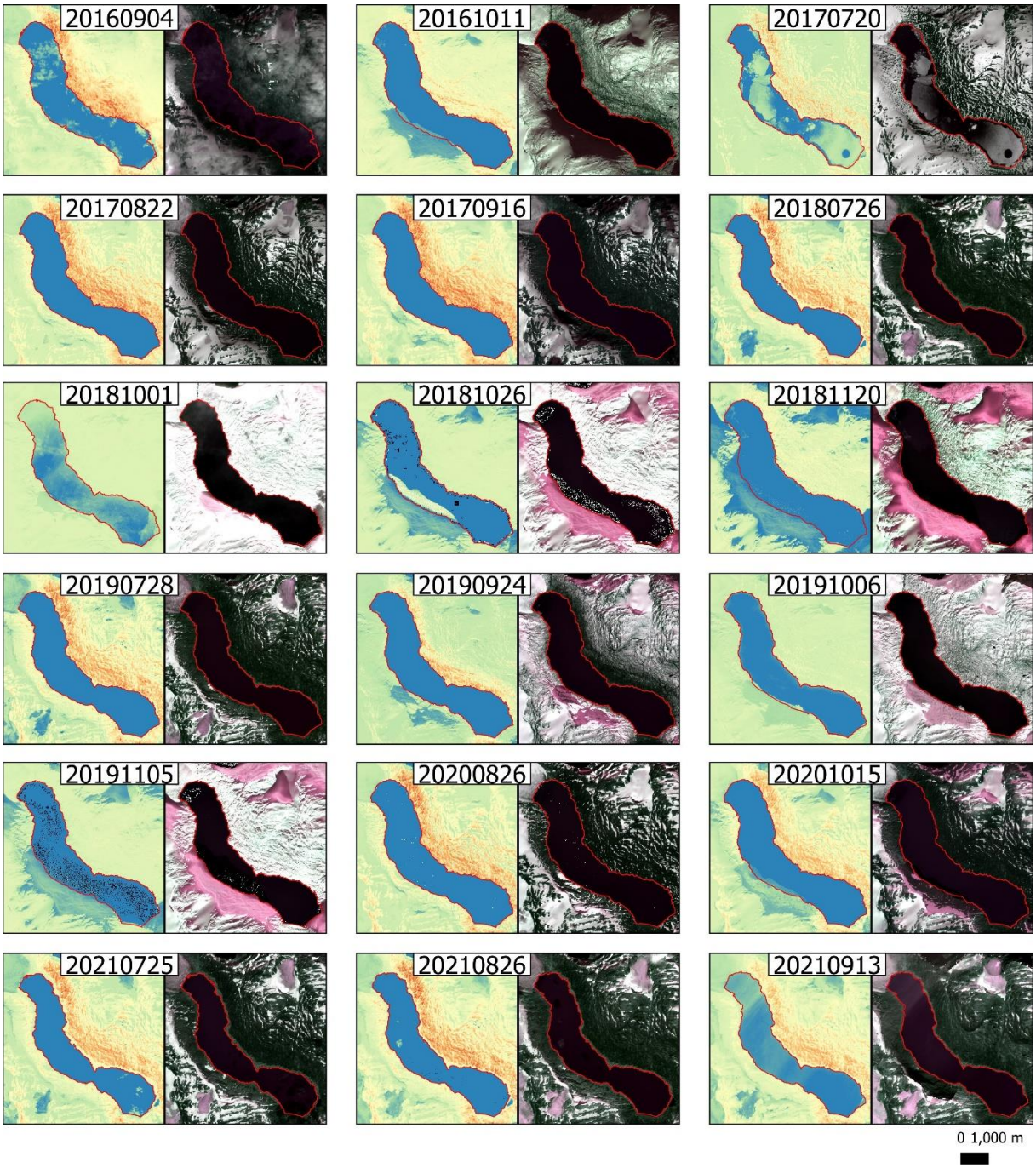

Figure 15: Outlines of L15 (GID: 2478) (Styggevatnet) which has the highest overall (6 years) variation in absolute surface area. The left frames represent NDWI images, and the right frames represent natural colour images

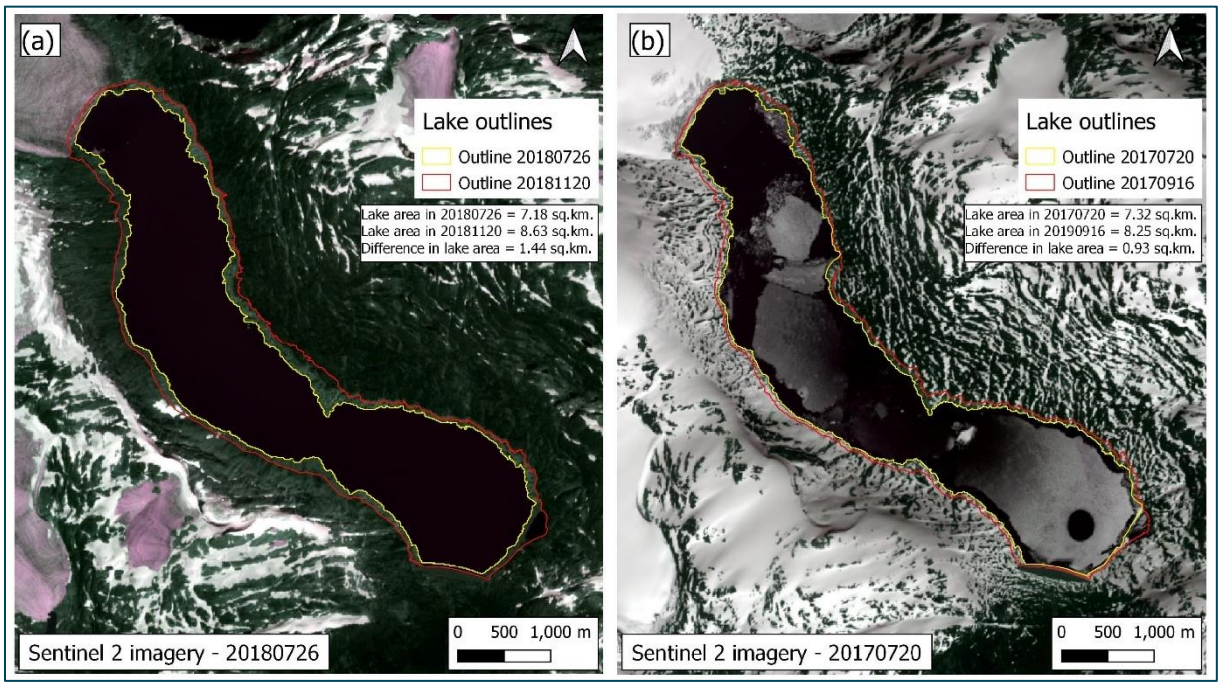

Figure 16: Difference in lake outlines in one melting season in L15 (GID: 2478) (Styggevatnet) in 2017 and 2018. (a) Outline mapped in 2018 and (b) Outline mapped in 2020

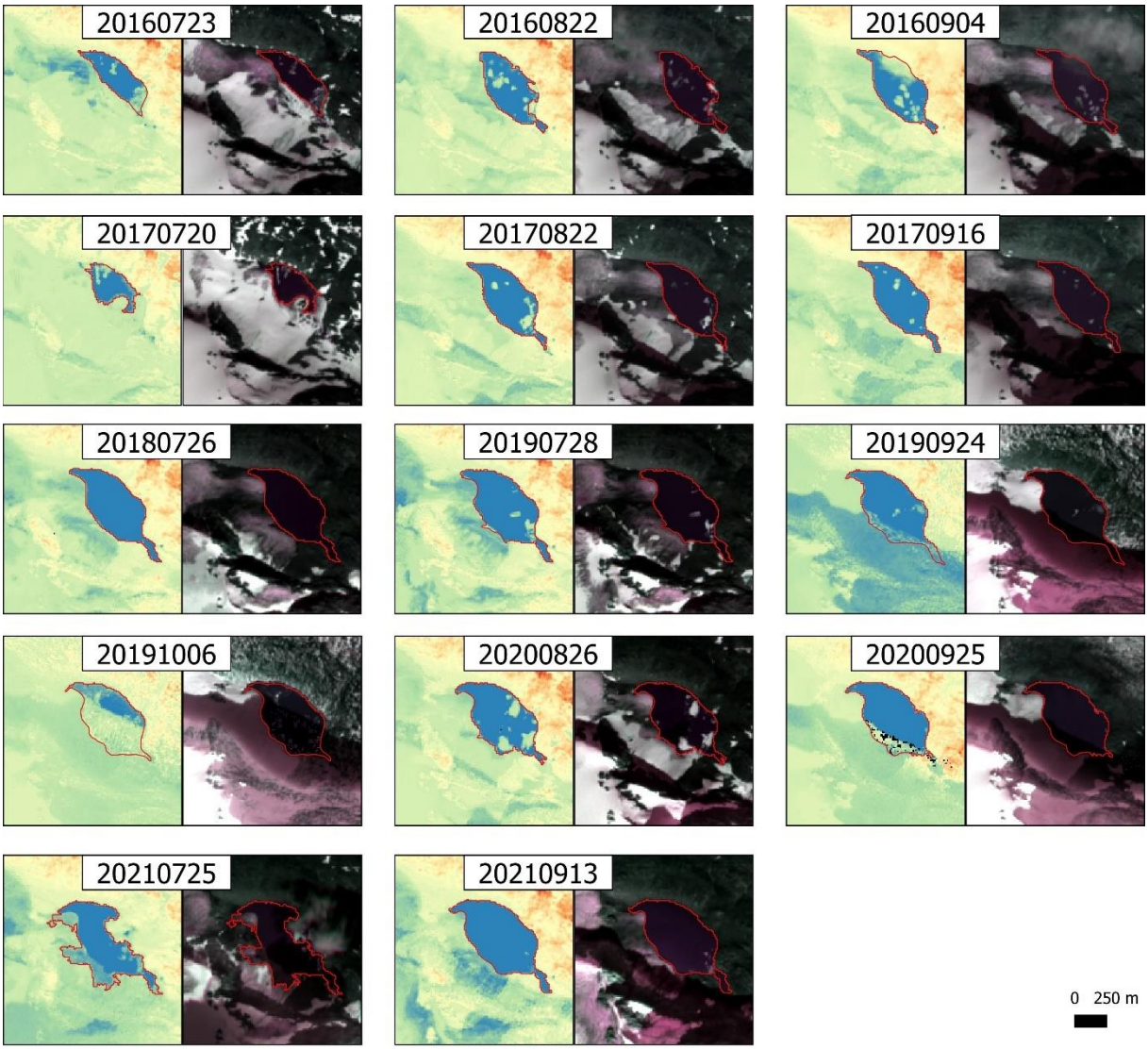

Figure 17: Outlines of L56 (GID: 2520) which has the second highest overall (6 years) variation in absolute surface area. The left frames represent NDWI images, and the right frames represent natural colour images

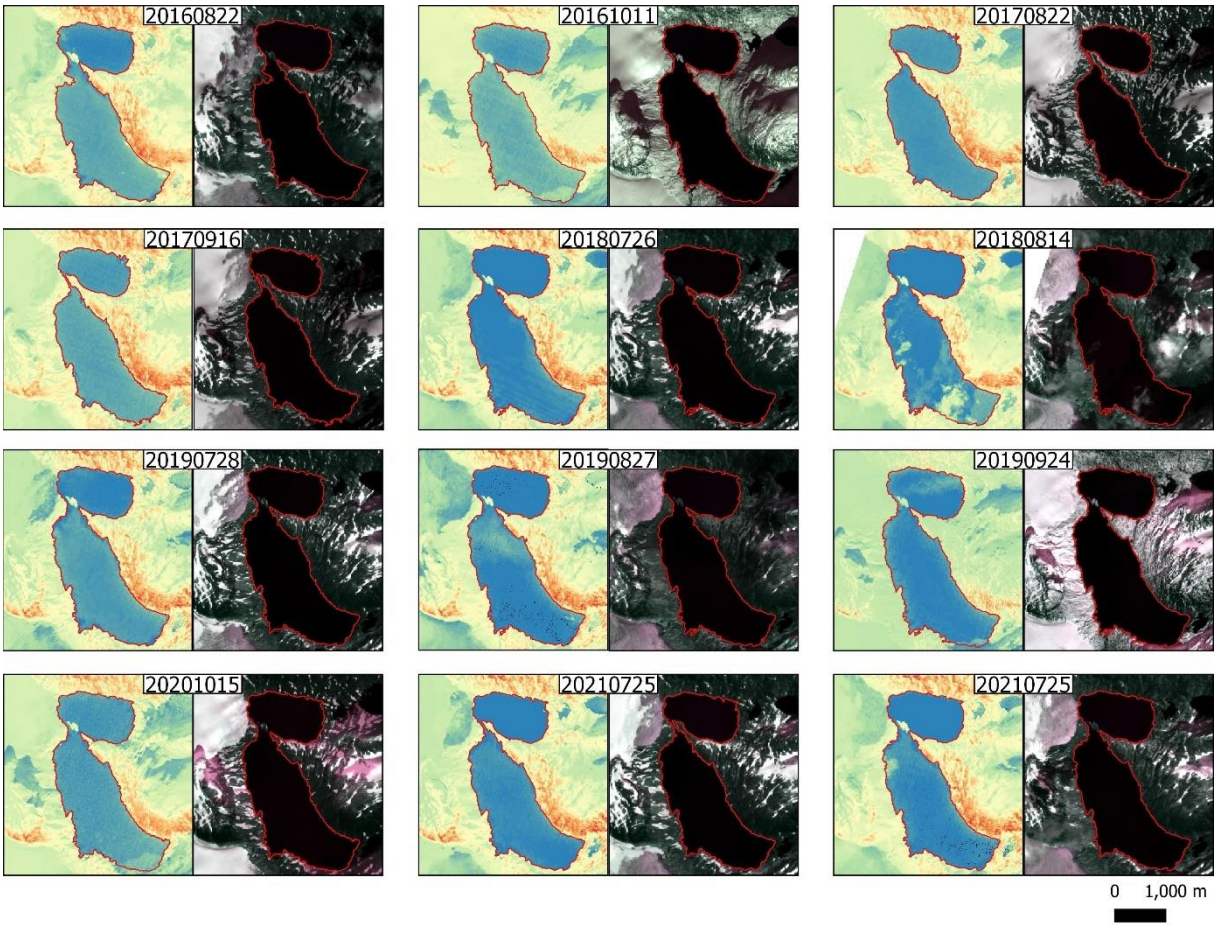

Figure 18: Outlines of L14 (Kupvatnet/GID: 2471) which has the third highest overall (6 years) variation in absolute surface area. The left frames represent NDWI images, and the right frames represent natural colour images

3.2.1.2 Annual seasonal and overall (6 years) variation in surface area of each lake and their types in normalized terms

Variation in surface area of glacial lakes is sensitive to their size so they were normalized based on their initial median size (2016). The second part of the Tab. 8b and Fig. 13 shows the highest overall (6 years) SD (1067.44%) in L23 (*GID: 2293*) (Fig. 19) and the lowest overall (6 years) SD (2.74%) in L10. Likewise, L34 (Fig. 20) and L55 (Fig. 21) stand at the second highest and the third highest positions. The top 10 lakes with the highest SD belong to type 2 (*connected-to-glacier*). L15 (*GID: 2478*) and L14 (*GID: 2471*) in lake type 5 (*Artificial-water-level-regulation*) with extremely large size and significantly higher absolute variation fall simultaneously on 46th and 47th places from top with 5.90% and 5.00% SD respectively in normalized variation. L58b and L2 (*GID: 2364*) in lake type 3 (*glacier-dammed*) fall on 27th and 35th places from top with 27.94% and 17.83% SD respectively. All lakes in lake type 1 (*not-connected-to-glacier*) have less than 80% SD in 6 years. Therefore, the Tab. 8b and Fig. 13 show that glacial lakes in lake type 2 (*connected-to-glacier*) are more variable compared to

type 1 (*not-connected-to-glacier*), 3 (*glacier-dammed*), 4 (*moraine-dammed*) and 5 (*Artificial-water-level-regulation*) in terms of percentage change.

According to the Tab. 8b and Fig. 13, L1 (*GID: 2364*) had the highest SD (78.58%) in 2016. In 2017, L55 had the highest SD (194.5%). In 2018 and 2019, L34 had the highest SDs, (781.21%), and (438.19%) respectively. Likewise, in 2020, L56 (*GID: 2520*) had the highest SD (431.60%) and in 2021, L23 had the highest SD (1004.63%) which is also the highest normalized annual seasonal variation among all lakes. On the other hand, L58a, L6, L15, L11 had the lowest SD in 2016 (0.27%), 2017 (0.18%), 2020 (0.38%), 2021 (0.54%) respectively. Likewise, L14 (*GID: 2471*) had the lowest variation in 2018 (0.01%) and 2019 (0.71%).

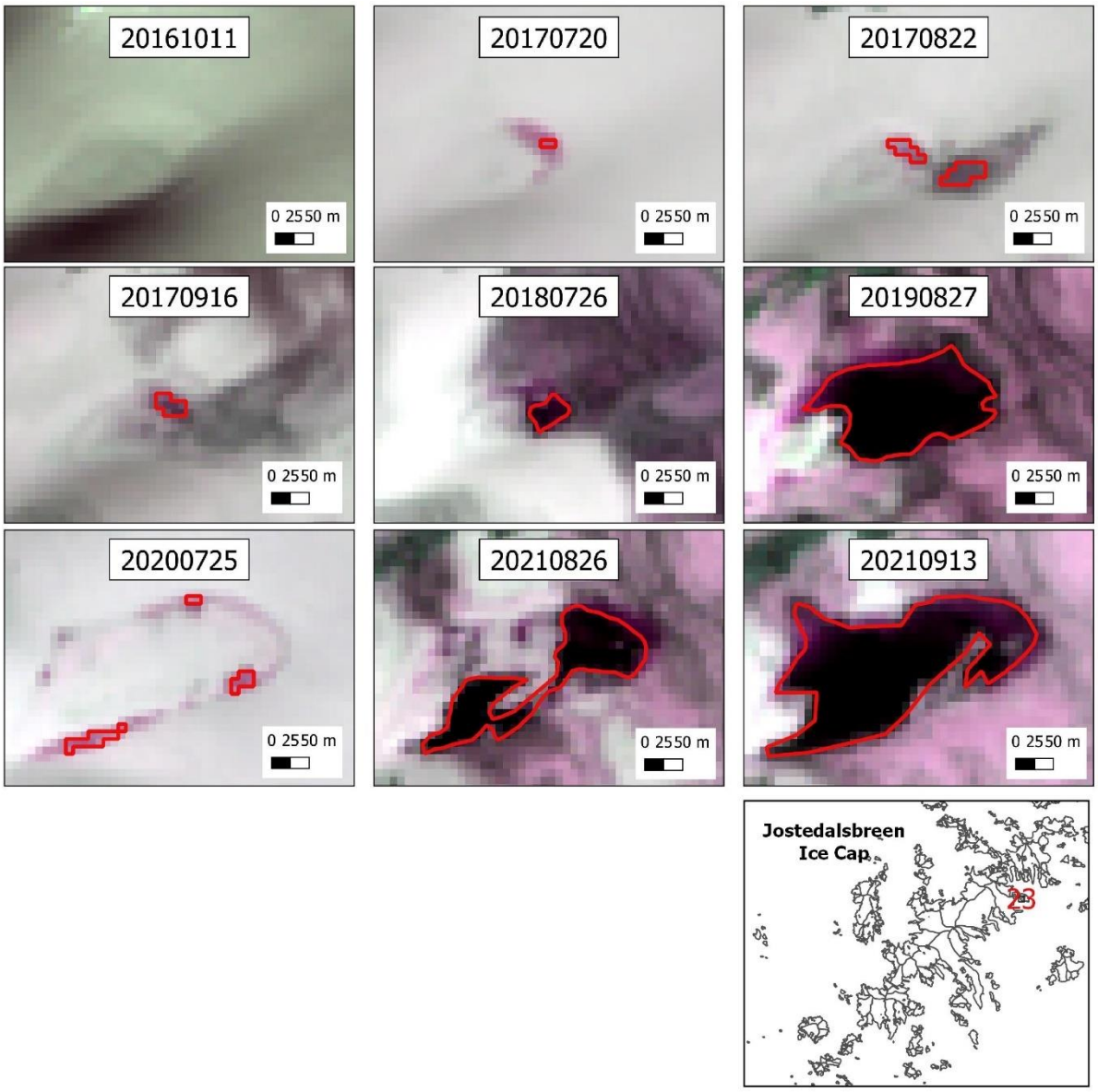

Figure 19: Outlines of L23 (GID: 2293) which has the first highest overall (6 years) variation in (%) surface area. The left frames represent NDWI images, and the right frames represent natural colour images

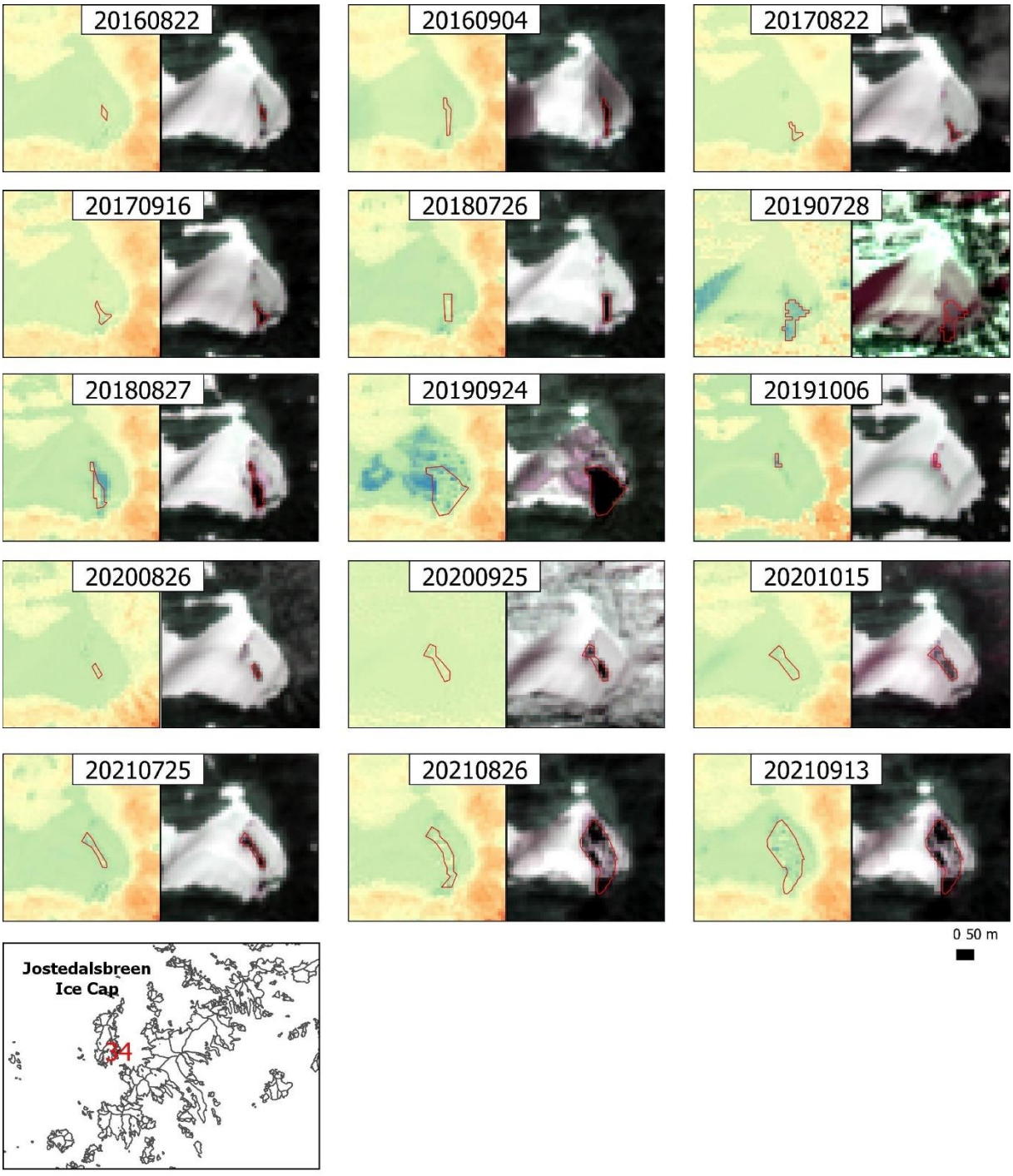

Figure 20: Outlines of L34 (GID: 2303) which has the second highest overall (6 years) variation in (%) surface area. The left frames represent NDWI images, and the right frames represent natural colour images.

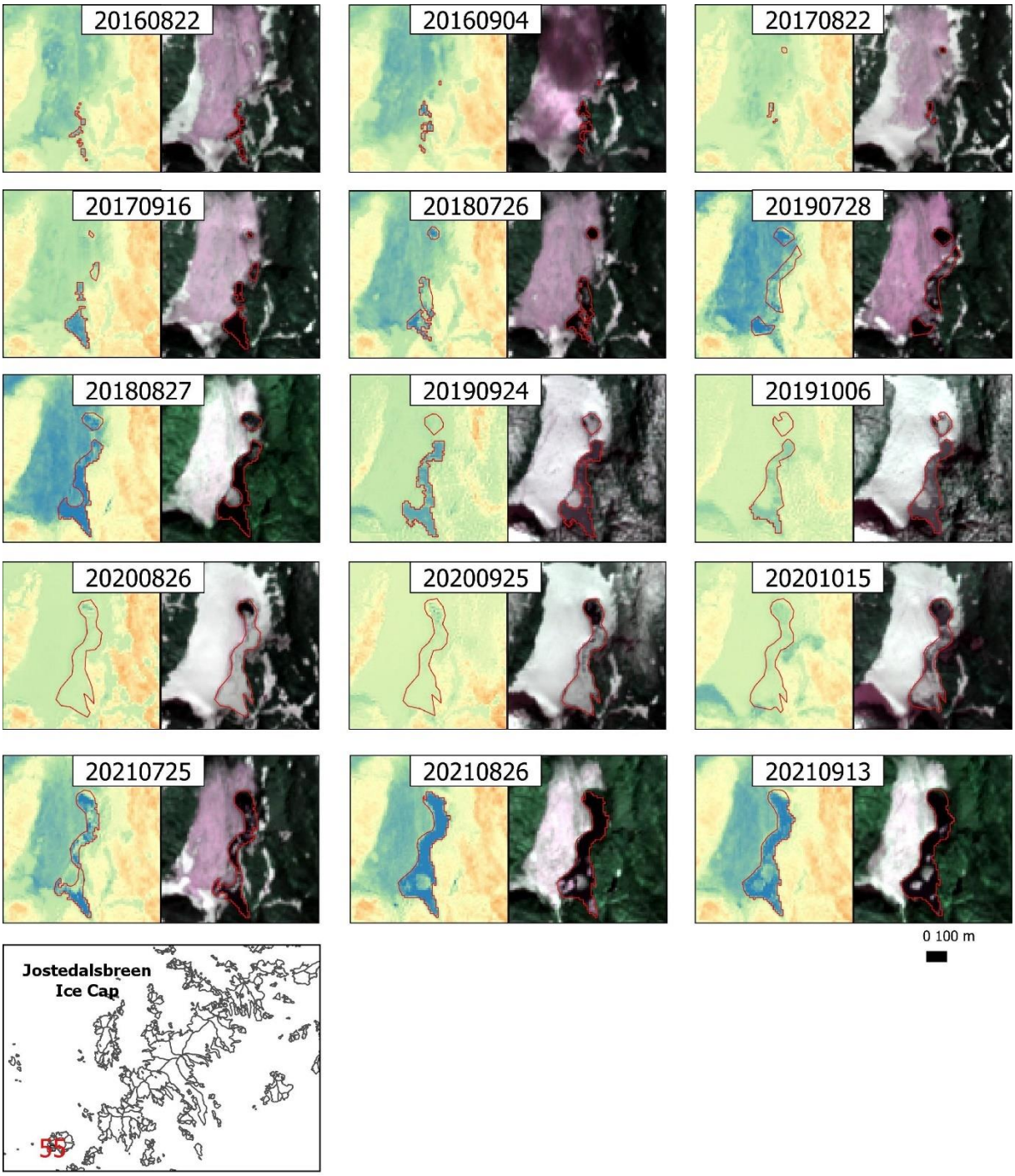

Figure 21: Outlines of L55 (GID: 2124) which has the third highest overall (6 years) variation in (%) surface area. The left frames represent NDWI images, and the right frames represent natural colour images

Fig. 22 shows the boxplot of each lake types with their % SD in surface area. As mentioned earlier, lake type 4 (*moraine-dammed*) contains just one lake, whereas lake types 3 (*glacier-dammed*), and 5 (*artificial-water-level-regulation*) contain just 2 lakes each. Lake type 1 (*not-connected-to-glacier*), and 2 (*connected-to-glacier*) contain considerably more lakes than

others, and so the difference in overall (6 years) variation (% SD) in surface area between these two lake types was tested with a Mann Whitney U test (Wilcoxon rank sum exact test). The result from the test shows that the % SD of these two groups are not significantly different (p-value = 0.06) with 95% confidence interval. Therefore, there is no sufficient statistical evidence to say that lake type 1 (*Not-connected-to-glacier*) and lake type 2 (*Connected-to-glacier*) vary differently in % annual seasonal surface area change in overall (6 years).

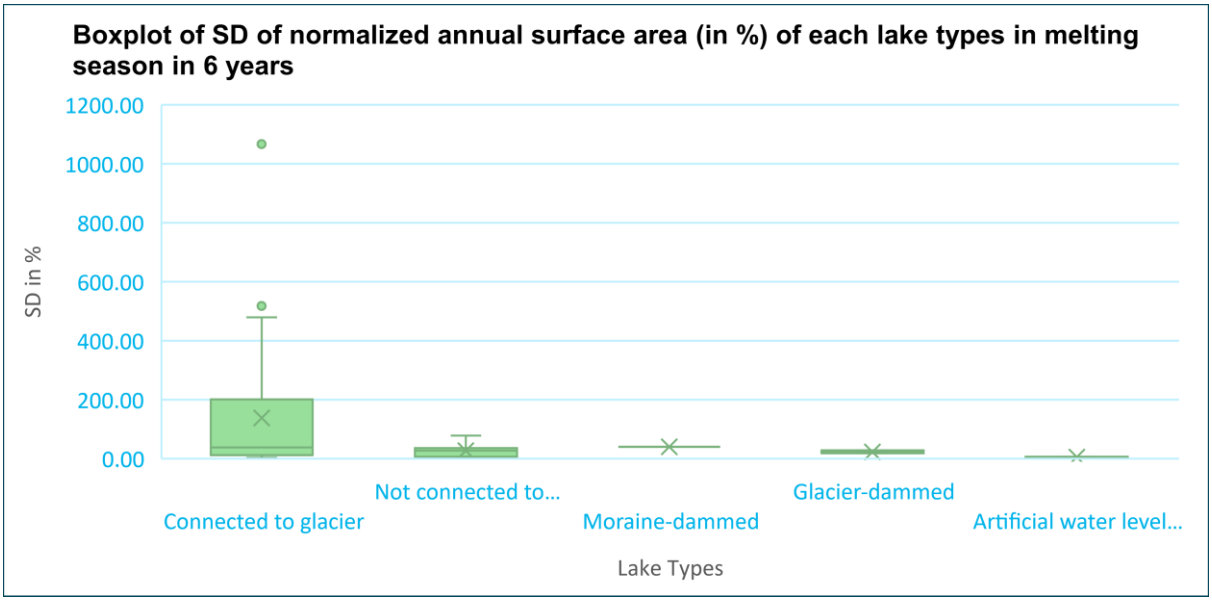

Figure 22: Boxplot of normalized annual surface area (in %) of each lake types in melting season in 6 years

3.2.2 Overall (6 years) variation in maximum surface area of each lake and their types (in both absolute and normalized terms)

Maximum surface area of lake is important to study as the impact of GLOF increases with more volume of water flowing through it. Therefore, maximum surface area recorded from the lake outline inventory in each year was noted for 6 years (2016-2021) and their variation in overall (6 years) was calculated in SD in both absolute and normalized terms. The absolute and normalized SD of annual maximum surface area is presented in Tab. 9, and graphically represented in Fig. 23 and Fig. 24.

Table 9: SD of absolute and normalized annual maximum recorded surface area of each lake in 6 years

Lakes	Lake Type	SD in Km^2.	SD in %
L23	2	0.013	617.3
L34	2	0.006	472.4
L55	2	0.019	342.7
L56	2	0.548	320.3
L13	2	0.005	294.5
L41	2	0.013	278.6
L1	2	0.004	243.5
L40	2	0.011	121.9
L18	2	0.036	121.1
L54	2	0.03	108.4
L22	2	0.001	99.39
L35	2	0.004	90.66
L45	2	0.009	70.59
L37	2	0.002	68.59
L12	2	0.003	60.45
L42	1	0.007	56.02
L19	4	0.003	43.34
L24	1	0.004	40.16
L38	2	0.005	36.33
L25	2	0.022	28.19
L29	1	0.001	23.98
L30	1	0.004	22.5
L9	2	0.034	21.65
L5	2	0.007	20.65
L49	2	0.002	15.65
L43	1	0.002	14.72
L6	1	0.004	11.99
L7	1	0.001	11.76
L2	3	0.006	11.48
L17	2	0.029	10.7
L48	2	0.002	9.8
L58b	3	0.012	8.95
L4b	2	0.003	6.65
L58c	2	0.026	6.54
L58a	2	0.01	6.4
L51	1	0.003	6.16
L52	2	0.003	5.67
L14	5	0.204	4.98
L44	2	0.015	4.58
L3	2	0.008	4.45
L15	5	0.36	4.28
L4a	2	0.003	4.11
L50	2	0.0006	3.92
L11	1	0.0008	3.81
L31	1	0.0002	3.38
L36	1	0.005	3.17
L47	1	0.004	2.75
L46	1	0.007	2.67
L10	2	0.01	2.13
L57	1	0.001	1.58
L53	2	0.003	0.99

Note: Red highlighted number represents highest SD and green highlighted number represents lowest SD

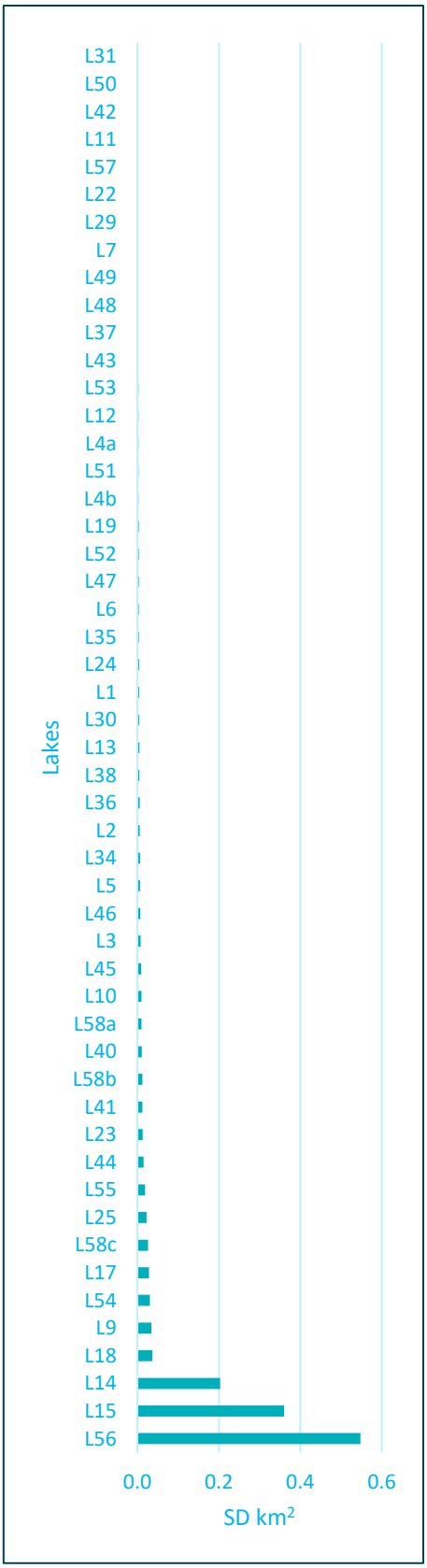

Figure 23: SD of absolute annual maximum recorded surface area of each lake in 6 years

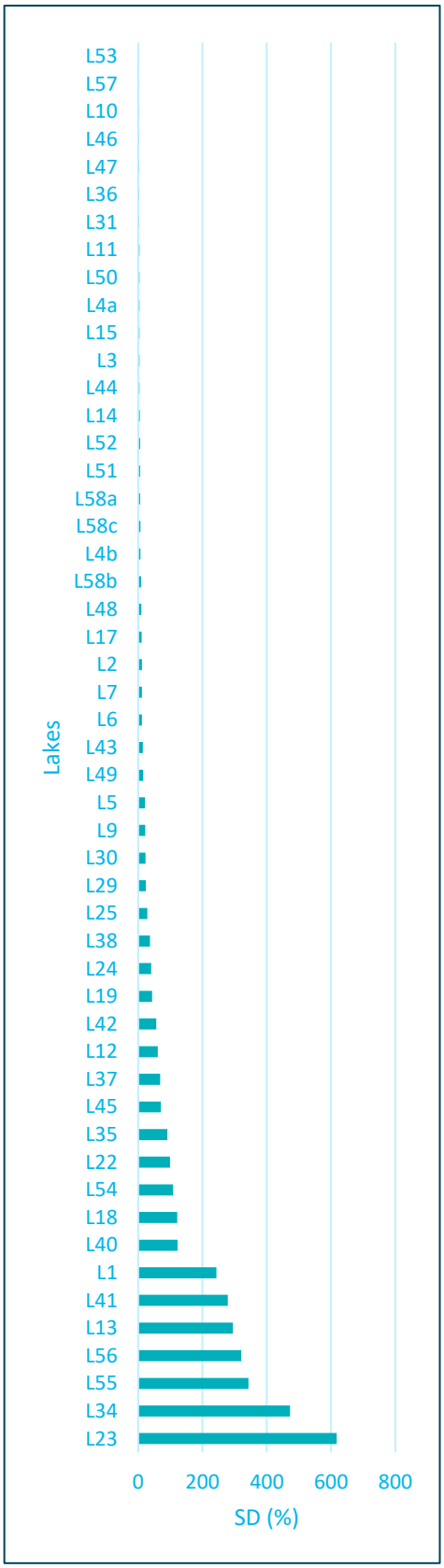

Figure 24: SD of normalized annual maximum recorded surface area of each lake in 6 years

3.2.2.1 Overall (6 years) variation in annual maximum surface area of each lake and their types in absolute terms

The SD of annual seasonal maximum absolute surface area of 51 lakes in overall (6 years) is shown in Tab. 9 and Fig. 23. According to the Tab. 9, L56 (*GID: 2520*) has the highest SD (0.5480 km^2) whereas L31 has the lowest SD (0.0002 km^2). L15 (*GID: 2478*) and L14 (*GID: 2471*) in lake type 5 (*Artificial-water-level-regulation*) stand at 2nd and 3rd position with SD (0.3604 km^2) and (0.2035 km^2) respectively. In top 20 lakes with highest absolute SD, 16 lakes belong to lake type 2 (*Connected-to-glacier*) which means they are more variable compared to other lake types. L58b and L2 (*GID: 2364*) in lake type 3 (*Glacier-dammed*) stand at 14th (0.0121 km^2) and 23rd (0.0059 km^2) positions. L19 (*GID: 2352*) in lake type 4 (*Moraine-dammed*) stand at 34th place with SD (0.0033 km^2).

As mentioned earlier, lake type 5 (*Artificial-water-level-regulation*) has two extremely large-sized lakes, and so they show very high variation as compared to others. Lake type 3 (*Glacier-dammed*) has higher variation than lake type 4 (*Moraine-dammed*) lakes. Moreover, the lake type 2 (*Connected-to-glacier*) is more variable than lake type 1 (*Not-connected-to-glacier*). L56, as an outlier in the plot, shows extremely high variation among all and even overtops the variation in type 5 (*Artificial-water-level-regulation*) lakes.

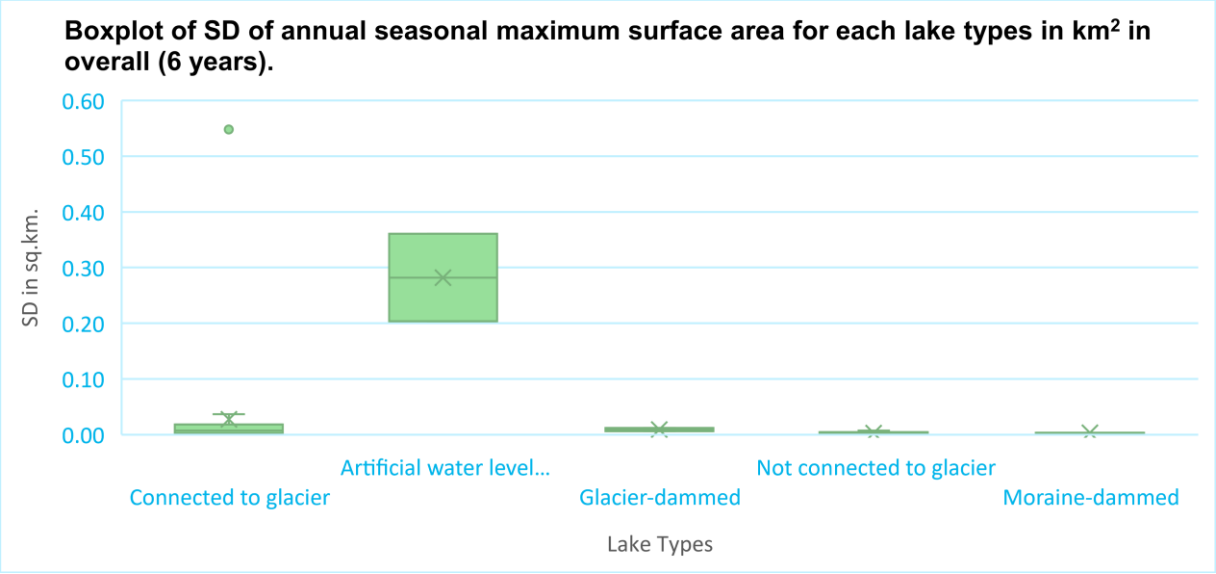

Figure 25:Boxplot of SD of annual seasonal maximum surface area for each lake types in km² in overall (6 years)

3.2.2.2 Overall (6 years) variation in annual maximum surface area of each lake and their types in normalized terms

To make better comparison between the lakes and their types, the annual seasonal maximum surface area was normalized based on the maximum surface area of initial year (2016) and their overall (6 years) SD was calculated for 51 lakes. The SD of each lake was represented graphically in Fig. 24.

The Tab. 9 shows that L23 (*GID: 2293*) has the highest SD (617.29 %) and L53 has the lowest SD (0.99 %) of their surface area compared to that in 2016. L34, L55 and L56 stand at 2nd, 3rd, and 4th places with SD 472.36%, 342.74%, and 320.27% respectively. 17 out of top highest 20 lakes belong to lake type 2 (*connected-to-glacier*) so they are more variable compared to others. L2 (*GID: 2364*) and L58b, lake type 3 (*glacier-dammed*), stand at 29th (11.48%) and 32nd (8.95%) respectively, whereas L19 (*GID: 2352*), lake type 4 (*moraine-dammed*), stands at top 17th place with SD 43.34%. Likewise, L14 (*GID: 2471*) and L15 (*GID: 2478*), lake type (*Artificial-water-level-regulation*), stand at 38th (4.98%) and 41st (4.28%) places respectively.

Fig. 26 shows the SD of normalized annual seasonal maximum surface area of each lake types in % in 6 years. Lake type 2 (*Connected-to-glacier*) has higher % variation in maximum surface area as compared to other lake types. Variation in some lakes in lake type 2 are extremely higher as compared to other lakes.

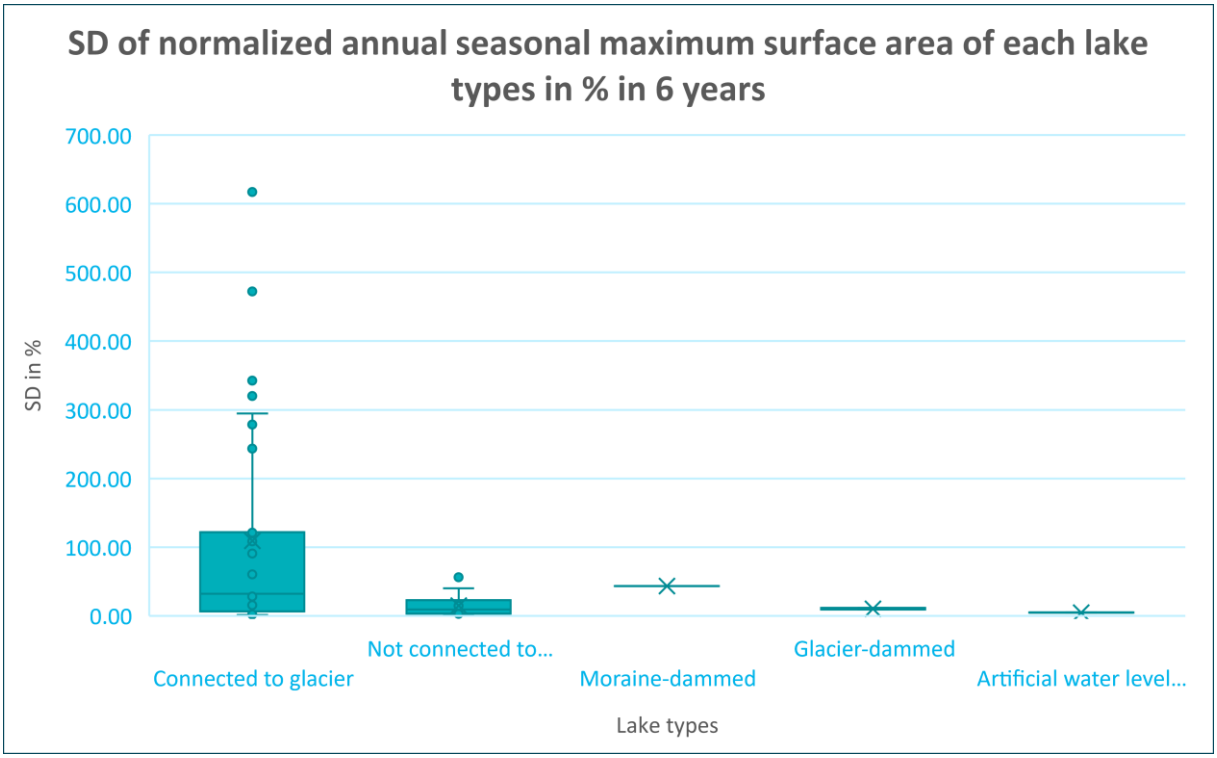

Figure 26: SD of normalized annual seasonal maximum surface area of each lake types in % in 6 years

Since the lake type 1 (*not-connected-to-glacier*), and lake type 2 (*connected-to-glacier*) contain considerably more lakes than others, the difference in % SD on annual seasonal maximum surface area between these two lake types was tested with a Mann Whitney U test (Wilcoxon rank sum exact test). The result from the test shows that the % SD of these two groups are significantly different (p-value = 0.01) from each other with 95% confidence interval. Therefore, lake type 1 (*Not-connected-to-glacier*) and lake type 2 (*Connected-to-glacier*) vary differently in % annual seasonal maximum surface area change in overall (6 years).

3.3 Trend in maximum annual surface area of each lake type over the 6-years period (2016-2021)

Despite having very few years in consideration, the probable trends of different lake types were studied both in absolute and normalized terms.

3.3.1 Trend in maximum annual surface area of each lake type over the 6-years period (2016-2021) in absolute terms

In order to check the trend in absolute maximum annual surface area of each lake type over the 6-years period (2016-2021), the mean of lakes belonging to each lake types were calculated for each year. There were 14 lakes in lake type 1 (*not-connected-to-glacier*) and 31 lakes in lake

type 2 (*connected-to-glacier*), but all lakes were not included in some years to calculate the mean due to absence of data (Tab. 10). There were just 2 lakes for each lake types; 3 (*glacier-dammed*) and 5 (*artificial-water-level-regulation*) but in 2020, there was data for just one lake in lake type 3 (*glacier-dammed*), so the mean calculation was not possible for that year. In case of lake type 4 (moraine-dammed), the actual data was used because of just one lake available in the category. The Tab. 10 shows the summary of total number of lakes available for calculating total and mean maximum surface area for each lake types each year.

Table 10: Summary of available lakes for calculating mean of annual seasonal maximum surface area of each lake types in km²

Lake types	Description	2016	2017	2018	2019	2020	2021
Type 1 (*Not-connected-to-glacier*)	Total Area (km²)	0.7745	0.7455	0.8285	0.8184	0.7376	0.8095
	No. of Lakes	12	12	14	14	13	14
	Mean Area (km²)	0.0645	0.0621	0.0592	0.0585	0.0567	0.0578
Type 2 (*Connected-to-glacier*)	Total Area (km²)	2.8278	3.0050	3.4400	3.5240	4.6430	3.6818
	No. of Lakes	31	32	32	32	27	32
	Mean Area (km²)	0.0912	0.0939	0.1075	0.1101	0.1720	0.1151
Type 3 (*Glacier-dammed*)	Total Area (km²)	0.1871	0.1944	0.2019	0.2063	0.0238	0.2060
	No. of Lakes	2	2	2	2	1	2
	Mean Area (km²)	0.0935	0.0972	0.1009	0.1031	0.0238	0.1030
Type 4 (*Moraine-dammed*)	Total Area (km²)	0.0077	0.0047	0.0129	0.0144	0.0102	0.0126
	No. of Lakes	1	1	1	1	1	1
	Mean Area (km²)	0.0077	0.0047	0.0129	0.0144	0.0102	0.0126
Type 5 (*Artificial-water-level-regulation*)	Total Area (km²)	12.5030	11.8526	12.7910	12.2806	12.7388	11.7433
	No. of Lakes	2	2	2	2	2	2
	Mean Area (km²)	6.2515	5.9263	6.3955	6.1403	6.3694	5.8716

Fig. 27 shows the mean of maximum annual surface area of lakes in each lake types in absolute term. Because of extremely high variation, the graph for lake type 5 (artificial-water-level-regulation) is presented separately in Fig. 28. The number of lakes used for calculation of mean is listed on the graph along with the line of mean at corresponding points (years).

Fig. 27 shows that mean maximum annual surface area for lake type 1 (*Not-connected-to-glacier*) was 0.0645 km^2 in 2016, but it slightly declined until 2018, and remained constant until 2021. Lake type 2 (*Connected-to-glacier*) had a mean maximum surface area of 0.0912 km^2 in 2016. It remained almost same in 2017 and then rose slightly up to 0.1075 km^2 until 2018. It remained constant again in 2019 and ascended to 0.1720 km^2 in 2020 followed by a descend to 0.1151 km^2 in 2021. Lake type 3 (*Glacier-dammed*) had a mean maximum surface area of 0.0935 km^2 in 2016. It then kept on ascending gently until 2019 to 0.1031 km^2 and sharply dropped to 0.0238 km^2 in 2020. The shape drop is because no available data for L58b which was among the 2 lakes in type 3. In 2021, it came back to 0.1030 km^2 again, so if we ignore the

plot for 2020, we can see a gradual rise in mean of seasonal annual maximum surface area of lake type 3 from 2016 until 2019 followed by a constant mean. The only lake in type 4 (*moraine-dammed*), L19 (*GID: 2352*), had its actual maximum surface area of 0.0077 km^2 in 2016. The size of this lake slightly decreased in 2017 and rose back again followed by almost constant area until 2021.

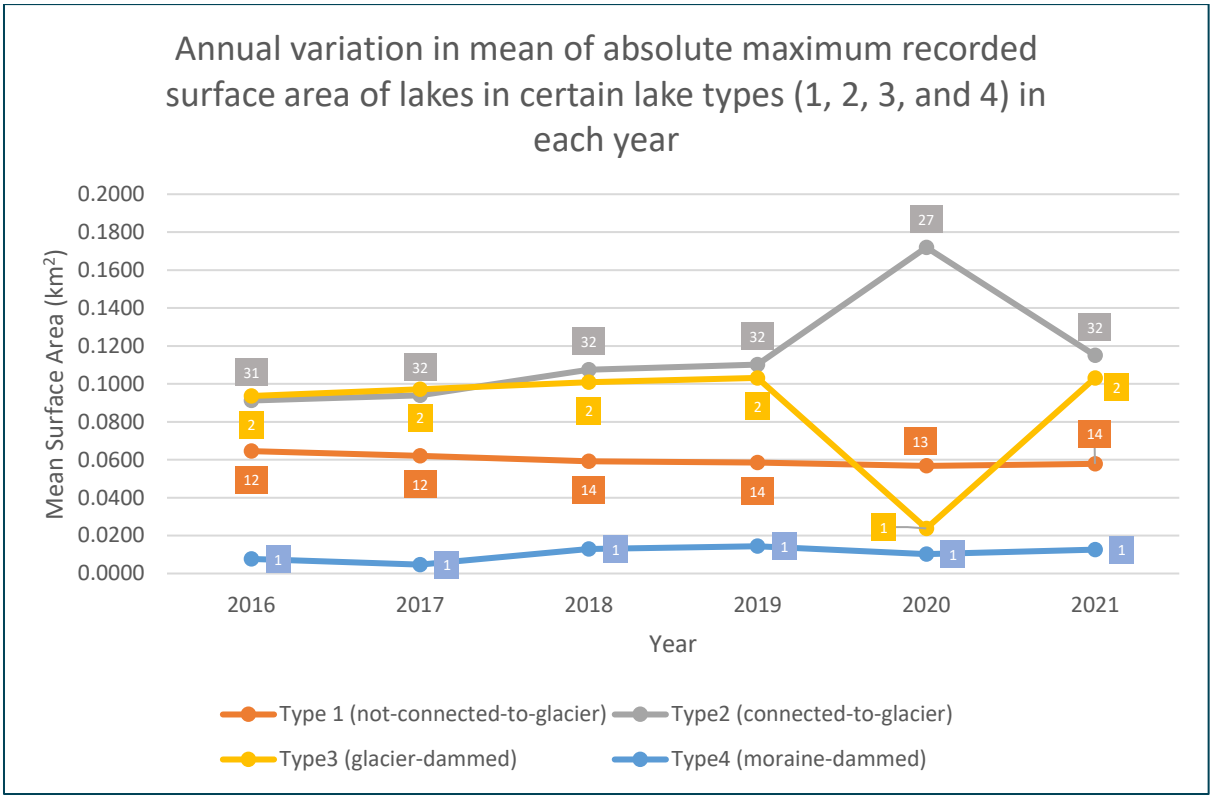

Figure 27: Mean of absolute maximum recorded surface area of lakes in certain lake types (1, 2, 3, and 4) in each year. Numbers in different coloured-boxes represents the number of lakes included to calculate the mean for particular year and for particular lake type.

Fig. 28 shows that the mean of maximum surface area of lake type 5 (*Artificial-water-level-regulation*) is fluctuating each year. In 2016, it was 6.2515 km^2 It became the highest in 2018 (6.3955 km^2) and the least in 2021 (5.8716 km^2). However, the change in maximum surface area of lake type 5 is because of artificial water level regulation system, therefore, these changes may not be concerned with climate change.

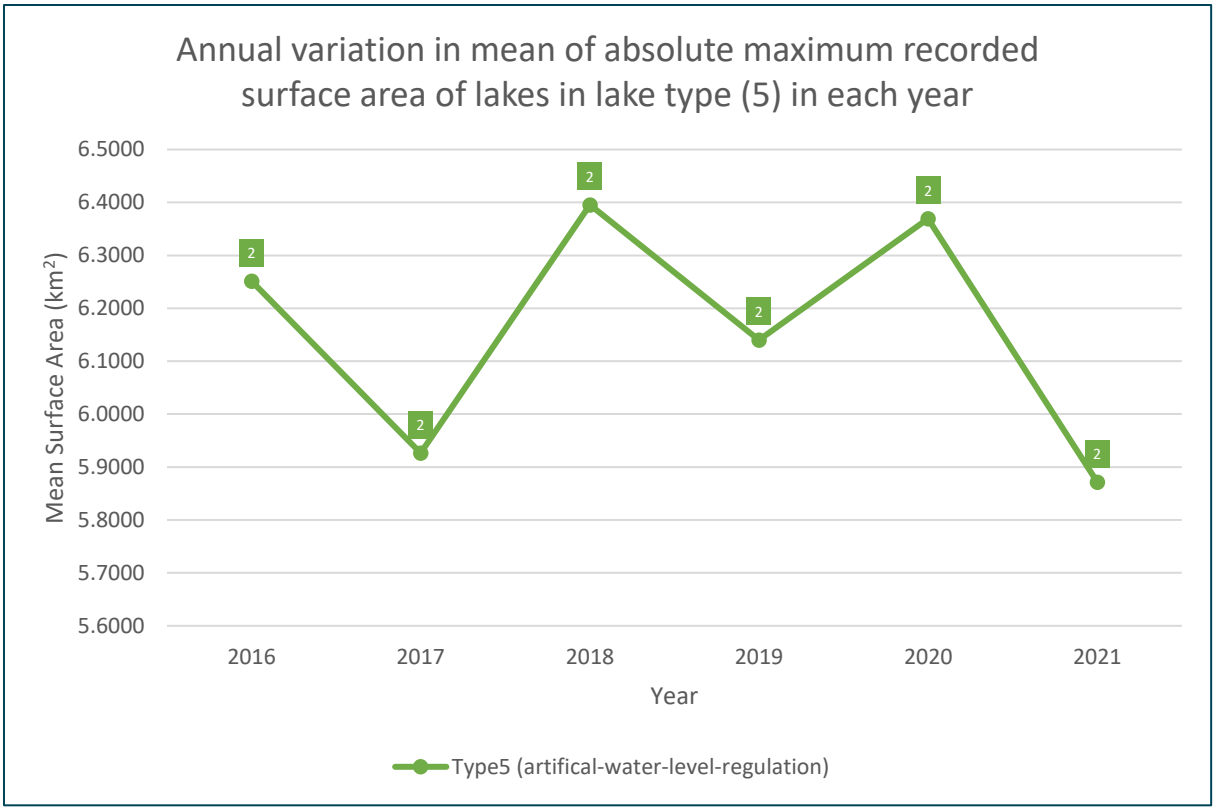

Figure 28: Mean of absolute maximum recorded surface area of lakes in lake type (5) in each year. Numbers in different coloured-boxes represents the number of lakes included to calculate the mean for particular year and for particular lake type.

3.3.2 Trend in maximum annual surface area of each lake type over the 6-years period (2016-2021) in normalized terms

To check the percentage change in mean of maximum annual surface area of lakes in each lake type, their mean was calculated for each year and presented graphically in Fig. 29. The Tab. 11 shows the total number of lakes available for calculating total and mean maximum surface area for each lake types.

Table 11: Summary of available lakes for calculating mean of annual seasonal maximum surface area of each lake types (in %)

Lake types		2016	2017	2018	2019	2020	2021
Type 1 (*Not-connected-to-glacier*)	Total Area (%)	1200.0	1181.3	1595.7	1535.0	1032.2	1524.6
	No. of Lakes	12	12	14	14	13	14
	Mean Area (%)	100.0	98.4	114.0	109.6	79.4	108.9
Type 2 (*Connected-to-glacier*)	Total Area (%)	3100.0	4062.1	8699.5	8565.5	5985.6	9860.7
	No. of Lakes	31	32	32	32	27	32
	Mean Area (%)	100.0	126.9	271.9	267.7	221.7	308.1
Type 3 (*Glacier-dammed*)	Total Area (%)	200.0	197.7	203.8	206.6	46.3	192.7
	No. of Lakes	2	2	2	2	1	2
	Mean Area (%)	100.0	98.8	101.9	103.3	46.3	96.3
Type 4 (*Moraine-dammed*)	Total Area (%)	100.0	61.0	167.9	186.6	132.5	163.6
	No. of Lakes	1	1	1	1	1	1
	Mean Area (%)	100.0	61.0	167.9	186.6	132.5	163.6
Type 5 (*Artificial-water-level-regulation*)	Total Area (%)	200.0	186.2	204.4	198.2	203.4	192.2
	No. of Lakes	2	2	2	2	2	2
	Mean Area (%)	100.0	93.1	102.2	99.1	101.7	96.1

Since the maximum surface area of each lake in each lake types in 2016 are normalized to 100 %, the mean of maximum surface area of each lake type is also 100 % as shown in Fig. 29. This makes easy comparison between different lake types in terms of percentage change in surface area annually. Therefore, according to Fig. 29, lake type 1 (*Not-connected-to-glacier*) does not show considerable changes from 2016 to 2021. It increased by around 10 % in 2018 and 2019, decreased by around 20 % in 2020 and again increased by around 10 % in 2021. On the other hand, lake type 2 (*Connected-to-glacier*) shows an increasing trend in 6 years period. It increased by 27 % in 2017, and sharply ascended by 172 % of the initial year in 2018. It remained somehow constant in 2019 and slightly dropped to 122 % followed by 208 % increase of the initial year. This is the highest record of % increase in lake surface area among all types of lakes in this study. The only lake in lake type 4 (*moraine-dammed*) shows a similar trend as of type 2 (*connected-to-glacier*) but with a slightly less increment. In 2017, it reduced by 41 % but it rose gradually in the following years; 2018 (68 %) and 2019 (87 %). In 2020 and 2021, it was 33 % and 64 % of the initial year.

The lake type 3 (glacier-dammed) shows very negligible amount of change (+/- 2 %) throughout the 6 years period. There was just one lake available for 2020, so the mean was not computed for that year which is why the depression is observed in the graph (Fig. 29). The lake type 5 (*artificial-water-level-regulation*), which showed high variation in absolute term has almost no change in terms of percentage change.

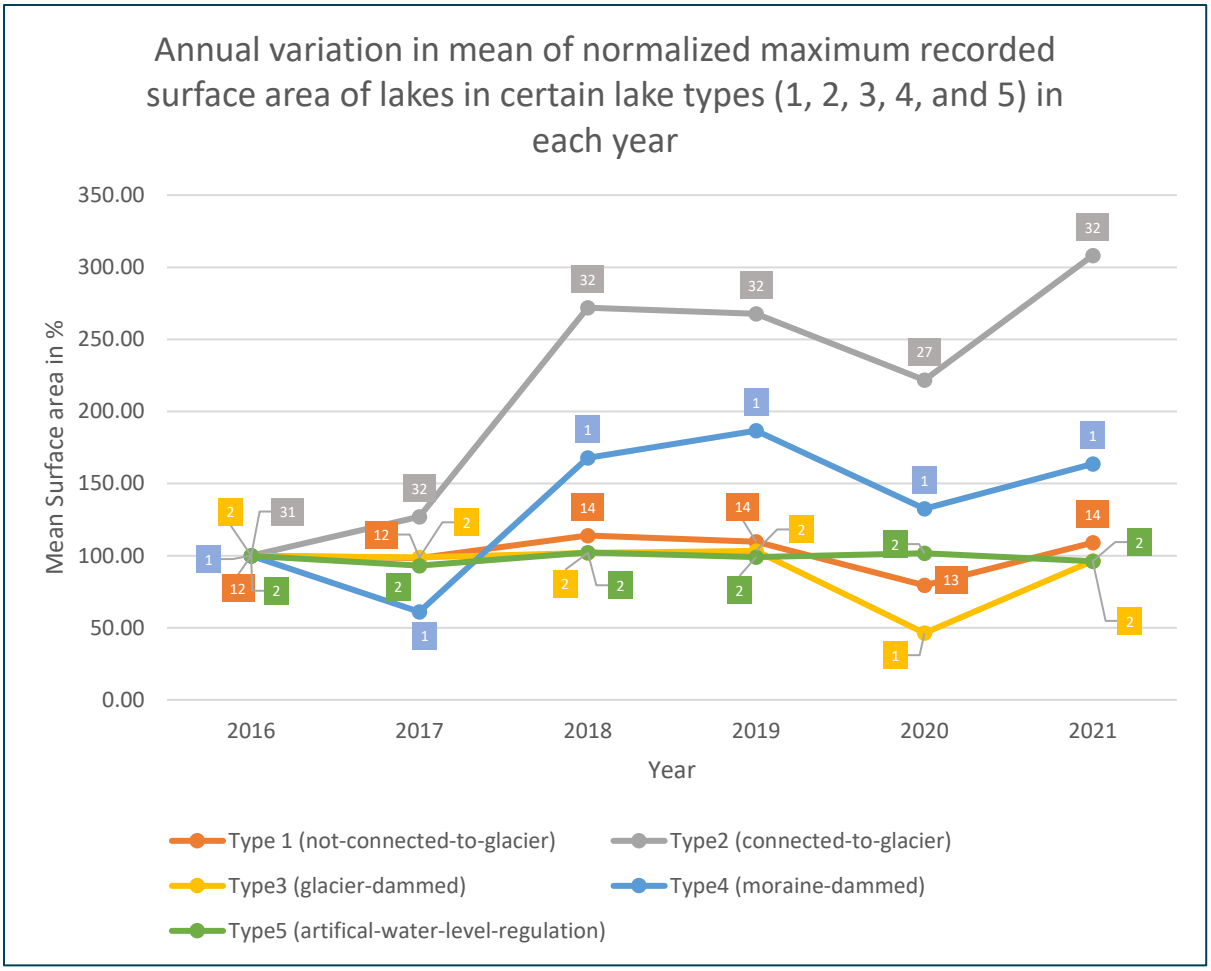

Figure 29: Mean of normalized maximum recorded surface area of lakes in certain lake types (1, 2, 3, 4, and 5) in each year. Numbers in different coloured-boxes represents the number of lakes included to calculate the mean for particular year and for particular lake type.

4 DISCUSSION

4.1 Lake area change indicative of GLOF event

Out of 4 lakes with history of outburst in Jostedalsbreen, there was no evidence of water accumulation (or lake formation) in L27 and L28 from 2016 to 2021, but the lakes L2 (*AG: Marabreen/GID: 2364/type - Glacier-dammed*) and L19 (*AG: Supphellebreen/GID: 2352*) (*Moraine-dammed*) demonstrated a considerable reduction in surface area implying to actual lowering of water level in most of the years. The normalized seasonal variation for L2 was the highest in the year 2019 (16.65 %) with maximum and minimum normalized area of 88 % and 55 % respectively. This means that the maximum amount of water collected in L2 was lower than the median (100 %) of surface area in 2016. The normalized maximum surface area in 2017 (88 %), 2018 (89 %), 2020 (72 %), and 2021 (66 %) were also similar or even lower. Since L2 is a *glacier-dammed* lake, and the mechanism for potential GLOF event to happen are overtopping and ice-dam floatation, the first mechanism is very unlikely as the maximum surface area (which corresponds to maximum water level) of L2 is decreasing each year (Fig. 30). On the other hand, due to decreased surface area (or decreased water level), the hydrostatic pressure of lake water may not be able to sufficiently overcome the ice overburden pressure of glacier to lift the ice and create a subglacial conduit to drain out more water. These might be the reasons why the lake L2 did not undergo rapid and complete drainage in 6 years' time interval.

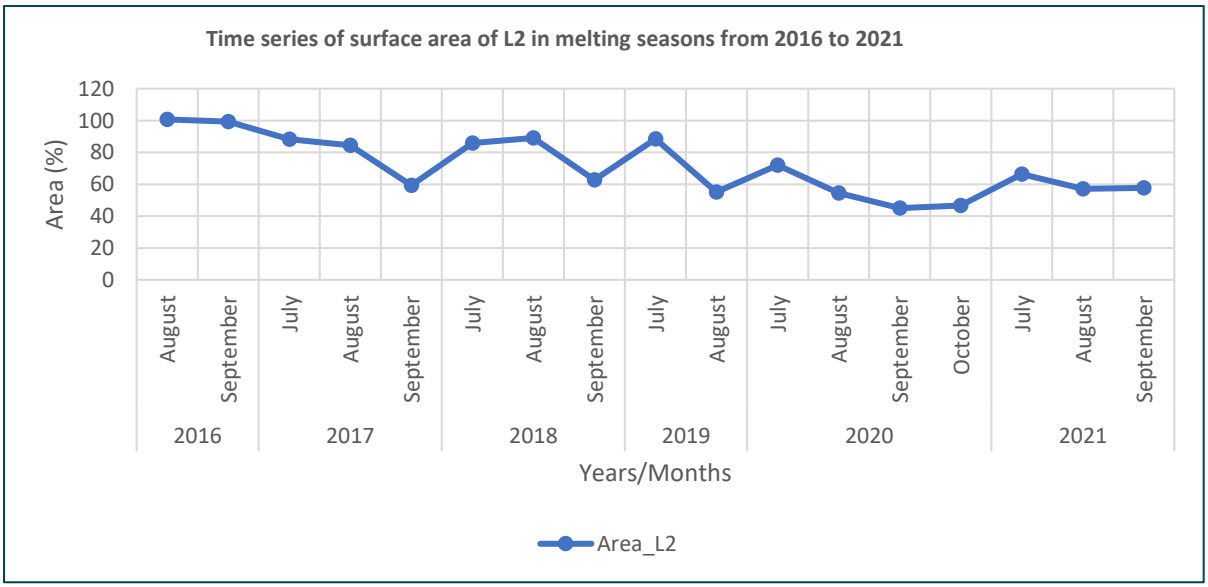

Figure 30: Time series of surface area of L2 (GID: 2364) in melting seasons from 2016 to 2021

Likewise, the normalized seasonal variation for L19 was the highest in the year 2021 (33.45 %) with the maximum and minimum normalized area of 173 % and 92 % respectively. The second highest normalized seasonal variation for L19 was in 2019 (23.85 %) with maximum and minimum normalized area of 197 % and 140 % respectively. In both these years, the regional surface temperature in summer was about 1.5 ºC to 1.7 ºC higher than the 1961- 1990 normal (Meteorological Institute Norway, 2021). So, the melting of glacier-ice was higher resulting in higher accumulation of water. However, in none of the years, the lake was drained completely and abruptly. This seems like the moraine dam at the frontal side of the glacier is stabilized after the last GLOF event in 2004 (Norwegian Water Resources and Energy Directorate, 2022a), letting the water drain out naturally from the incision at the side of the dam (Fig.s 32a; b). However, if the glacier continues to retreat making room for more water to collect, there is still a chance to break the dam near the weak incision part where there are unconsolidated materials collected from glacier retreat.

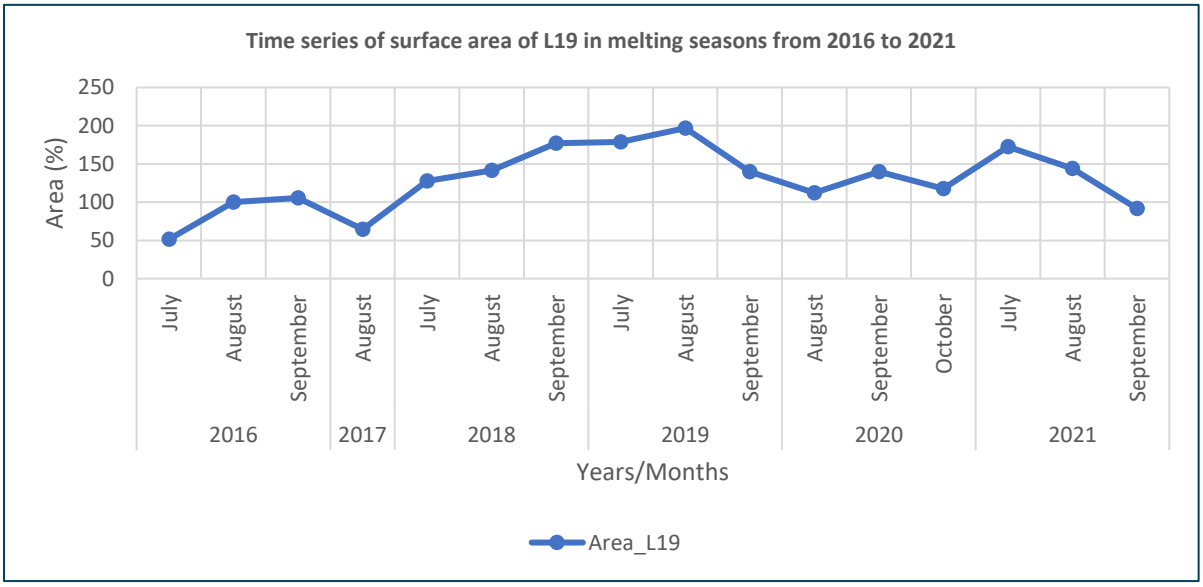

Figure 31: Time series of surface area of L19 (GID: 2352) in melting seasons from 2016 to 2021

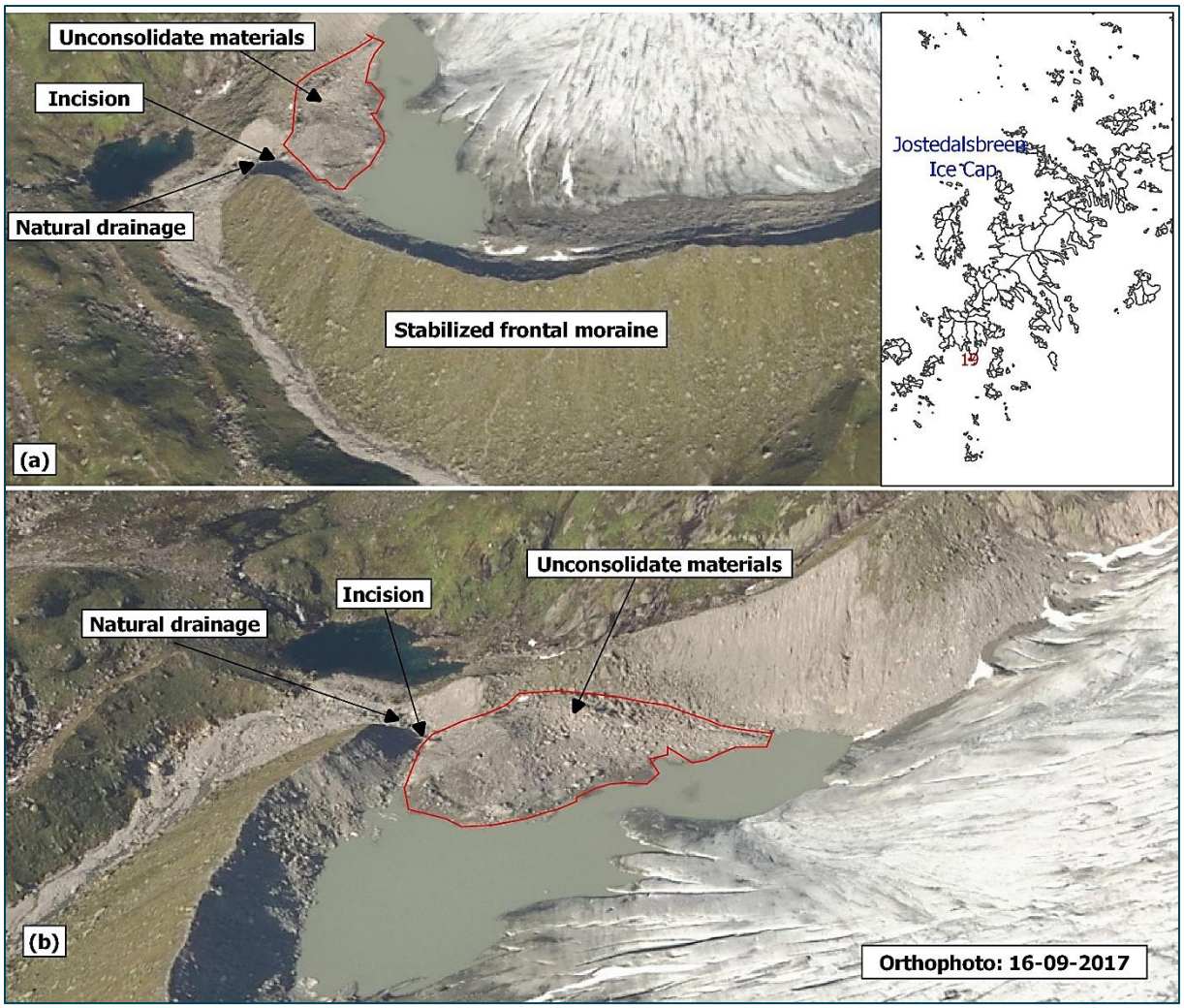

Figure 32: Impounding and outburst potentiality of lake L19 (GID: 2352). (a) Front view and (b) Side view. The back ground orthophoto is derived from (norgeibilder, 2022)

L5 (*AG: Melkevollbreen/GID: 2324/type: connected-to-glacier*) is one of the gradually increasing lakes threatening the human settlements downstream in Olden in Vestland county. In 6 years' time interval, there is no significant reduction in the surface area, rather it is gradually increasing in size each year (Fig.s 33; 34). The time series of annual maximum surface area of L5 shows an increasing trend in Fig. 35, though not statistically significant (p-value = 0.07). An annual increase in 10.40 % of surface area with reference to that of 2016 was observed for L5.

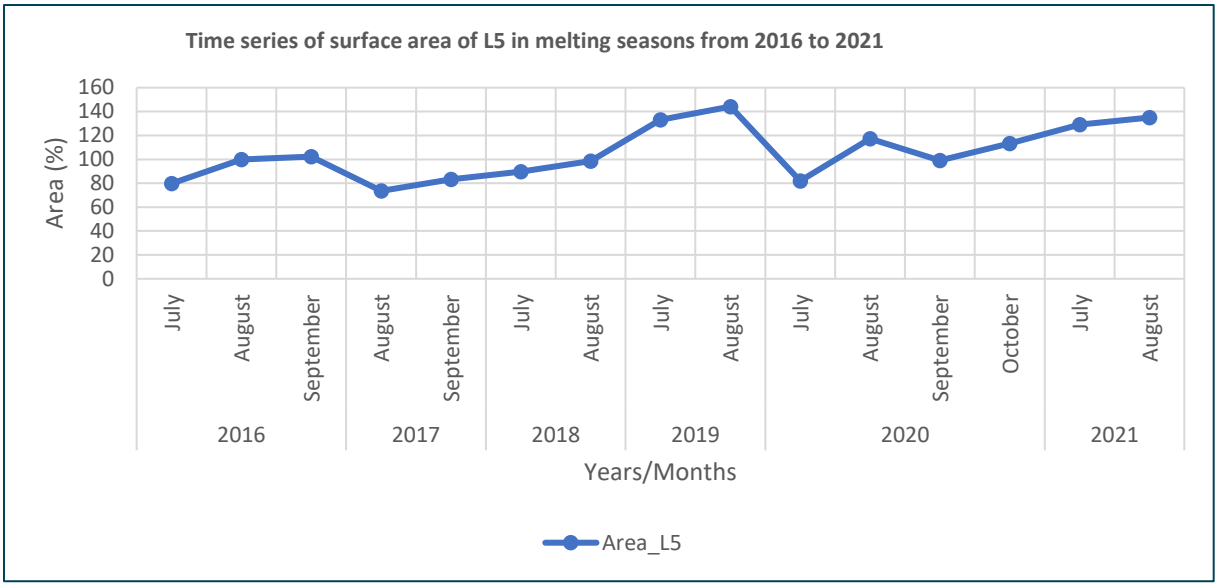

Figure 33:Time series of surface area of L5 (GID: 2324) in melting seasons from 2016 to 2021

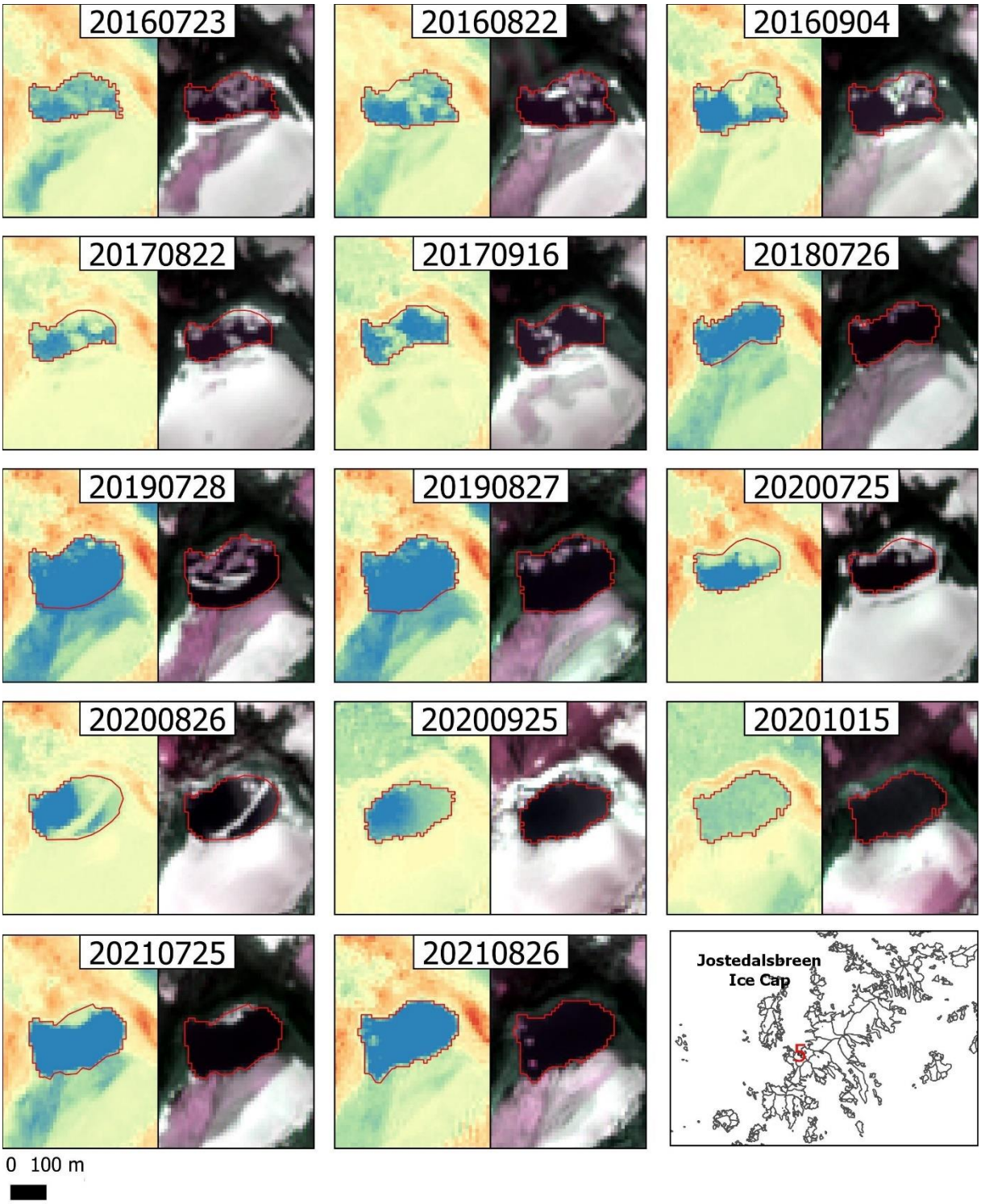

Figure 34: Outlines of L5 (AG: Melkevollbreen/GID: 2324/type: connected-to-glacier) which is increasing in surface area in a faster rate. The left frames represent NDWI images, and the right frames represent natural colour images

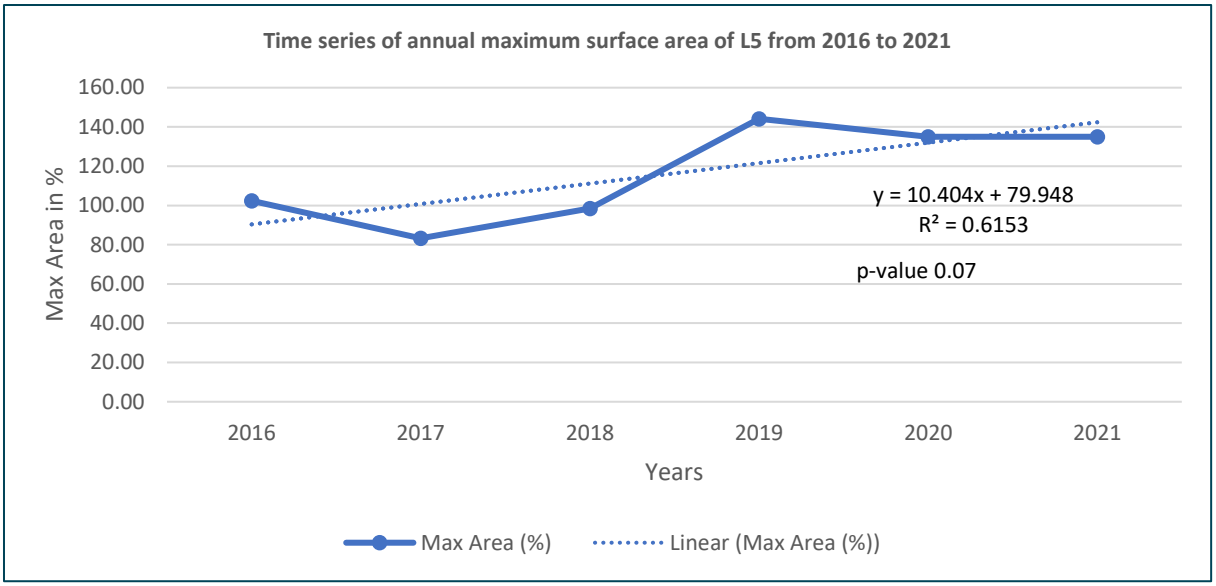

Figure 35: Time series of annual maximum surface area of L5 (GID: 2324) from 2016 to 2021

The lake has natural drainage which can been seen in the orthophoto taken in 06-07-2013 (Fig 36), but the glacier ice is continuously calving into the lake and the size of the lake is increasing each year at a faster rate. In such a scenario, there might be the chance of occurring displacement wave overtopping the moraine dam causing GLOF, and as the size of the lake is bigger, the impact of GLOF hence produced will be higher. It is also clearly seen in the Fig. 37 that the height of the damming structure is not so high, so overtopping due to displacement wave caused by ice-calving is very likely to happen. However, it is required to check the geology and morphology of damming structure to assure how strong it is to withstand such displacement waves.

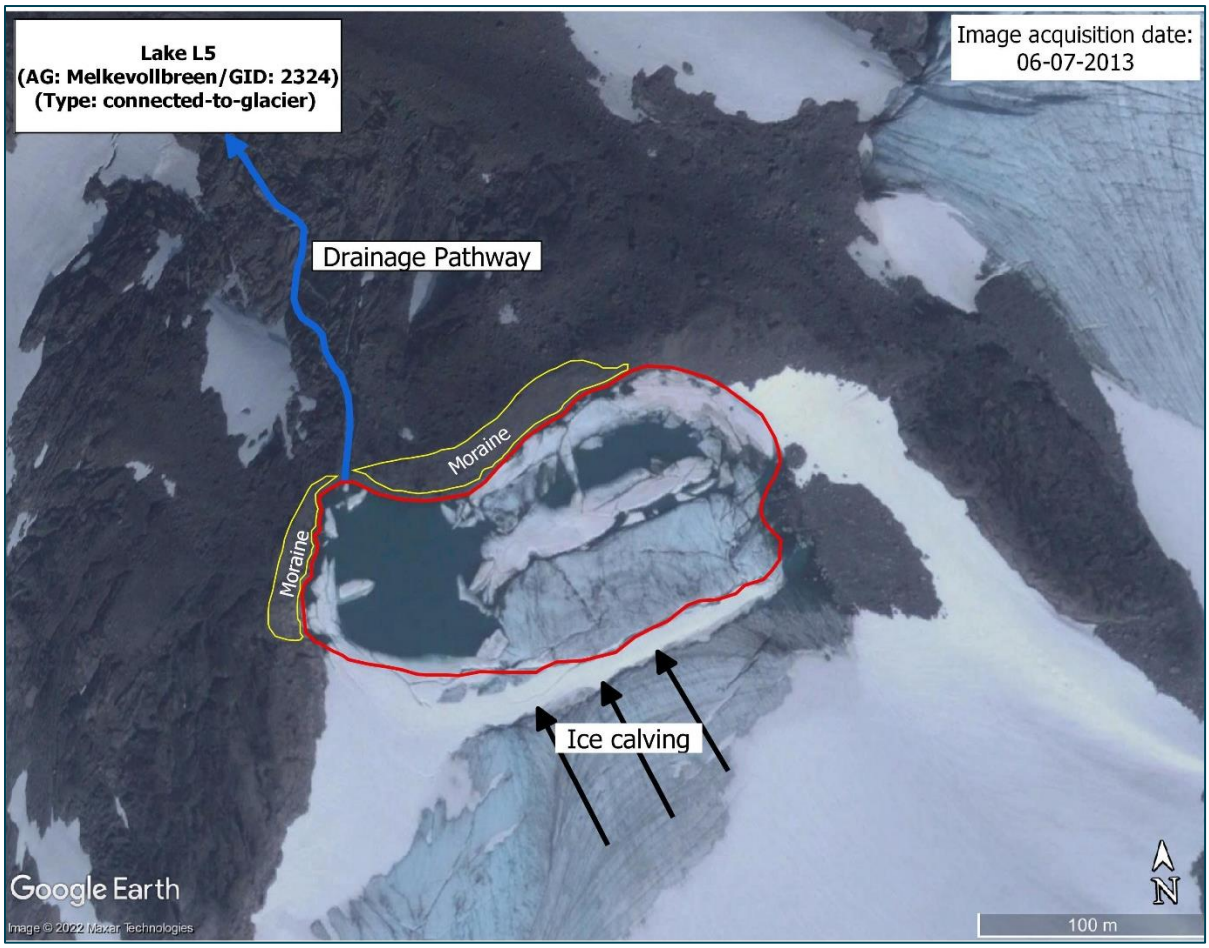

Figure 36: L5 (AG: Melkevollbreen/GID: 2324/type: connected-to-glacier) with its drainage path, moraine, and ice calving. Image acquisition date: 06-07-2013. Source: Google Earth

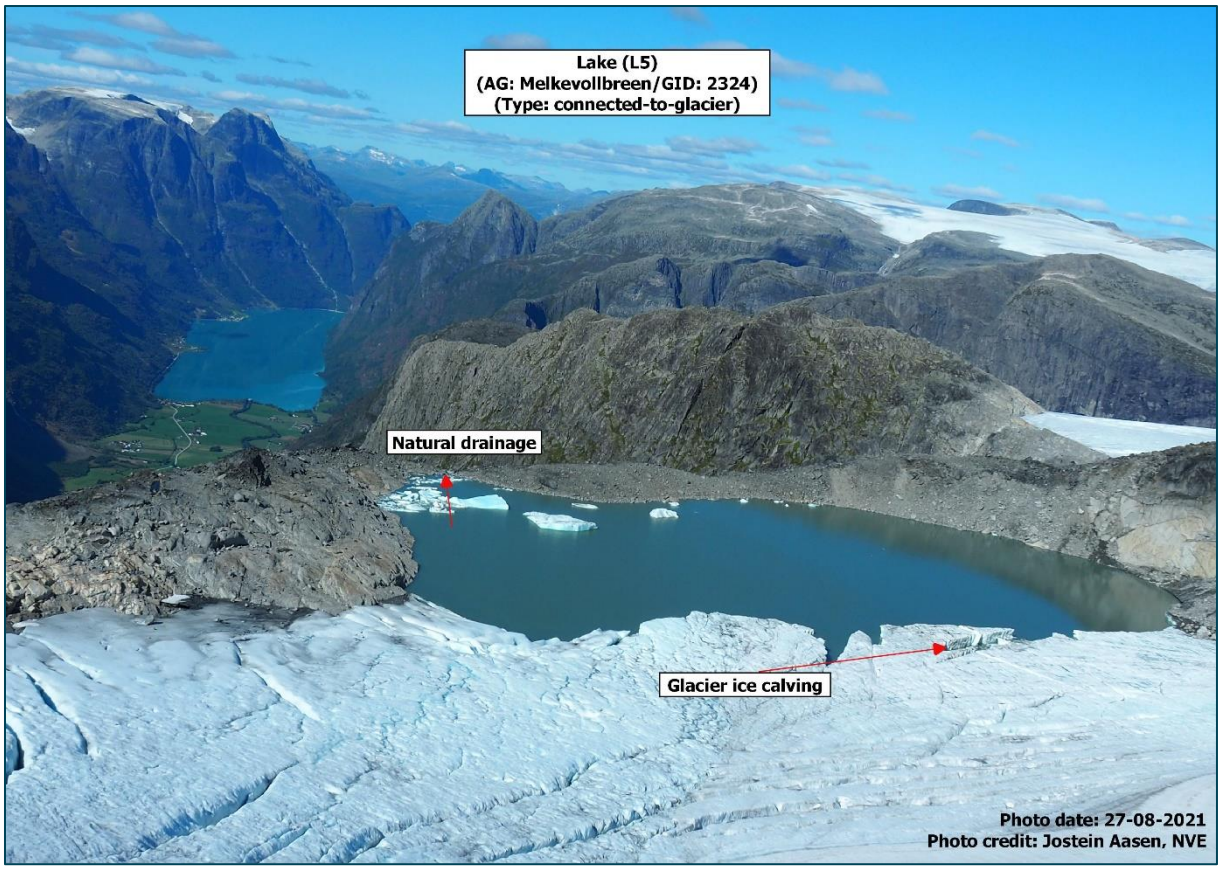

Figure 37: Recent picture of L5 (AG: Melkevollbreen/GID: 2324/type: connected-to-glacier). Photo date: 27-08-2021. Photo Credit: Jostein Aasen, NVE

Despite the fact that lakes *not-connected-to-glaciers* have remained almost constant for the last six years, outburst flood events can occur if a massive rockfall, an avalanche, or landslide occurs nearby. In addition, an earthquake can also trigger outburst in lakes *not-connected-to-glaciers*.

4.2 Sensitivity of lakes connected-to-glaciers including moraine-dammed and glacier-dammed lakes

The result of this study clearly shows that lakes *connected-to-glacier*s are more variable in surface area compared to lakes *not-connected-to-glacier*s which is in line with different studies conducted in other parts of the world (Aggarwal et al., 2017; Bajracharya et al., 2008; Komori, 2008; Mohanty & Maiti, 2021; Wang et al., 2015). The changes observed in lakes *connected-to-glacier*s are so dramatic that they show very high percentage change within short period of time i.e., 6 years. The top 9 lakes in highest % SD namely L23 (*GID: 2293*), L34 (*GID: 2303*), L55 (*GID: 2124*), L13 (*GID: 2459*), L41 (*GID: 3628*), L56 (*GID: 2520*), L18 (*GID: 2327*), L1 (*GID: 2364*), and L54 (*GID: 2118*) show extremely high percentage increase in surface area over 6 years ranging from 161 % (L56) to 3452 % (L23) which is more than what is observed in glacial lakes in other parts of the world. For instance, lake Imja Tsho in Everest region, Nepal

grew to almost 1 km^2 in 5 decades from non-existence in 1960 and some glacial lakes in Pho Chu basin of Bhutan Himalaya expanded by around 800 % in 4 decades (Bajracharya et al., 2008). Even if no significant rapid drainage events have been recorded indicative of outburst, the annual seasonal variation and overall (6 years) variation in surface area is so severe for lakes *connected-to-glacier* which indicates that the impact due to their potential outburst will be significantly higher than experienced in some glacial lakes in the past.

As indicated by (Aggarwal et al., 2017) in their study in Sikkim, India, lakes in contact with glaciers are expanding at high rate in the last two decades and the major factors affecting this expansion are frequent glacier calving, glacier retreat and ice loss which are similar to the findings of this study. For instance, L17 (*AG: Tunsbergdalsbreen/GID: 2320/Type: connected-to-glacier*) and L18 (*AG: Austerdalsbreen/GID: 2327/Type: connected-to-glacier*) clearly show the impact of these factors for lake expansion. As these lakes grow along with exposing land mass at the terminus, they may slide down to the lake as the melting continues causing shock waves and leading to outburst. Therefore, lakes *connected-to-glacier* are potentially more dangerous as compared to others.

4.3 Change in lake types

Along glacier retreat over time, some lakes have been changed from one type to another. Specially, lakes initially *connected-to-glacier* such as L48 (Fig. 38) and L52 (Fig. 39) are disconnected by the end of 2021, whereas some lakes like L42 (Fig. 40) remained connected in 2016, 2017 and 2019 and was disconnected in 2018, 2020, 2021. L22 (Fig. 41) was detached once in 2019-08-27. Likewise, some lakes remained frozen in some years and reappeared in 2021. L13 (*GID: 2459*) (Fig. 42) is one lake of such type. L50 (Fig. 43) is a lake with peculiar example where it is detached along with a small portion of glacier. L23 (Fig. 44) which showed highest variation among all lakes was actually a *supraglacial-lake* which eventually expanded and found an outlet. In 2016, there was no sign of its formation. In 2017, a clear sign of water accumulation was observed. In 2018-07-26, a clear *supraglacial-lake* was observed but it remained frozen for rest of the year. Similarly, it appeared again in 2019-08-27 with significantly large surface area and again remained frozen for rest of the year. Surprisingly, it remained frozen in 2020, but opened up again in 2021-09-13 with its largest area observed since 2016. The lakes which eventually disconnected from the glacier by the end year 2021 such as L42, L48, L50, and L52 (Tab.s 8; 9) showed a medium variation in surface area ranging from 10.06% SD (L50) to 39.90% SD (L42). It also indicates that lakes in transition phase from type

2 (*connected-to-glacier*) to type 1 (*not-connected-to-glacier*) tend to be stable in surface area as there will be less influence of glacier terminus which advance and retreat in a single season and in a couple of years changing the surface area coverage of lake.

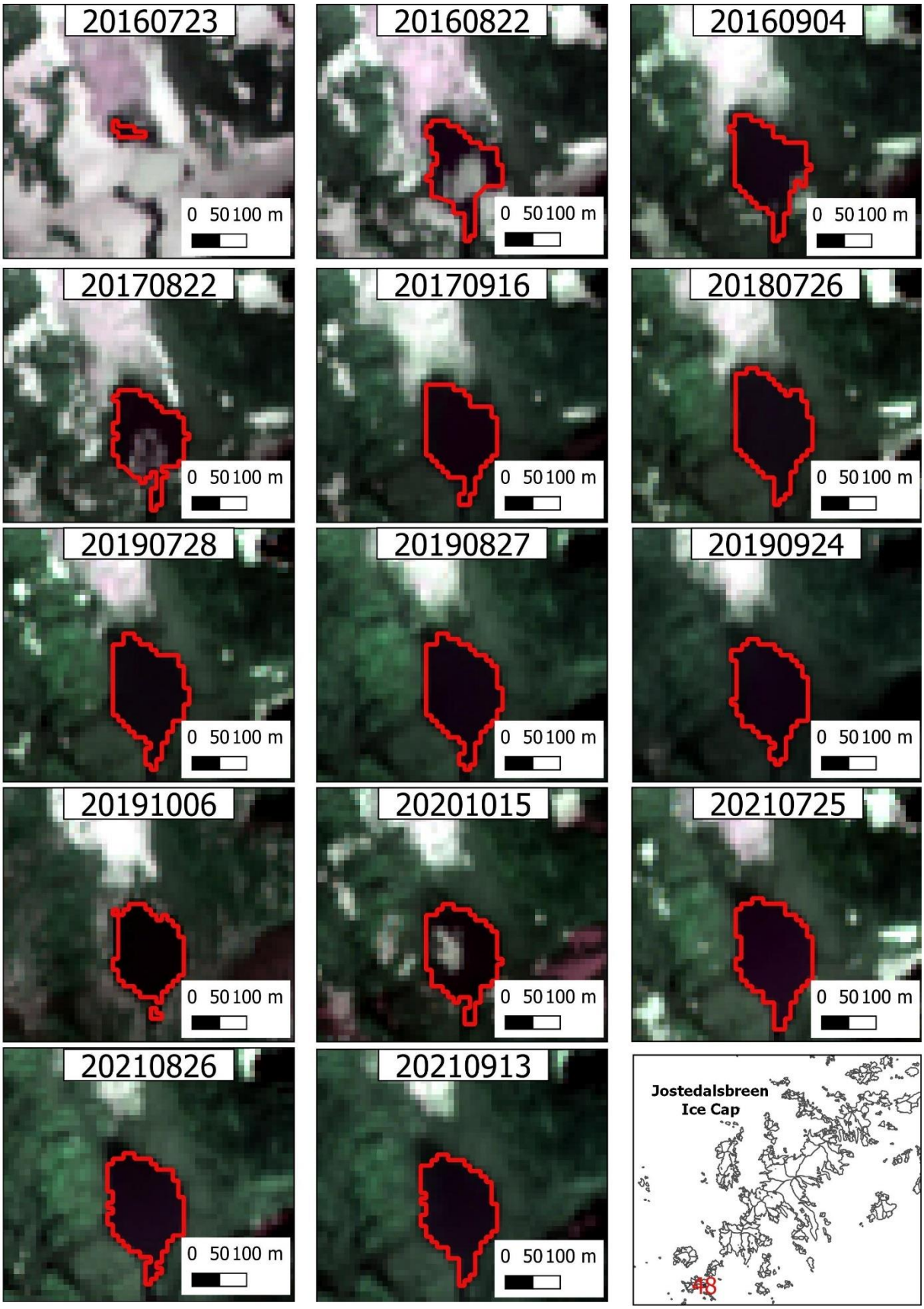

Figure 38: L48 (GID: 2145) which is disconnected from the glacier by 2021

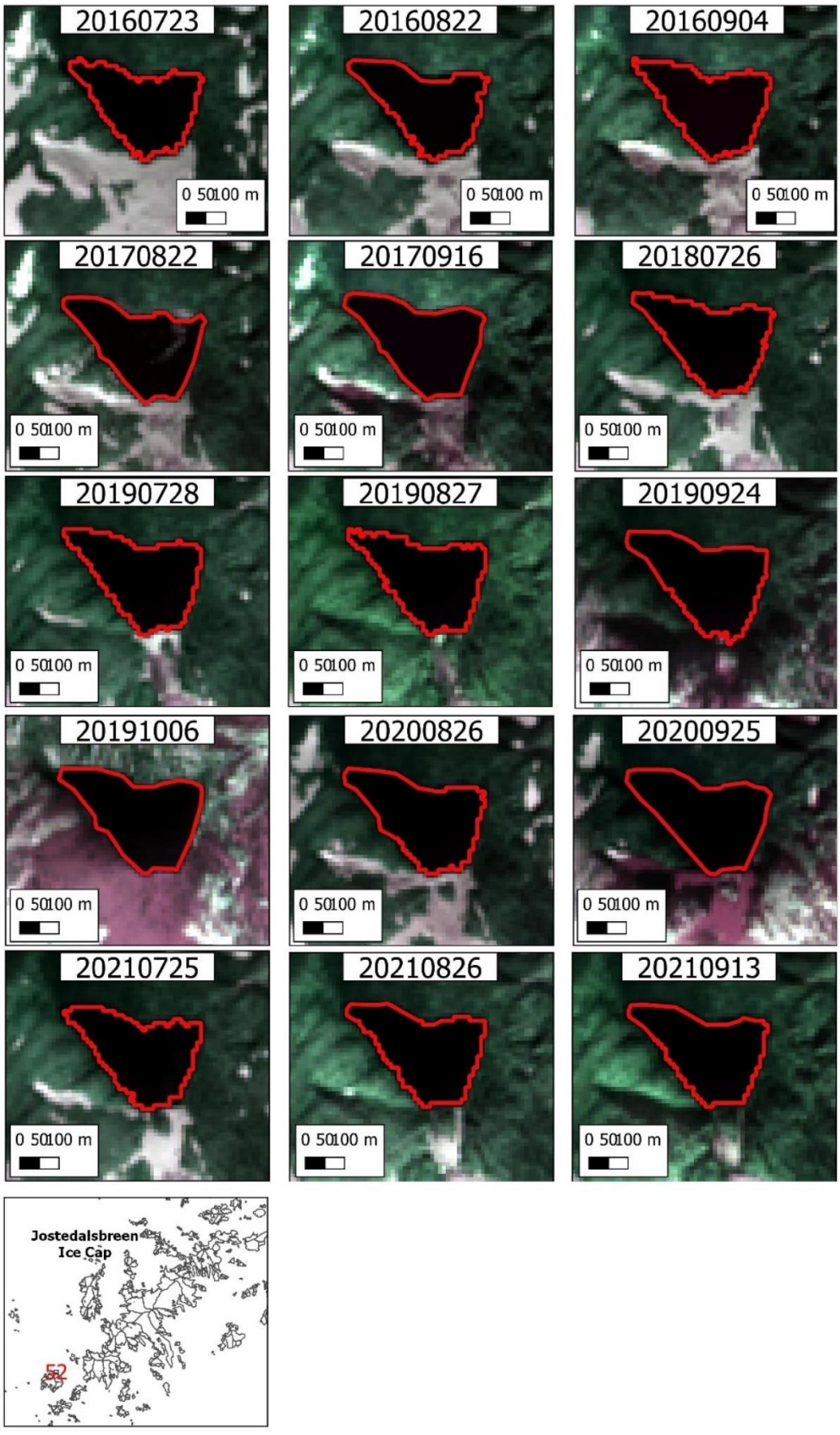

Figure 39: L52 (GID: 2119) which is disconnected from the glacier by 2021

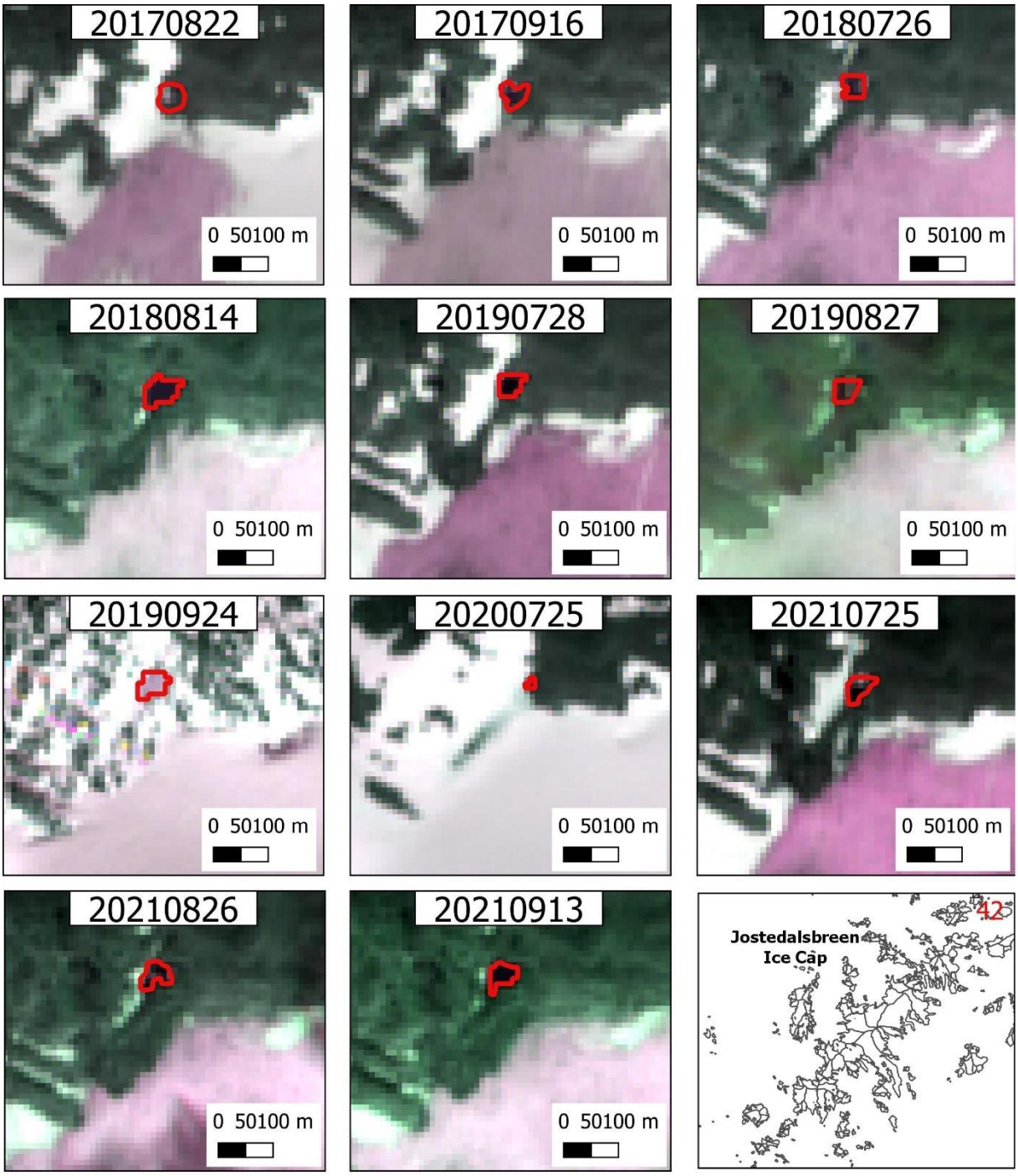

Figure 40: L42 which remained connected and disconnected in alternative years

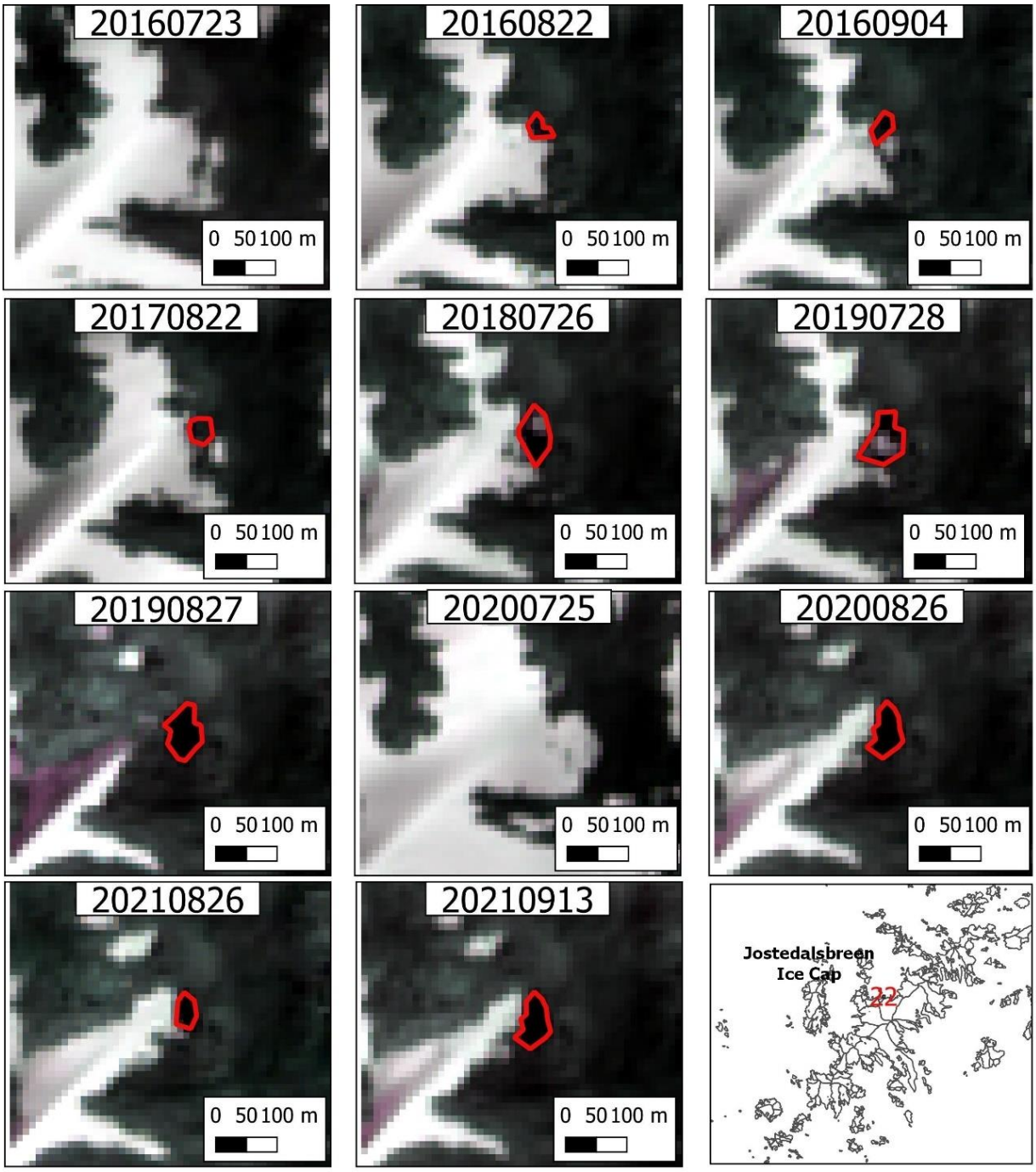

Figure 41: L22 (GID: 2294) which remains mostly frozen throughout the year

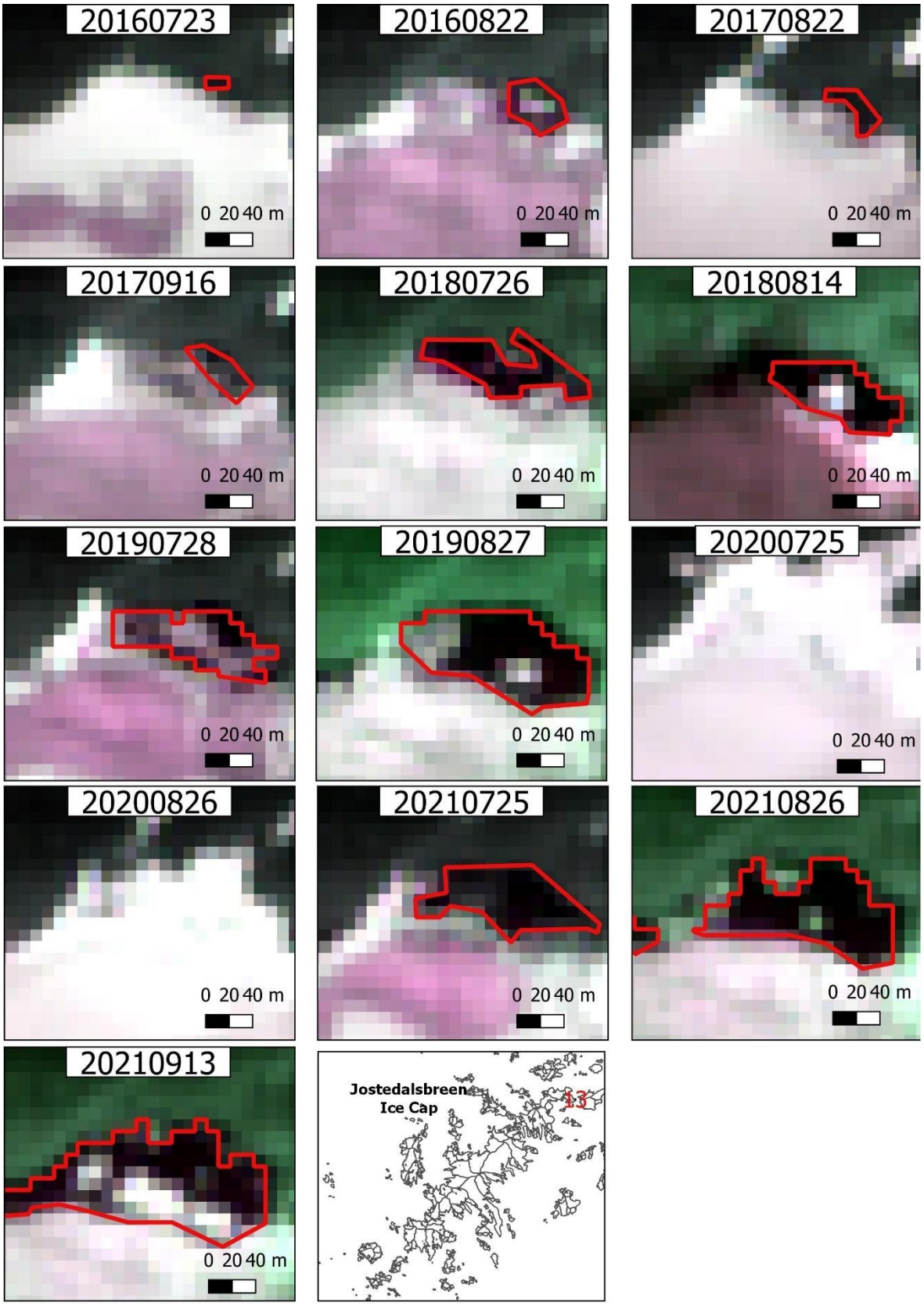

Figure 42: L13 (GID: 2459) which is covered in ice in alternative years

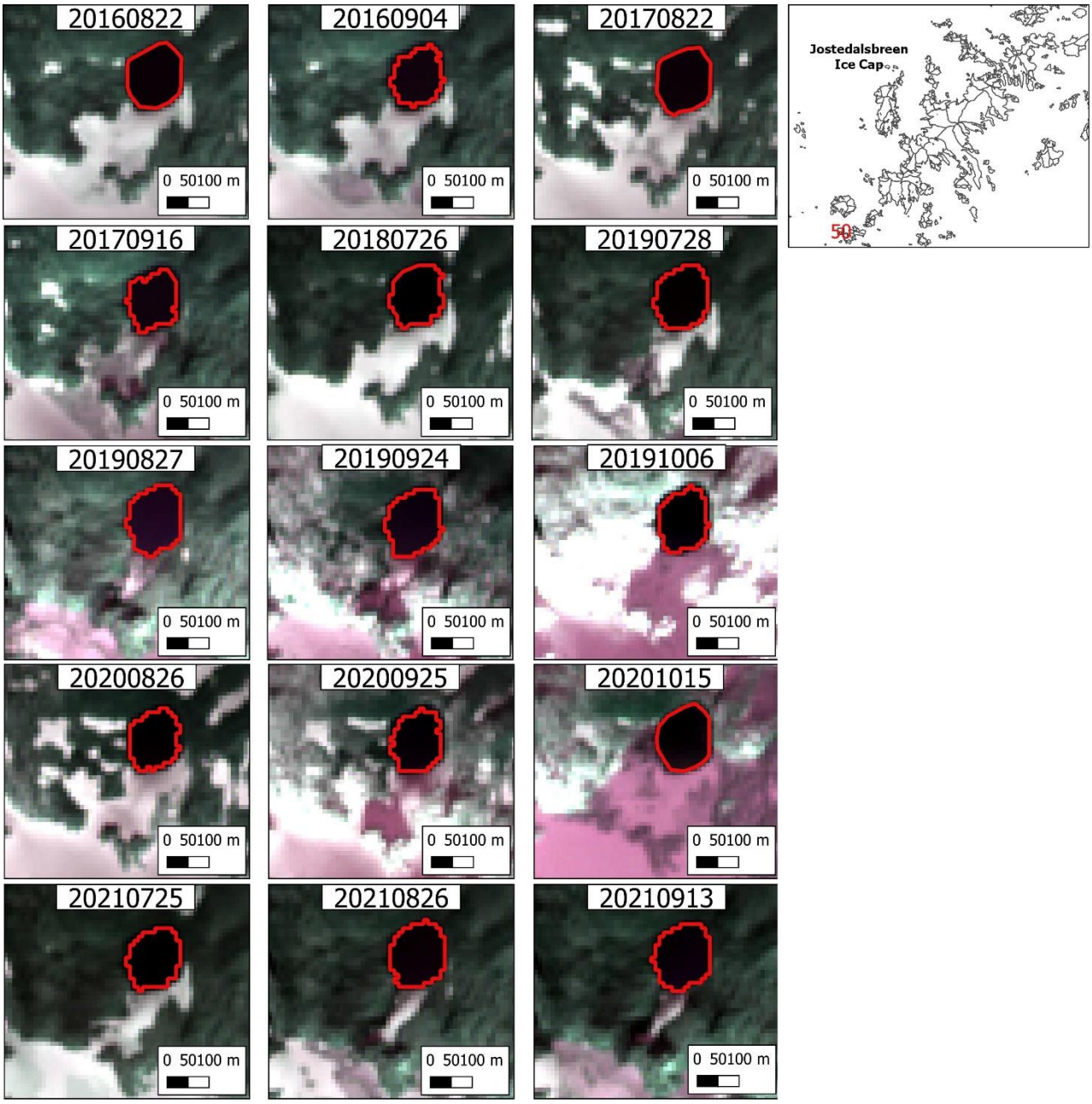

Figure 43: L50 (GID: 3848) which is disconnected along with a part of glacier

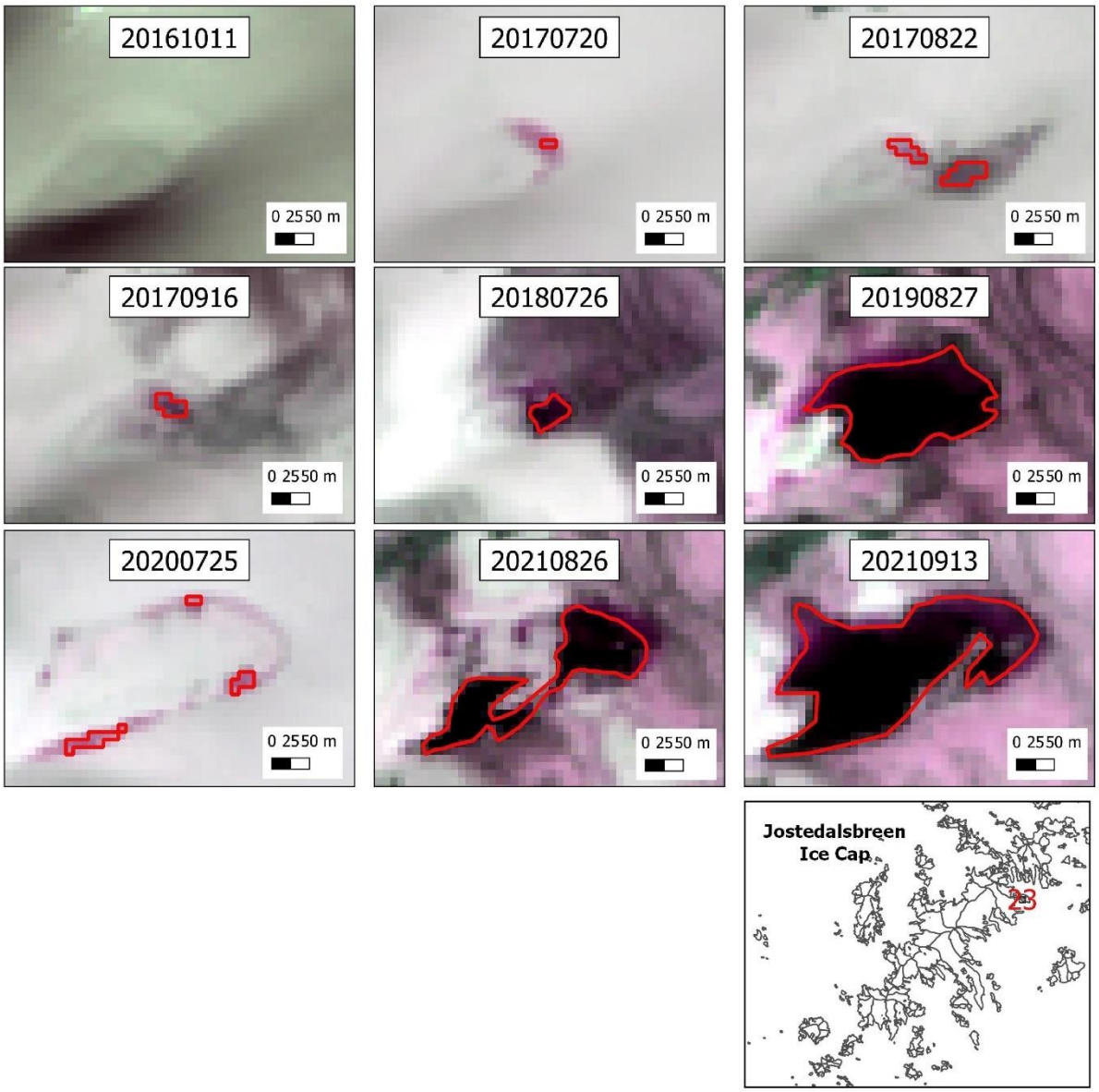

Figure 44: Evolution of supraglacial-lake (L23 (GID: 2293)) which has the highest % variation among all lakes

4.4 Relation of glacial lake surface area variation with variation in mass balance of glacier and regional surface temperature

Mass balance is an important factor contributing to the size of the glacial lakes but, due to intensive process, not all glaciers in Jostedalsbreen have continuous updated data available on this. However, there is a study on Nigardsbreen and Austdalsbreen glaciers which has glacier mass balance data until 2020 updated through glaciological investigations by the Norwegian Water Resources and Energy Directorate (NVE; Kjøllmoen, Andreassen, Elvehøy, & Melvold, 2021). These glaciers fall within my study area. Mass balance data of 2020 in the paper by

(Kjøllmoen et al., 2021) showed that Nigardsbreen had the highest (1.65 m w.e.) annual mass balance and Austdalsbreen has the 3rd highest (0.78 m w.e.) annual mass balance of 9 glaciers considered under study, but the figures were negative in 2018 and 2019 indicating that the glacial lakes formed at the terminus of the glaciers should have increased in size because of ablation, and calving with some time lag (Fig.s 45; 46). Unfortunately, there was no lakes in direct contact with the glacier under study in Nigardsbreen. However, L23 (*Supraglacial lake*) (*GID: 2293*) and L24 closer to Nigardsbreen glacier showed results resonating with its mass balance. Both these lakes were enlarged in 2018 and 2019 whereas they remained frozen all-round the year in 2020 (Fig.s 47; 48). This variation can be better explained by the rise in both seasonal (summer) and annual temperature in 2018 and 2019 as shown in the Fig.s 49 and 50. Due to slight drop in seasonal (summer) temperature in 2020, lake L23 was still covered with ice but with marginal opening at the periphery of the lake.

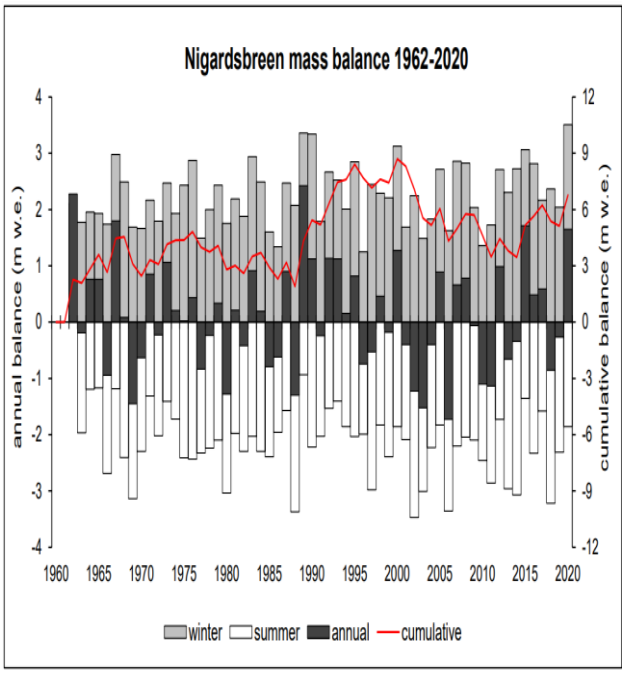

Figure 45: Mass balance of Nigardsbreen for winter, summer and annual from 1962 to 2020. Red line indicates cumulative mass balance (source: (Kjøllmoen et al., 2021) *)*

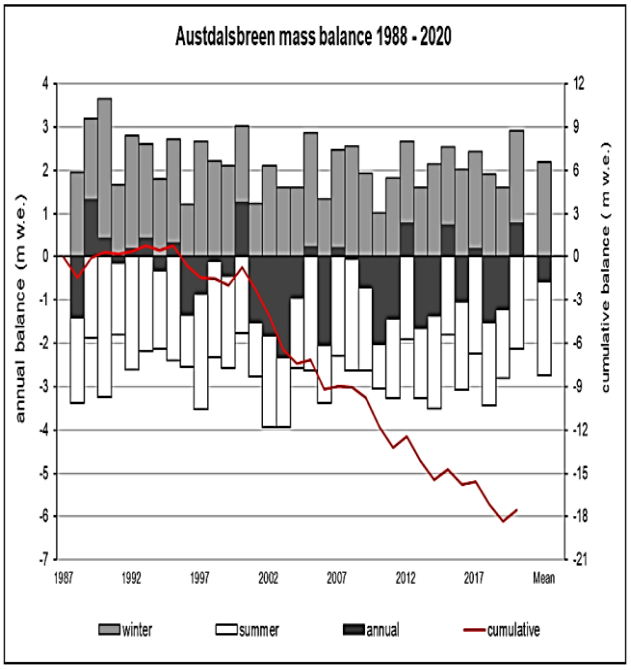

Figure 46: Mass balance of Austdalsbreen for winter, summer and annual from 1962 to 2020. Red line indicates cumulative mass balance (source: (Kjøllmoen et al., 2021)*)*

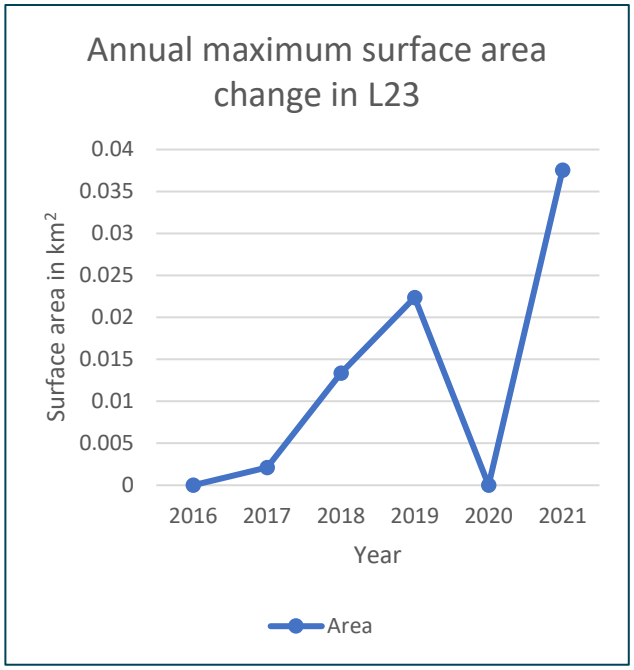

Figure 47: Annual maximum surface area changes in L23 (supraglacial lake)

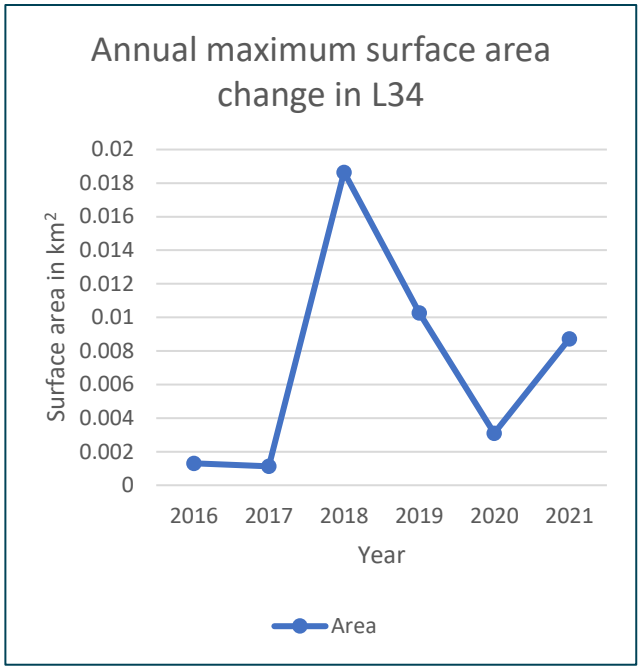

Figure 48: Annual maximum surface area changes in L34

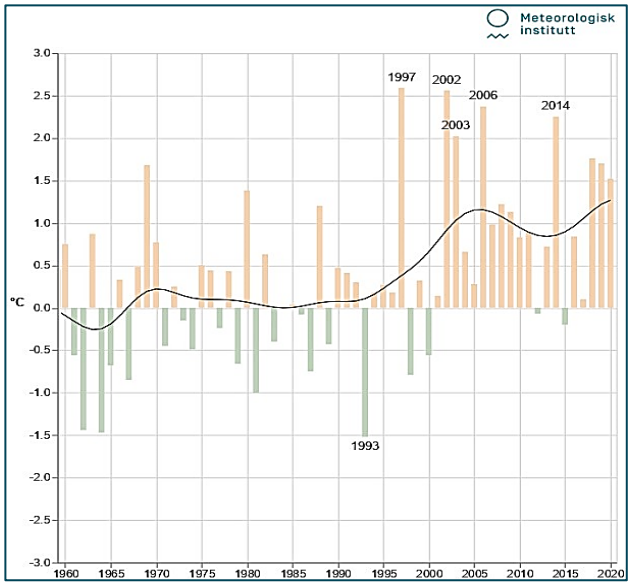

Figure 49: Temperature development in Western Norway annually in summer season from 1961-1990 normal. Green bars represent temperature below normal, and orange-coloured bars represent temperature above normal. Black-coloured bars represent the trend in temperature variation. Source: Meteorological Institute Norway, 2021

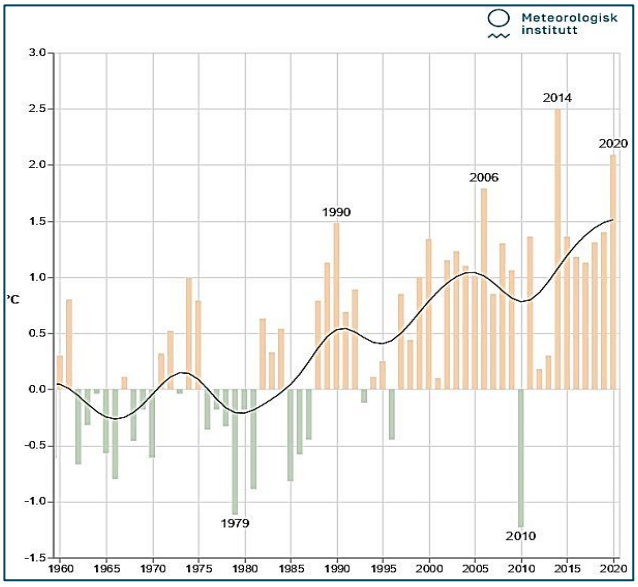

Figure 50: Temperature development in Western Norway annually from 1961-1990 normal. Green bars represent temperature below normal, and orange-coloured bars represent temperature above normal. Black-coloured bars represent the trend in temperature variation. Source: Meteorological Institute Norway, 2021

Likewise, the terminus in Austdalsbreen at L15 (*AG: Styggevatnet/GID: 2478/type: artificial-water-level-regulation*) retreated to around 60 m in 2018 with an ice loss of 0.0434 km^2 and 120 m in 2019 with an ice loss of 0.0838 km^2 as compared to that of 2017 outline. But the

following year in 2020, it extended forward to around 60 m with an ice gain of 0.0287 km^2 (Fig. 50). Satellite images well captured these variations of glacier terminus, including advances, but it is difficult to interpret the results with climate change in lakes with *artificial-water-level-regulation* system. As a matter of fact, Austdalsbreen (*GID: 2480*) is not selected as a reference series for climate change studies as it is regulated (Andreassen & Elvehøy, 2021). Austdalsbreen (*GID: 2480*) was excluded as reference glacier because it was calving into a hydro-power reservoir, and consequently the glacier is influenced by the water level regulations (Fleig et al., 2013).

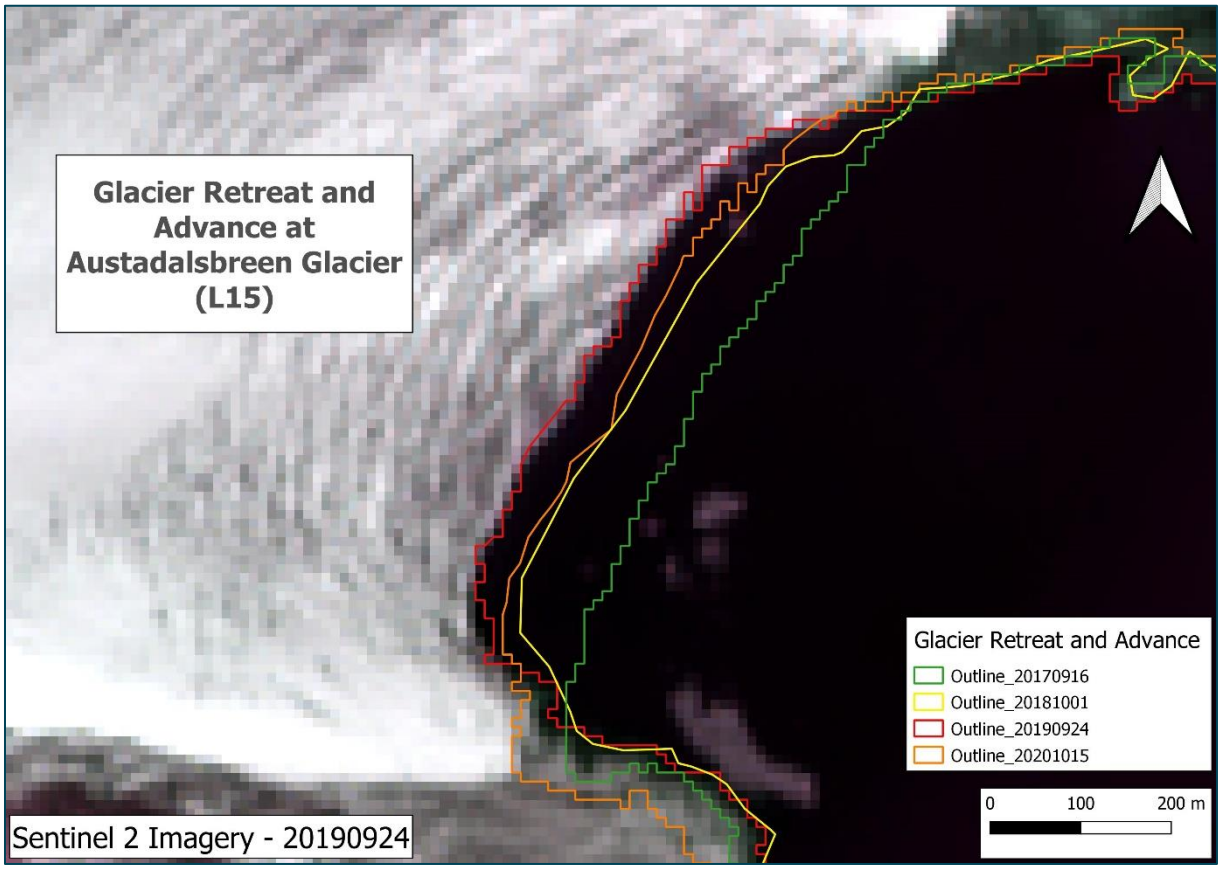

Figure 51: Glacier retreat and advance in Austdalsbreen Glacier (L15 (GID: 2478))

Assuming the similar trend of mass balance (though not so confident due to time lag) and regional annual and seasonal (summer) temperature of all glaciers in the study area and comparing the trend with the trend of lake surface area change in Fig. 29 in Results section, we can observe that lakes *connected-to-glacier* including *moraine-dammed* lakes show significantly high rise in surface area in the year 2018 and 2019, and a significant fall in 2020. Specially in low lying lakes where most of the ablation and calving occurs such as in L17 (*AG: Tunsbergdalsbreen/GID: 2320*) (535 m from m.s.l) and L18 (*AG: Austerdalsbreen/GID: 2327*) (387 m from m.s.l.), the glacier retreat is clearly visible exposing rocks underneath and

expanding the surface area for lakes. The glacial-ice calving can be seen distinctly in the Fig.s 52 and 53.

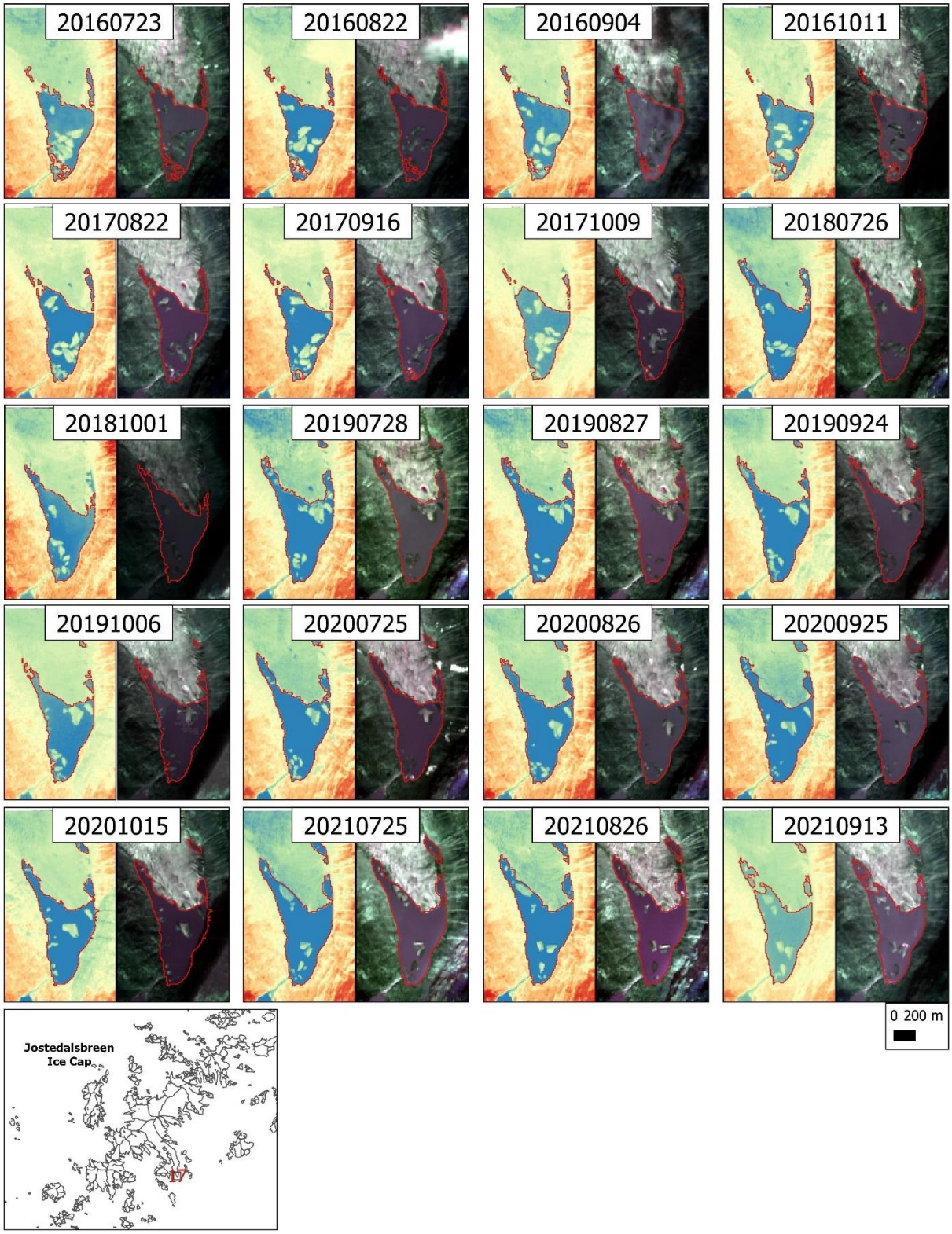

Figure 52: L17 (AG: Tunsbergdalsbreen/GID: 2320) (ice calving and glacier retreat). The left frames represent NDWI images, and the right frames represent natural colour images

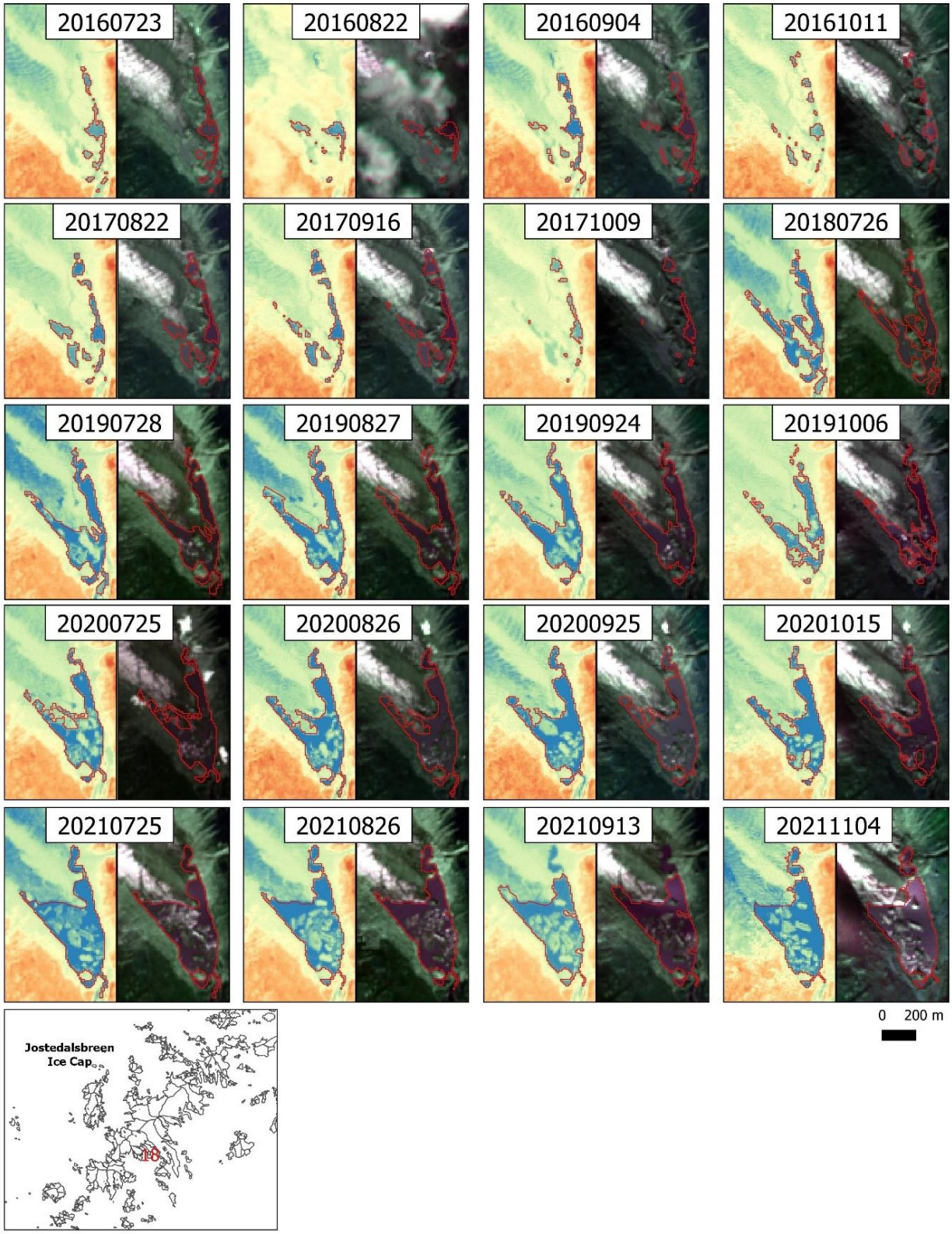

Figure 53: L18 (AG: Austerdalsbreen/GID: 2327) (ice calving and glacier retreat). The left frames represent NDWI images, and the right frames represent natural colour images

4.5 Sensitiveness of lake size in area change and inter-lake comparison

Inter-lake comparison of lake area variation (SD) is subject to their size as bigger lakes exhibit bigger area change in absolute terms as compared to smaller lakes and vice-versa. For example, L14 (*Kupvatnet/GID: 2471*) and L15 *(Styggevatnet/GID: 2478*), which have extremely large surface area stood at the top list in absolute SD (Tab. 8a and Fig. 12). Meanwhile, there was no significant difference between the mean lake areas of lake type 1 (*Not-connected-to-glacier*) and lake type 2 (*Connected-to-glacier*) (p-value = 0.54). Therefore, the lakes under these lake types fall within same group in terms of size and so the SD calculated for these lakes are not much affected by their initial size. However, for significant comparison, normalized SD was used.

4.6 Significance of Mann-Whitney U test on type 1 (*Not-connected-to-glacier*) and 2 (*connected-to-glacier*)

The result of Mann-Whitney U test conducted between lake type 1 (*Not-connected-to-glacier*) and lake type 2 (*Connected-to-glacier*) showed that there was no significant difference (p-value = 0.06) between their SD in normalized annual seasonal (month-to-moth) surface area over 6 years meaning that the variation they showed over 6 years in their surface area is no different to each other. However, this might be because of lack of data available in some months of the year to sufficiently represent the SD. In addition, there are some years where some lakes do not have data available for even a month or have data for just one or two months. In such a scenario, the confidence interval of 95% may be high enough to test the hypothesis, so if we reduce the confidence interval to, let's say 90%, then the obtained p-value, which is 0.06 would be significant meaning that there is significant difference in SD of normalized annual seasonal (month-to-month) surface area in lake type 1 (*Not-connected-to-glacier*) and lake type 2 (*Connected-to-glacier*). Meanwhile, the result of Mann-Whitney U test conducted between lake type 1 (*Not-connected-to-glacier*) and lake type 2 (*Connected-to-glacier*) showed that there was significant difference (p-value = 0.01) between their SD in normalized annual seasonal maximum (year-to-year) surface area over 6 years meaning that the variation they showed over 6 years in their surface area is significantly different from each other. Here, the data were available for all years and for almost all lakes, so the confidence level (95%) was logical enough to test the hypothesis and therefore, we are 95% confident that lake type 1 (*Not-connected-to-glacier*) and lake type 2 (*Connected-to-glacier*) vary differently in terms of normalized annual seasonal maximum (year-to-year) surface area over 6 years.

4.7 Comparison of outline mapping with previously performed inventories

Inventory of glacial lakes was in mainland Norway conducted by (Nagy & Andreassen, 2019) in 2018 with the help of Semi-automatic Classification Technique. The inventory was conducted on images acquired for 26-07-201 which is one of the dates for which images were acquired for analysis of glacial lakes in Jostedalsbreen region in this study. Therefore, the results of both outline mappings were compared with each other and represented in the Tab. 12.

Table 12: Comparison of outline mapping for glacial lakes with the mapping performed by (Andreassen et al., 2019) with semi-automatic classification

Lake name	Lake type	Date of image acquisition	Area in km² (Andreassen et. al., 2019) (a)	Area in km² (Manoj Pariyar - 2022) (b)	Difference (b-a)
L14	Artificial-water-level-regulation	20180726	4.1877	4.1631	-0.0246
L15	Artificial-water-level-regulation	20180726	7.2271	7.1825	-0.0446
Sub-total (Artificial-water-level-regulation)			**11.4148**	**11.3456**	**-0.0692**
L1	Connected-to-glacier	20180726	0.0024	0.0023	-0.0001
L10	Connected-to-glacier	20180726	0.4793	0.4811	0.0018
L12	Connected-to-glacier	20180726	0.0052	0.0050	-0.0002
L13	Connected-to-glacier	20180726	0.0024	0.0040	0.0016
L17	Connected-to-glacier	20180726	0.3166	0.3128	-0.0038
L18	Connected-to-glacier	20180726	0.1176	0.0844	-0.0333
L25	Connected-to-glacier	20180726	0.0936	0.0916	-0.0020
L3	Connected-to-glacier	20180726	0.1878	0.1831	-0.0047
L35	Connected-to-glacier	20180726	0.0104	0.0096	-0.0008
L37	Connected-to-glacier	20180726	0.0042	0.0032	-0.0010
L38	Connected-to-glacier	20180726	0.0173	0.0165	-0.0008
L40	Connected-to-glacier	20180726	0.0294	0.0259	-0.0036
L41	Connected-to-glacier	20180726	0.0283	0.0319	0.0036
L44	Connected-to-glacier	20180726	0.3800	0.3714	-0.0086
L48	Connected-to-glacier	20180726	0.0230	0.0223	-0.0007
L49	Connected-to-glacier	20180726	0.0108	0.0107	-0.0001
L4a	Connected-to-glacier	20180726	0.0725	0.0696	-0.0029
L4b	Connected-to-glacier	20180726	0.0410	0.0403	-0.0007
L5	Connected-to-glacier	20180726	0.0280	0.0287	0.0007
L50	Connected-to-glacier	20180726	0.0155	0.0146	-0.0009
L52	Connected-to-glacier	20180726	0.0570	0.0514	-0.0055
L53	Connected-to-glacier	20180726	0.2568	0.2564	-0.0004
L54	Connected-to-glacier	20180726	0.0476	0.0483	0.0007
L55	Connected-to-glacier	20180726	0.0161	0.0200	0.0039
L56	Connected-to-glacier	20180726	0.2053	0.2006	-0.0046
L58a	Connected-to-glacier	20180726	0.1780	0.1707	-0.0073
L58c	Connected-to-glacier	20180726	0.4450	0.4392	-0.0058
L9	Connected-to-glacier	20180726	0.1587	0.1720	0.0133
Sub-total (Connected-to-glacier)			**3.2299**	**3.1676**	**-0.0623**
L2	Glacier-dammed	20180726	0.0456	0.0438	-0.0018
L58b	Glacier-dammed	20180726	0.1543	0.1519	-0.0024
Sub-total (Glacier-dammed)			**0.1998**	**0.1957**	**-0.0042**
L19	Moraine-dammed	20180726	0.0078	0.0093	0.0015
Sub-total (Moraine-dammed)			**0.0078**	**0.0093**	**0.0015**
L11	Not-connected-to-glacier	20180726	0.0198	0.0185	-0.0013
L36	Not-connected-to-glacier	20180726	0.1761	0.1746	-0.0015
L42	Not-connected-to-glacier	20180726	0.0015	0.0015	0.0000
L46	Not-connected-to-glacier	20180726	0.2786	0.2716	-0.0070
L47	Not-connected-to-glacier	20180726	0.1298	0.1279	-0.0019
L51	Not-connected-to-glacier	20180726	0.0503	0.0484	-0.0019
L57	Not-connected-to-glacier	20180726	0.0631	0.0606	-0.0025
L6	Not-connected-to-glacier	20180726	0.0319	0.0307	-0.0012
L7	Not-connected-to-glacier	20180726	0.0115	0.0104	-0.0011
Sub-total (Not-connected-to-glacier)			**0.7626**	**0.7442**	**-0.0184**
Total			**15.6150**	**15.4624**	**-0.1526**

Altogether 42 lakes included in this study were also mapped by (Nagy & Andreassen, 2019) in the same date and these lakes belong to 5 different types – *connected-to-glacier (28), not-connected-to-glacier (9), glacier-dammed (2), moraine-dammed (1), and artificial-water-level-*

regulation (2). The sum of outlines mapped in both the mappings were almost the same in km^2. The total sum lake area obtained in this study was 15.4624 km^2 which is 0.1526 km^2 (1 %) less than the previous (2018) inventory. The outlines of lakes *connected-to-glacier, not-connected-to-glacier, glacier-dammed,* and *artificial-water-level-regulation* were underestimated by 0.0623 km^2, 0.0184 km^2, 0.0042 km^2 and 0.0692 km^2 respectively in this study, whereas the outlines of lake type *moraine-dammed* was overestimated by 0.0015 km^2 which is less difference. Therefore, the lake type *moraine-dammed* is more accurately represented. On the other hand, the lake types *artificial-water-level-regulation* and *connected-to-glacier* are less accurately represented than other types which is obviously due to ice-water interface in case of lake types *connected-to-glacier* where the NDWI technique of automatic classification often fails to work properly, and manual digitization is needed and in case of lake type *artificial-water-level-regulation*, more errors accumulate from larger circumferences.

Inventory of glacial lakes in mainland Norway conducted by (Nagy & Andreassen, 2019) in 2018 was later updated by (Andreassen et al., 2022) with lake outlines mapped in 2019. Manual digitization was done to optimize the number of lakes in the inventory conducted in 2019. The satellite images were acquired for 27-08-2019. Coincidentally, the images used for this study also included the images of glacial lakes in Jostedalsbreen region for the same date. Therefore, the results of both outline mappings were compared with each other and represented in the Tab. 13.

Table 13: Comparison of outline mapping for glacial lakes with the mapping performed by (Andreassen et al., 2022) with manual digitization

Lake name	Lake type	Date of image acquisition	Area in km2 (Andreassen et. al., 2022) (a)	Area in km2 (Manoj Pariyar (MP)- 2022) (b)	Diff. (b-a)	Mean Annual Seasonal Area (MP) (c)	Median Annual Seasonal Area (MP) (d)	Diff. from Mean (c-a)	Diff. from Median (d-a)
L14	Artificial-water-level-regulation	27/08/19	4.1903	4.1489	-0.0414	4.1209	4.1318	-0.0694	-0.0585
Sub-total (Artificial-water-level-regulation)			**4.1903**	**4.1489**	**-0.0414**	**4.1209**	**4.1318**	**-0.0694**	**-0.0171**
L1	Connected-to-glacier	27/08/19	0.0114	0.0113	-0.0002	0.0079	0.0077	-0.0036	-0.0037
L3	Connected-to-glacier	27/08/19	0.1859	0.1931	0.0072	0.1887	0.1903	0.0027	0.0044
L4a	Connected-to-glacier	26/07/18	0.0725	0.0695	-0.0030	0.0695	0.0700	-0.0030	-0.0025
L5	Connected-to-glacier	27/08/19	0.0468	0.0461	-0.0006	0.0444	0.0444	-0.0024	-0.0024
L9	Connected-to-glacier	27/08/19	0.1893	0.2312	0.0419	0.2100	0.2238	0.0207	0.0346
L10	Connected-to-glacier	27/08/19	0.4881	0.4825	-0.0056	0.4787	0.4810	-0.0094	-0.0071
L12	Connected-to-glacier	27/08/19	0.0096	0.0069	-0.0027	0.0073	0.0075	-0.0023	-0.0021
L13	Connected-to-glacier	27/08/19	0.0092	0.0089	-0.0003	0.0069	0.0069	-0.0023	-0.0023
L17	Connected-to-glacier	27/08/19	0.3392	0.3381	-0.0011	0.3257	0.3312	-0.0135	-0.0080
L18	Connected-to-glacier	27/08/19	0.0727	0.1078	0.0351	0.0918	0.0987	0.0191	0.0260
L25	Connected-to-glacier	27/08/19	0.0958	0.1236	0.0278	0.1142	0.1214	0.0185	0.0256
L34	Connected-to-glacier	27/08/19	0.0150	0.0103	-0.0048	0.0064	0.0064	-0.0086	-0.0086
L35	Connected-to-glacier	27/08/19	0.0104	0.0105	0.0001	0.0101	0.0105	-0.0003	0.0001
L38	Connected-to-glacier	27/08/19	0.0045	0.0075	0.0030	0.0067	0.0072	0.0022	0.0027
L40	Connected-to-glacier	27/08/19	0.0028	0.0014	-0.0014	0.0022	0.0022	-0.0006	-0.0006
L41	Connected-to-glacier	27/08/19	0.0315	0.0377	0.0062	0.0361	0.0361	0.0046	0.0046
L44	Connected-to-glacier	27/08/19	0.3723	0.3694	-0.0029	0.3487	0.3591	-0.0236	-0.0132
L45	Connected-to-glacier	27/08/19	0.0188	0.0246	0.0058	0.0165	0.0217	-0.0023	0.0029
L48	Connected-to-glacier	27/08/19	0.0234	0.0218	-0.0016	0.0201	0.0208	-0.0033	-0.0026
L49	Connected-to-glacier	27/08/19	0.0142	0.0144	0.0002	0.0140	0.0146	-0.0002	0.0004
L54	Connected-to-glacier	27/08/19	0.0745	0.0758	0.0012	0.0638	0.0700	-0.0107	-0.0045
L55	Connected-to-glacier	27/08/19	0.0445	0.0368	-0.0077	0.0377	0.0380	-0.0068	-0.0065
L58a	Connected-to-glacier	27/08/19	0.1809	0.1741	-0.0068	0.1723	0.1738	-0.0086	-0.0071
L58c	Connected-to-glacier	27/08/19	0.4590	0.4568	-0.0022	0.4497	0.4563	-0.0094	-0.0027
Sub-total (Connected-to-glacier)			**2.7724**	**2.8601**	**0.0878**	**2.7294**	**2.7998**	**-0.0429**	**0.0275**
L2	Glacier-dammed	27/08/19	0.0290	0.0281	-0.0009	0.0366	0.0366	0.0076	0.0076
L58b	Glacier-dammed	27/08/19	0.1698	0.1612	-0.0085	0.1577	0.1571	-0.0120	-0.0126
Sub-total (Glacier-dammed)			**0.1987**	**0.1893**	**-0.0094**	**0.1943**	**0.1937**	**-0.0044**	**-0.0050**
L19	Moraine-dammed	15/08/19	0.0093	0.0144	0.0050	0.0125	0.0131	0.0032	-0.0013
Sub-total (Moraine-dammed)			**0.0093**	**0.0144**	**0.0050**	**0.0125**	**0.0131**	**0.0032**	**-0.0013**
L37	Not-connected-to-glacier	27/08/19	0.0042	0.0061	0.0019	0.0044	0.0041	0.0002	-0.0001
Sub-total (Not-connected-to-glacier)			**0.0042**	**0.0061**	**0.0019**	**0.0044**	**0.0041**	**0.0002**	**-0.0020**
		Total	7.1749	7.2188	**0.0439**	**7.0616**	**7.1425**	**-0.1133**	**-0.0763**

Altogether 29 lakes included in this study were also mapped by (Andreassen et al., 2022) in the same date and these lakes belong to 5 different types – *connected-to-glacier (24), not-connected-to-glacier (1), glacier-dammed (2), moraine-dammed (1), and artificial-water-level-regulation (1).* The sum of outlines mapped in both the mappings were almost the same in km^2. The total sum obtained in this study was 7.2188 km^2 which is 0.0439 km^2 (0.6 %) more than the previous (2019) inventory. The outlines of lakes *connected-to-glacier, not-connected-to-glacier, and moraine-dammed* were over-estimated by 0.0878 km^2, 0.0019 km^2, and 0.0050 km^2 in this study, whereas the outlines of lake types *glacier-dammed* and *artificial-water-level-regulation* were underestimated by 0.0094 km^2 and 0.0414 km^2. Therefore, the lake type *not-connected-to-glacier* is more accurately represented. It is because of no ice-water interface. On the other hand, the lake types *connected-to-glacier* are less accurately represented than other types which is obviously due to ice-water interface as mentioned earlier in case of 2018 inventory.

Meanwhile, the glacial lake outlines areas from inventory by (Andreassen et al., 2022) was also compared with the mean annual seasonal area and median annual seasonal area of same lakes in 2019 computed in this study. The result showed that the outlines computed by (Andreassen et al., 2022) were very close to the mean (7.0616 km^2) and median (7.1425 km^2). In fact, it was just 1.5 % and 1.1 % more than the mean and median respectively. Therefore, the result of the inventory by (Andreassen et al., 2022) is representative for 2019.

Manual digitization often encounters bias from the digitizer, so chances of error is high. There are also some discrepancies in both outline mappings where manual digitization was done. These discrepancies can be seen clearly in lakes L1 (*GID: 2364*), L18, L25, L40, and L55 in Fig. 54. Since the glacier ice are often in the process of calving, it is tricky for the digitizer to include or omit them. Ideally, the glacier ice which is completely detached from the glacier is included in the lake water, but it is always challenging for a digitizer to verify that with Sentinel imageries. Therefore, use of false color images with bands combination enhancing the distinct visibility of the lake water is important.

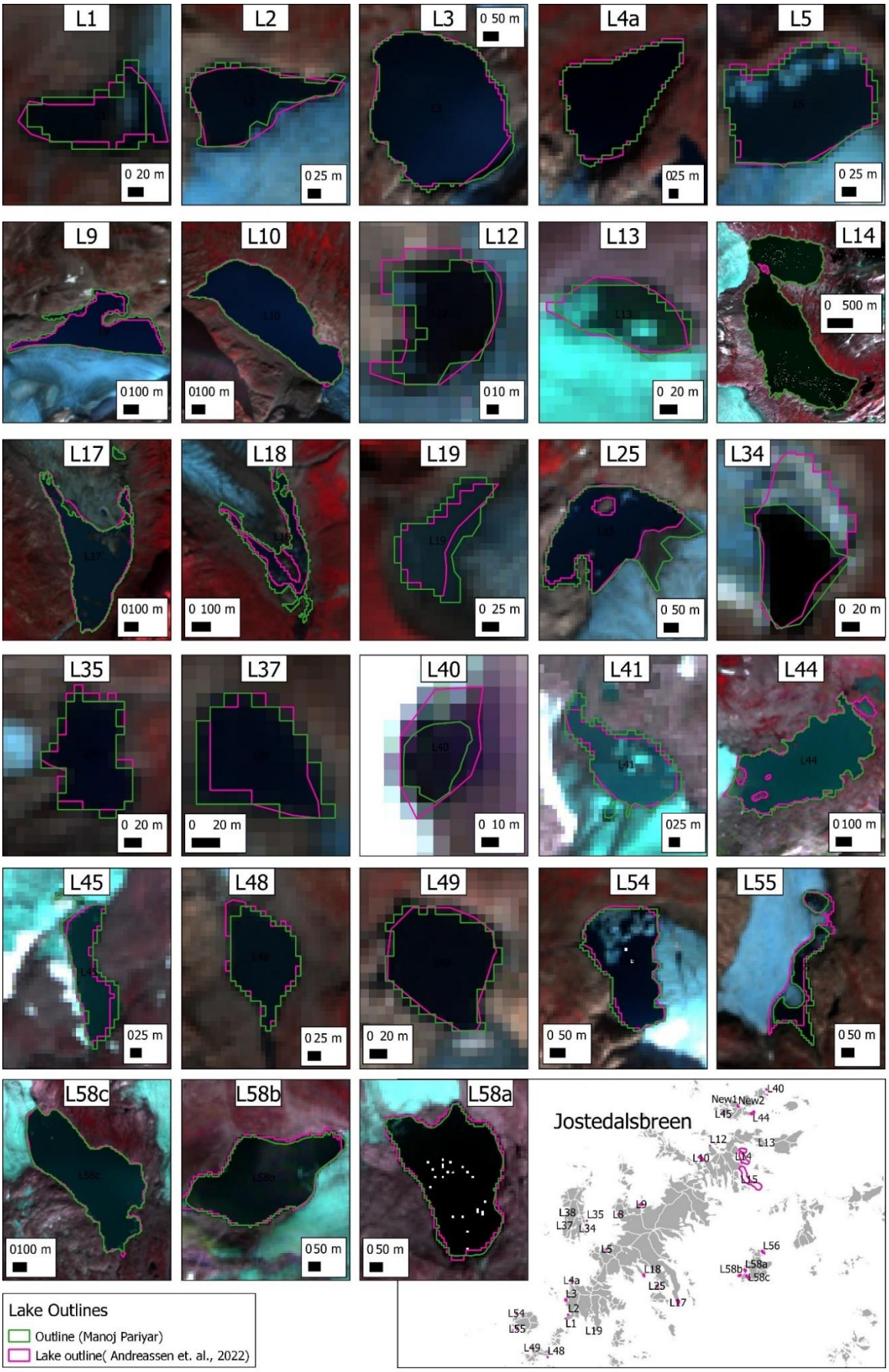

Figure 54: Comparison of outline mapping for glacial lakes with the one performed by (Andreassen et al., 2022). *The background images are false colour images to enhance the visibility of the lake.*

5 CONCLUSIONS

Time series analysis of glacial lakes using optical remote sensing is a challenging task as it is difficult to get a continuous series and high temporal resolution data due to atmospheric conditions. However, the combination of PS and S2 optimized the number of images included in the analysis. In addition, the outline mapping conducted in this study was close enough to that conducted by NVE in 2018 and 2019 with less than 1 % difference in area (Andreassen et al., 2022; Nagy & Andreassen, 2019), which enhanced the reliability of the results obtained in this study.

Scrutinizing all 51 lakes from Jostedalsbreen region included in the analysis, the study concludes that there was no significant evidence of GLOF events from 2016 to 2021. However, the lakes L2 (*AG: Marabreen/GID: 2364/type: Glacier-dammed*) and L19 (*AG: Supphellebreen/GID: 2352/type: Moraine-dammed*), both with history of GLOF events were found to be apparently reduced in size in the month of August and September compared to that of July, but the intermediate images confirmed that the drainage was not rapid and still they had significant amount of water impounded in them. During these 6 years, the regional surface temperature in Western Norway has increased in summer seasons (Meteorological Institute Norway, 2021), resulting in an increased surface area of other lakes *connected-to-glacier*, but both these *glacier-dammed* and *moraine-dammed* lakes, yet having a history of GLOF events and registered as potentially dangerous lakes by NVE (Nagy & Andreassen, 2019), did not undergo any rapid drainage events - rather they were just reduced in their size in an interval of 1 to 2 months. This suggests that both these lakes were drained partially through natural drainage pathways and so they did not pose any risk during the years. In addition, L5 (*AG: Melkevollbreen/GID: 2324/type: connected-to-glacier*) which showed a comparatively rapid increase in size in 6 years, was also draining out through natural drainage. This confirms that there is no risk of an outburst in situations with natural drainage. However, such lakes in future may pose risk of outburst due to displacement waves overtopping the dam caused by huge chunks of ice calving into the lake. In fact, it is imperative to check the geology and morphology of the dam if it can withstand the shock wave thus produced. While lakes that aren't connected to glaciers remained almost constant in 6 years, they might also experience outburst flood events if a massive rock fall, an avalanche, or landslide occurs into the lake. The outbursts of glacial lakes are particularly prominent in the early summer (Jackson & Ragulina, 2014), but the images exposed a reduction in glacial lake area in late autumn due to glacier advances at

the terminus. Therefore, all images should be subjectively reviewed to confirm the actual drainage events while performing such remote sensing image analysis.

The month-to-month (seasonal) and year-to-year (interannual) variation analysis of lake surface area showed that lakes *connected-to-glacier* were more variable in % SD as compared to lakes *not-connected-to-glacier*, though not statistically significant (p-value = 0.06). These variations were accounted for ablation and calving due to changes in regional seasonal surface temperature. Especially at the beginning and end of the melting season, the presence of ice cover at the margin of lakes highly influenced the area coverage observed in the images but the lakes were clearly open with their maximum surface area in August and September. In addition, the change in glacier terminus through retreat, and advance in lakes *connected-to-glacier*, for instance in lakes L17, L18, and L5, are also major factors for causing the variation. Further, the study showed that % variation (SD) in normalized maximum annual surface area of lakes *not-connected-to-glacier* and *connected-to-glacier* were significantly different (p value =0.01) from each other and lakes *connected-to-glacier* were more variable as compared to lakes *not-connected-to-glacier*. This variation is accounted for the changes in regional annual surface temperature in alternative years influencing the ice-melting process.

In addition, the lake types *connected-to-glacier* including *moraine-dammed* lake showed an increasing trend in normalized annual maximum recorded surface area in recent years which is in line with regional annual and seasonal (summer) surface temperature trend in recent years in the study area. The percentage change in surface area observed in some lakes is so huge (several thousand %) within 6 years' time that the impact can be huge in case of outburst in future. Considering that a trigger factor (for instance calving ice) causing displacement waves overtops the dam and the dam is weak, especially the lake L23 (*GID: 2293/type: supraglacial-lake*), which has the highest % variation in lake area, could be very dangerous in case of an outburst.

To no surprise, like in other parts of the world with increasing surface temperatures, the glacier terminus in Jostedalsbreen region connected to lakes are retreating leaving earth surface underneath exposed and losing direct contact with the lake. As a result, a significant number of lakes *connected-to-glacier* are now disconnected from the glacier. Such lakes in transitioning phase showed a medium variation during 6 years' time interval (Tab.s 8; 9) as compared to rest of the lakes as they have moderate interface with the glacier. During a complete separation, the variation in surface area as a result of retreat or advance is rare, and the surface area will somehow remain constant as long as there is a balance between input and output water.

In this study, out of a total 1479 imageries for 51 lakes in 6 years (29 imageries per lake in total), only 826 imageries were usable whereof 702 imageries were obtained from S2 and 124 imageries were obtained from PS. However, most of the images were obtained from the core melting months (July (207), August (272), September (228) and October (101), so the result of lake surface area variation in this study sufficiently captures the lake expansion phase of the year which is crucial to outburst. Meanwhile, the semi-automatic classification method applying NDWI used to identify and delineate glacial lake area was a very suitable method to fulfill the objective of this study. There was not much difference in percentage representation of water pixels using the best suitable NDWI thresholds for S2 and PS imageries so the combination of S2 and PS imageries for time series analysis of lake area data was significantly helpful.

As mentioned earlier, the major cause observed behind the expansion of lake area in Jostedalsbreen region was glacier retreat prompted by ablation and ice calving which can be seen clearly in low lying lakes (L17 and L18). Since the annual mass balance of glaciers in Jostedalsbreen region in recent years are negative and as this continues, the rate of melting is sure to be increased, expanding the lakes even further posing risk of higher damage due to potential outburst as well as new lakes are formed. This can be surveyed with continued use of high frequency satellite imageries (Andreassen, Engeset, et al., 2021; Andreassen, Moholdt, et al., 2021). Therefore, the need for a regular monitoring of glacial lakes, especially lakes with high potential of outburst, is a most in Jostedalsbreen region.

6 DATA AVAILABILITY

The outlines (polygons) of glacial lakes produced in this study will be available in NVE's Copernicus Glacier Service Website.

https://www.nve.no/hydrology/glaciers/copernicus-glacier-service/glacier-lakes/

References:

Aggarwal, S., Rai, S. C., Thakur, P. K., & Emmer, A. (2017). Inventory and recently increasing GLOF susceptibility of glacial lakes in Sikkim, Eastern Himalaya. *Geomorphology*, *295*, 39–54. https://doi.org/10.1016/J.GEOMORPH.2017.06.014

Andreassen, L. M., & Elvehøy, H. (2021). *Norwegian Glacier Reference Dataset for Climate Change Studies*. Retrieved from www.nve.no

Andreassen, L. M., Engeset, R. V., Melvold, K., Müller, K., Orthe, N. K., Sund, M., & Winsvold, S. H. (2021). *Developing Satellite Services for Hydrology, Glaciers and Avalanches in Norway*. Retrieved from www.nve.no

Andreassen, L. M., Moholdt, G., Kääb, A., Messerli, A., Nagy, T., & Winsvold, S. H. (2021). *Monitoring glaciers in mainland Norway and Svalbard using Sentinel*. Retrieved from https://publikasjoner.nve.no/rapport/2021/rapport2021_03.pdf

Andreassen, L. M., Nagy, T., Kjøllmoen, B., & Leigh, J. R. (2022). An inventory of Norway ' s glaciers and ice-marginal lakes from 2018 – 19 Sentinel-2 data. *Journal of Glaciology*, *1*(22). https://doi.org/https://doi.org/10.1017/jog.2022.20

Andreassen, L. M., Winsvold, S. H., Paul, F., & Hausberg, J. E. (2012). Inventory of Norwegian Glaciers. In *NVE Rapport* (Vol. 38).

Askheim, S. (2022). Jostedalsbreen. In *Store norske leksikon*. Retrieved from https://snl.no/Jostedalsbreen

Bajracharya, S. R., Mool, P. K., & Shrestha, B. R. (2008). Global climate change and melting of Himalayan glaciers. *Melting Glaciers and Rising Sea Levels: Impacts and Implications*, 28–46. Retrieved from http://hpccc.gov.in/pdf/glaciers/global climate change and melting of himalayan glaciers.pdf

Bashiri, A., Moghaddam, H. H., Khodam, M. J., Afghahi, S. M., Tabarsi, H., & Eng, M. (2021). A novel method for Sentinel-2 satellite images radiometric calibration. *JOURNAL OF NATURE AND SPATIAL SCIENCES*, *1*(2), 27–37. https://doi.org/10.30495/jonass.2021.1929310.1011

Begam, S., Sen, D., & Dey, S. (2018). Moraine dam breach and glacial lake outburst flood generation by physical and numerical models. *Journal of Hydrology*, *563*, 694–710. https://doi.org/10.1016/J.JHYDROL.2018.06.038

Bendle, J. (2020). Glacial Lake Outburst Floods. Retrieved June 3, 2022, from AntarcticGlaciers.org website: https://www.antarcticglaciers.org/glacier-processes/glacial-lakes/glacial-lake-outburst-floods/

Braithwaite, R. J., & Zhang, Y. (1999). Modelling Changes in Glacier Mass Balance that may Occur as a Result of Climate Changes. *Geografiska Annaler, Series A: Physical Geography*, *81*(4), 489–496. https://doi.org/10.1111/1468-0459.00078

Carrivick, J. L., Andreassen, L. M., Nesje, A., & Yde, J. C. (2022). A reconstruction of

Jostedalsbreen during the Little Ice Age and geometric changes to outlet glaciers since then. *Quaternary Science Reviews*, *284*, 107501. https://doi.org/10.1016/j.quascirev.2022.107501

Copernicus Open Access Hub. (n.d.). Open Access Hub. Retrieved May 26, 2022, from https://scihub.copernicus.eu/

Dai, K., Wen, N., Fan, X., Deng, J., Zhang, L., Liang, R., … Xu, Q. (2022). Seasonal Changes of Glacier Lakes in Tibetan Plateau Revealed by Multipolarization SAR Data. *IEEE Geoscience and Remote Sensing Letters*, *19*. https://doi.org/10.1109/LGRS.2021.3131717

Davies, B. (2020). Observing glacier change from space. Retrieved June 3, 2022, from AntarcticGlaciers.org website: https://www.antarcticglaciers.org/glaciers-and-climate/glacier-recession/observing-glacier-change-space/

Emmer, A., & Cochachin, A. (2013). The causes and mechanisms of moraine-dammed lake failures in the cordillera blanca, North American Cordillera, and Himalayas. *Acta Universitatis Carolinae, Geographica*, *48*(2), 5–15. https://doi.org/10.14712/23361980.2014.23

ESA. (n.d.-a). Calibration - Sentinel-2 MSI. Retrieved April 9, 2022, from https://sentinels.copernicus.eu/web/sentinel/technical-guides/sentinel-2-msi/calibration

ESA. (n.d.-b). Level-2A Product Formatting - Sentinel-2 MSI Technical Guide - Sentinel Online. Retrieved March 20, 2022, from https://sentinel.esa.int/web/sentinel/technical-guides/sentinel-2-msi/level-2a/product-formatting

ESA. (n.d.-c). Sentinel-2 - Mission Objectives - Sentinel Online. Retrieved March 20, 2022, from https://sentinel.esa.int/web/sentinel/missions/sentinel-2/mission-objectives

ESA. (n.d.-d). Sentinel-2 MSI - Resolutions - Sentinel Online. Retrieved March 20, 2022, from https://sentinel.esa.int/web/sentinel/user-guides/sentinel-2-msi/resolutions

ESA. (2013). *SENTINEL-2 User Handbook*. Retrieved from https://sentinel.esa.int/documents/247904/685211/Sentinel-2_User_Handbook

ESA. (2015). User Guides - Sentinel-2 MSI - Sentinel Online. Retrieved March 20, 2022, from Sentinels.copernicus.eu website: https://sentinel.esa.int/web/sentinel/user-guides/sentinel-2-msi/resolutions/spatial

Fischer, W. A., Hemphill, W. R., & Kover, A. (1976). Progress in remote sensing (1972–1976). *Photogrammetria*, *32*(2), 33–72. https://doi.org/10.1016/0031-8663(76)90013-2

Fleig, A. K., Andreassen, L. M., Barfod, E., Haga, J., Haugen, L. E., Hisdal, H., … Saloranta, T. (2013). *Norwegian Hydrological Reference Dataset for Climate Change Studies*. Retrieved from http://webby.nve.no/publikasjoner/rapport/2013/rapport2013_02.pdf

Gilmore, S., Saleem, A., & Dewan, A. (2015). Effectiveness of DOS (Dark-Object Subtraction) method and water index techniques to map wetlands in a rapidly urbanising megacity with Landsat 8 data. *CEUR Workshop Proceedings*, *1323*(October), 100–108.

Green, K. (2011). Interannual and seasonal changes in the ice cover of glacial lakes in the Snowy Mountains of Australia. *Journal of Mountain Science 2011 8:5*, *8*(5), 655–663. https://doi.org/10.1007/S11629-011-2084-9

Harrison, S., Kargel, J. S., Huggel, C., Reynolds, J., Shugar, D. H., Betts, R. A., … Vilímek, V. (2018). Climate change and the global pattern of moraine-dammed glacial lake outburst floods. *Cryosphere*, *12*(4), 1195–1209. https://doi.org/10.5194/TC-12-1195-2018

Imhof, P., Nesje, A., & Nussbaumer, S. U. (2012). Climate and glacier fluctuations at Jostedalsbreen and Folgefonna, southwestern Norway and in the western Alps from the "Little Ice Age" until the present: The influence of the North Atlantic Oscillation. *Holocene*, *22*(2), 235–247. https://doi.org/10.1177/0959683611414935

Jackson, M., & Ragulina, G. (2014). *Inventory of glacier-related hazardous events in Norway*. Retrieved from https://publikasjoner.nve.no/rapport/2014/rapport2014_83.pdf

Jóhannesson, T., Ahlstrøm, A. P., Andreassen, L. M., Björnsson, H., Woul, M. de, Elvehøy, H., … Radić, V. (2006). The impact of climate change on glaciers and glacial runoff in the Nordic countries. *European Conference on Impacts of Climate Change on Renewable Energy Sources*, 1–7. Retrieved from https://www.researchgate.net/publication/242249882_The_impact_of_climate_change_on_glaciers_and_glacial_runoff_in_the_Nordic_countries

Jóhannesson, T., Sigurdsson, O., Laumann, T., & Kennett, M. (1995). Degree-day glacier mass-balance modelling with applications to glaciers in Iceland, Norway and Greenland. *Journal of Glaciology*, *41*(138), 345–358. https://doi.org/10.3189/S0022143000016221

Karabulut, M., & Ceylan, N. (2005). The spectral reflectance responses of water with different levels of suspended sediment in the presence of algae. *Turkish Journal of Engineering and Environmental Sciences*, *29*(6), 351 – 360. Retrieved from https://journals.tubitak.gov.tr/engineering/abstract.htm?id=7951

Kjøllmoen, B., Andreassen, L. M., Elvehøy, H., & Melvold, K. (2021). Glaciological investigations in Norway 2020. In *www.nve.no*. Retrieved from http://publikasjoner.nve.no/rapport/2021/rapport2021_31.pdf

Komori, J. (2008). Recent expansions of glacial lakes in the Bhutan Himalayas. *Quaternary International*, *184*(1), 177–186. https://doi.org/10.1016/J.QUAINT.2007.09.012

Laumann, T., & Reeh, N. (1993). Sensitivity to climate change of the mass balance of glaciers in southern Norway. *Journal of Glaciology*, *39*(133), 656–665. https://doi.org/10.3189/S0022143000016555

Lindsey, R., & Dahlman, L. (2022). Climate Change: Global Temperature. Retrieved June 1, 2022, from ClimateWatch Magazine website: https://www.climate.gov/news-features/understanding-climate/climate-change-global-temperature

MacFarland, T. W., & Yates, J. M. (2016). Mann–Whitney U Test. *Introduction to Nonparametric Statistics for the Biological Sciences Using R*, 103–132. https://doi.org/10.1007/978-3-319-30634-6_4

McFeeters, S. K. (2007). The use of the Normalized Difference Water Index (NDWI) in the delineation of open water features. *International Journal of Remote Sensing*, *17*(7), 1425–1432. https://doi.org/10.1080/01431169608948714

McKnight, P. E., & Najab, J. (2010). Mann-Whitney U Test. *The Corsini Encyclopedia of Psychology*, 1–1. https://doi.org/10.1002/9780470479216.CORPSY0524

Meteorological Institute Norway. (2021). Western Norway since 1900 - Temperature. Retrieved June 1, 2022, from https://www.met.no/vaer-og-klima/klima-siste-150-ar/regionale-kurver/vestlandet-siden-1900

Mohanty, L., & Maiti, S. (2021). Probability of glacial lake outburst flooding in the Himalaya. *Resources, Environment and Sustainability*, *5*, 100031. https://doi.org/10.1016/J.RESENV.2021.100031

Nagy, T., & Andreassen, L. M. (2019). *Glacier lake mapping with Sentinel-2 imagery in Norway*. Retrieved from http://publikasjoner.nve.no/rapport/2019/rapport2019_40.pdf

Neupane, R., Chen, H., & Cao, C. (2019). Review of moraine dam failure mechanism. *Geomatics, Natural Hazards and Risk*, *10*(1), 1948–1966. https://doi.org/10.1080/19475705.2019.1652210

norgeibilder. (2022). Norge i bilder. Retrieved June 6, 2022, from https://www.norgeibilder.no/?id=2372

Norwegian Water Resources and Energy Directorate. (2022a). Glacier lake outburst floods. Retrieved from http://glacier.nve.no/glacier/viewer/GLOF/en/

Norwegian Water Resources and Energy Directorate. (2022b). Glacier lakes. Retrieved June 2, 2022, from https://www.nve.no/hydrology/glaciers/copernicus-glacier-service/glacier-lakes/

Planet Labs. (n.d.-a). Company | Planet. Retrieved June 1, 2022, from https://www.planet.com/company/

Planet Labs. (n.d.-b). Planet Explorer. Retrieved May 26, 2022, from https://www.planet.com/explorer/

Planet Labs. (n.d.-c). PlanetScope. Retrieved March 22, 2022, from https://developers.planet.com/docs/data/planetscope/

Planet Labs. (n.d.-d). PSScene4Band. Retrieved March 22, 2022, from https://developers.planet.com/docs/data/psscene4band/#available-asset-types

Qayyum, N., Ghuffar, S., Ahmad, H. M., Yousaf, A., & Shahid, I. (2020). Glacial lakes mapping using multi satellite PlanetScope imagery and deep learning. *ISPRS International Journal of Geo-Information*, *9*(10). https://doi.org/10.3390/ijgi9100560

Sadeh, Y., Zhu, X., Dunkerley, D., Walker, J. P., Zhang, Y., Rozenstein, O., … Chenu, K. (2021). Fusion of Sentinel-2 and PlanetScope time-series data into daily 3 m surface reflectance and wheat LAI monitoring. *International Journal of Applied Earth Observation and Geoinformation*, *96*, 102260.

https://doi.org/10.1016/J.JAG.2020.102260

Satellite Imaging Corporation. (n.d.). Sentinel-2A Satellite Sensor. Retrieved April 9, 2022, from https://www.satimagingcorp.com/satellite-sensors/other-satellite-sensors/sentinel-2a/

Shugar, D. H., Burr, A., Haritashya, U. K., Kargel, J. S., Watson, C. S., Kennedy, M. C., … Strattman, K. (2020). Rapid worldwide growth of glacial lakes since 1990. *Nature Climate Change 2020 10:10*, *10*(10), 939–945. https://doi.org/10.1038/s41558-020-0855-4

Song, C., Woodcock, C. E., Seto, K. C., Lenney, M. P., & Macomber, S. A. (2001). Classification and Change Detection Using Landsat TM Data. *Remote Sensing of Environment*, *75*(2), 230–244. https://doi.org/10.1016/s0034-4257(00)00169-3

Sugiyama, S., Minowa, M., Fukamachi, Y., Hata, S., Yamamoto, Y., Sauter, T., … Schaefer, M. (2021). Subglacial discharge controls seasonal variations in the thermal structure of a glacial lake in Patagonia. *Nature Communications 2021 12:1*, *12*(1), 1–9. https://doi.org/10.1038/s41467-021-26578-0

The European Space Agency. (n.d.). About Copernicus Sentinel-2. Retrieved from https://sentinel.esa.int/web/sentinel/missions/sentinel-2

Wang, W., Xiang, Y., Gao, Y., Lu, A., & Yao, T. (2015). Rapid expansion of glacial lakes caused by climate and glacier retreat in the Central Himalayas. *Hydrological Processes*, *29*(6), 859–874. https://doi.org/10.1002/HYP.10199

Yao, X., Liu, S., Han, L., Sun, M., & Zhao, L. (2018). Definition and classification system of glacial lake for inventory and hazards study. *Journal of Geographical Sciences*, *28*(2), 193–205. https://doi.org/10.1007/S11442-018-1467-Z

Zhang, G., Yao, T., Xie, H., Wang, W., & Yang, W. (2015). An inventory of glacial lakes in the Third Pole region and their changes in response to global warming. *Global and Planetary Change*, *131*, 148–157. https://doi.org/10.1016/J.GLOPLACHA.2015.05.013

Zhang, M., Chen, F., Tian, B., Liang, D., & Yang, A. (2020). High-frequency glacial lake mapping using time series of sentinel-1A/1B sar imagery: An assessment for the southeastern tibetan plateau. *International Journal of Environmental Research and Public Health*, *17*(3). https://doi.org/10.3390/ijerph17031072